

## CHAPTER 3 SURVEY RESULTS

### (1) Regional Survey Results

#### Geological Setting and Mineralization

The Erdenet copper deposit in the project area is the biggest porphyry copper-molybdenum deposit in eastern Asia. Many mineral showings related to different types of ore deposits exist in the project area, such as porphyry copper-molybdenum type, high sulphide gold deposit type, oxidized copper deposit type, high grade gold vein deposit type, etc.

Ore deposits and mineralized areas are widely distributed in an area set between two big scale structural lines along EW direction and occurring locally in cross points controlled by faults systems along NW-SE and NE-SW directions.

The geology of the project area is shown in Fig. 4.

The mineralizations are controlled by NW-SE trending geological structures, whereas the igneous post-mineralization activities tends to occur along N-S trending. The mineralized zones in the area, consisting of six known ore bodies and mineralizations including the Erdenet mine, show NW-SE trends elongated about 20km. Among the Erdenet ore deposit, which consists of five ore bodies and mineralized zones, the only developed ore body is the Erdenet northwest ore body. The remaining ore bodies present a small scale and low grade. The igneous rocks related to the mineralization are thought to correspond to the Erdenet complex consisting of granodiorite porphyry and diorite porphyry, which are confirmed as adakitic rocks according to the analytical results obtained by rock geochemical analysis.

Based on the interpretation of the geological map shown in Fig. 4, the area where the Erdenet ore deposit occurs is associated with plutonic rocks arrangements, small body structures, fault structure trending along NW-SE direction and fault structure trending along NE-SW direction. The Erdenet ore deposit is located in the northern margin of the ring structure, which also correspond to the southwestern end of the basin structure. The same kind of structure controls that occurred in the tectonic settings for the Erdenet ore deposit can also be observed in Mogoin gol/Khujiriin gol area and Zuukhiin gol area.

#### Conclusions of Airborne Geophysical Survey

The airborne geophysical survey consisting of both, magnetic survey and radiometric survey was carried out in the area shown in Fig. 2. The survey area covered an extension of 5,500km<sup>2</sup> with a total flight length of 26,538km. A reduced to pole field map is shown in Fig.10.

According to the results of airborne magnetic and radiometric surveys at the Western Erdenet area, in Area-1 it was detected an elongated magnetic lineament along NW-SE direction from the southeast corner to the center of the area with slight bending but showing a further westward continuation

Macroscopically, the geological structure is controlled by huge scale tectonic lines such as the Vitim Structure trending along the EW direction. The low magnetic zone, where Erdenet mine is located, is probably due to the effects of demagnetization during the alteration process. A tectonic line detected on the south part of Area-1 along an ENE-WSW seems to intersect the basement rocks and younger sedimentary basins. It is inferred that this tectonic line controls the Western Erdenet area. As shown in Fig. 10, several crossing structures were observed as formed by acute angles of low magnetic anomaly zones. The Erdenet ore deposit occurred in the place where the above mentioned crossing structures are located. The low magnetic anomaly is also reflected by the reverse magnetization of granitic rock of Erdenet complex.

According to the relationship between mineralization and radiometric anomalies, the Erdenet Mine area is located in the high potassium anomaly caused by granitic rocks of Selenge complex and Erdenet complex. High Potassium anomalies are seen distributed along the same trend as the magnetic NW-SE trend. Most of the strong potassium signatures were detected in the open-pit of Erdenet mine. This NW-SE trend spreads through the westward and continues to Khujiriin gol area.

Among the prospective zones extracted from the interpretation of the aeromagnetic and radiometric data, it is worth to mention a zone of high potassium anomaly which includes a NW-SE magnetic lineament that continues westward in the area and likely to be related to mineralization.

### **Low Magnetic Anomaly, Igneous Activity and Age of Mineralization**

In order to study the source of low magnetic anomaly and the igneous activity, rock samples were collected in several areas to analyze for natural remanent magnetization and K-Ar dating. The results were compiled in Fig. 12. Granodiorite (EM4) and syenite porphyry (EM3) of the Selenge complex and Erdenet complex gave indications of being reversely magnetized. The syenite porphyry (EM3) of the Erdenet complex is adakitic rock. A rock sample of andesite dyke (EM1) intruded in syenite porphyry was found to be normally magnetized.

The above results indicate that the magnetic pole changed probably from reverse magnetization to normal magnetization before intrusion of andesite dykes. The strong low magnetic anomaly detected in the Erdenet Mine area was caused by the intrusion of granitic rock of Erdenet complex.

The estimated ages of rock samples for K-Ar dating of granodiorite of Selenge complex, syenite porphyry of Erdenet complex and andesite dykes collected in the open-pit of Erdenet Mine were calculated in  $224.8 \pm 5.9\text{Ma}$ ,  $208.0 \pm 5.4\text{Ma}$  and  $191.1 \pm 5.8\text{Ma}$ , respectively. Consequently, the granodiorite (225Ma) of Selenge complex and the syenite porphyry (208Ma) of Erdenet complex

show reverse magnetization while the andesite dykes (191Ma) show normal magnetization. During the ages from 208Ma to 191Ma, the magnetic pole changed its polarization.

A sample with molybdenum mineralization that was collected from the drill core of MJME-Z2 in the Zuukhiin gol area was found useful to conduct the Re/Os isotope dating analysis. The age of the Re/Os dating was estimated in  $231.3 \pm 0.8$ Ma. Watanabe and Stein (2000) conducted the Re/Os isotope dating analysis of molybdenite collected from the Erdenet Mine and estimated an age of  $240.60 \pm 0.8$ Ma. The Re-Os age of the Erdenet Mine resulted 10Ma older than the Zuukhiin gol area. The K-Ar dating ages of granodiorite and syenite porphyry show  $224.8 \pm 5.9$ Ma and  $208.0 \pm 5.4$ Ma, respectively. However, their age estimations are younger than the Re/Os dating ages of molybdenite, indicating probably that original magma was melted first, then molybdenite crystallized during rising or emplating of magma and finally, the magma was completely emplaced in situ.

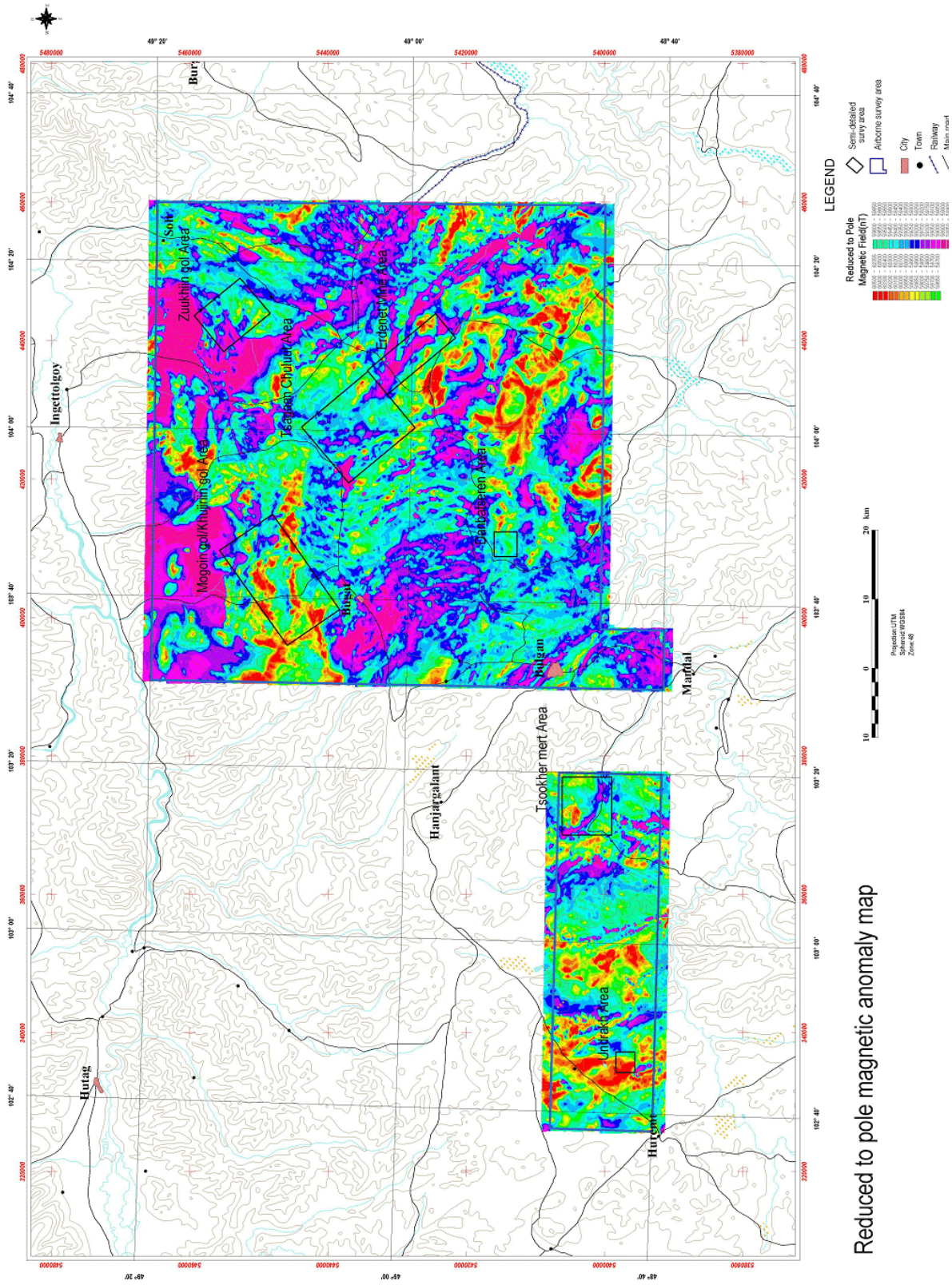
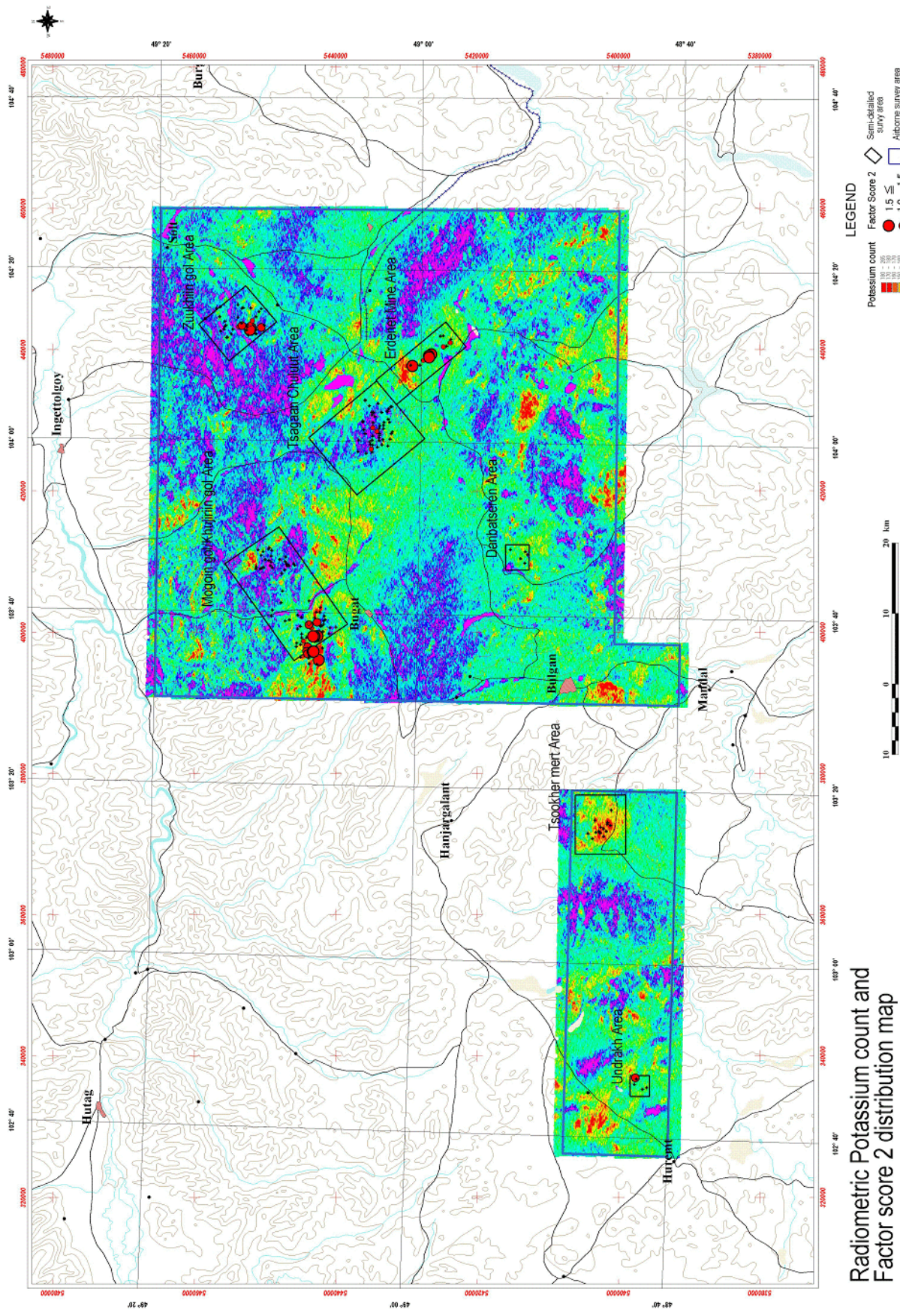


Fig. 10 Total magnetic intensity – reduced to pole color image and map in the Western Erdenet area.





**Radiometric Potassium count and Factor score 2 distribution map**

Fig. 11 Radiometric potassium count of airborne survey in the Western Erdenet area.

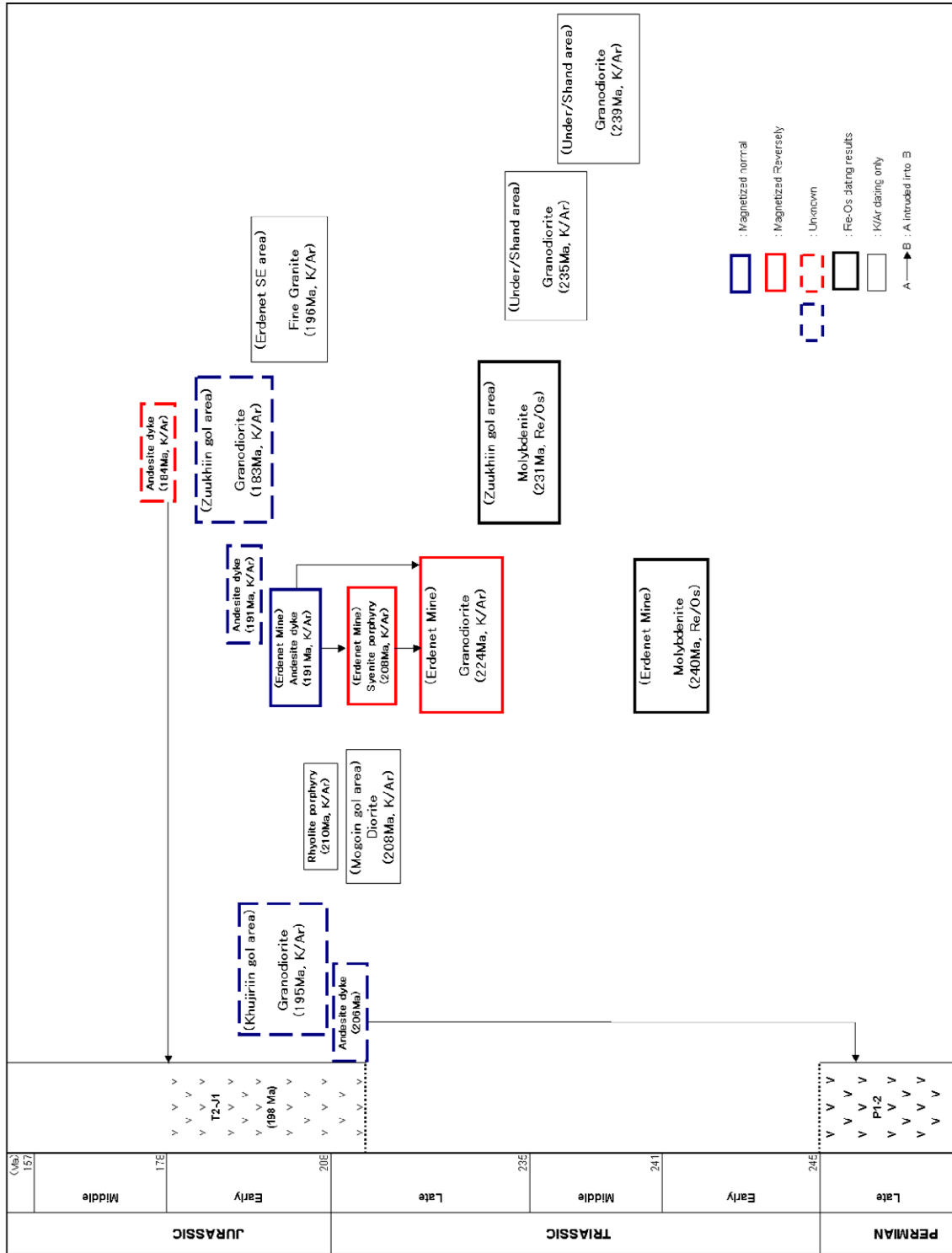


Fig. 12 Results of remanent magnetization, K/Ar dating and Re/Os dating on the geologic column.



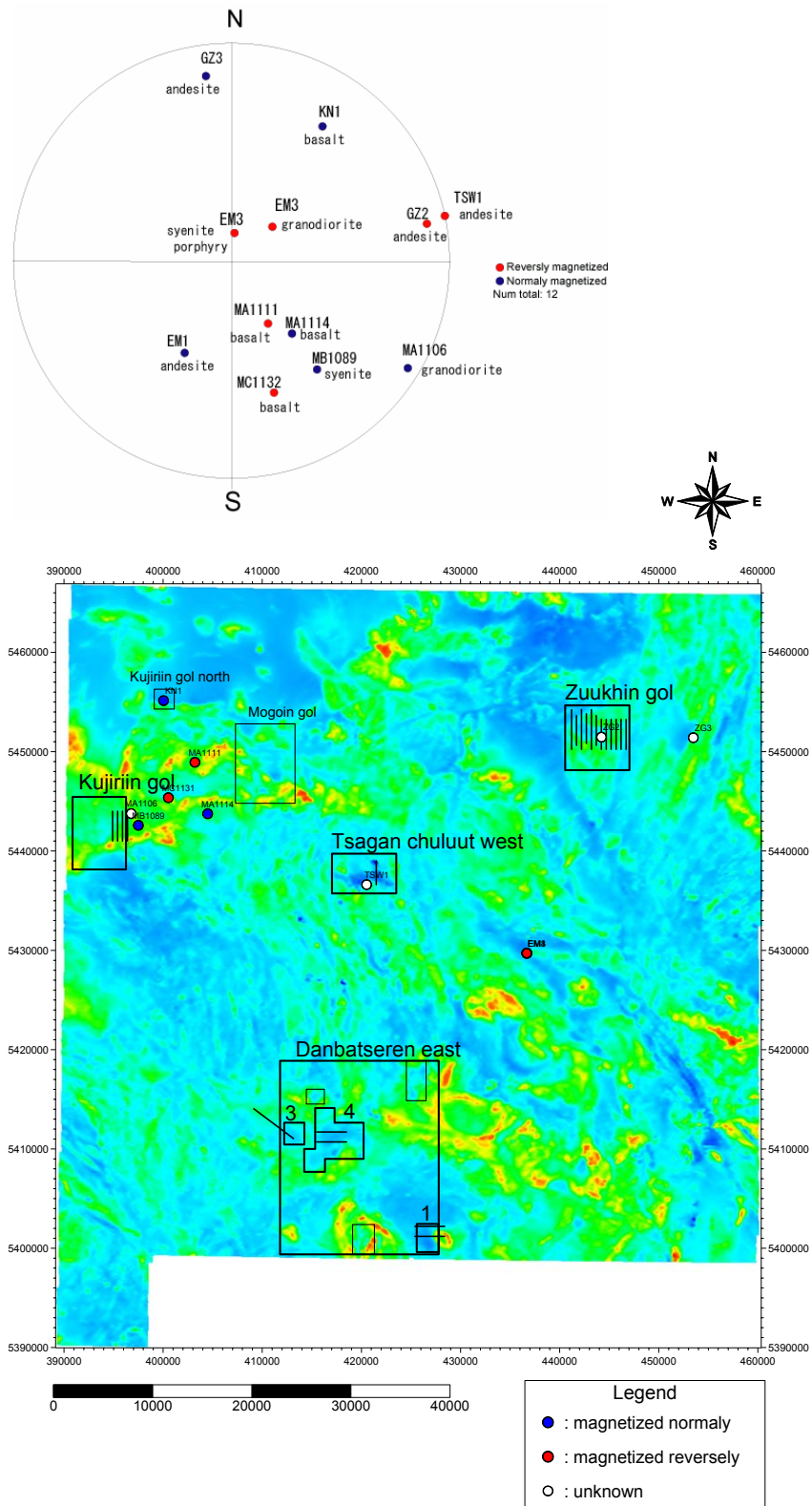


Fig. 13 Remanent magnetization measurements results.

## **(2) Mogoin gol Area**

### **Introduction**

The area is located approximately 25 km northwest from Erdenet city and about 1,240m to 1,700masl. As shown in Fig. 2, the topography consists of steep to gentle hills. The vegetation in the area is composed of coniferous forests and tall grass in the hill and valley and low grass along streams. Outcrop studies are difficult because of the high and abundant grass.

According to the previous existing data, the Mogoin gol mineralized zones were discovered in 1967. In 1971, a geological mapping survey was carried out in a scale of 1: 50,000, while in 1981, the 1: 25,000 geological mapping was performed. In the Mogoin gol mineral showing, secondary quartzite with copper minerals was confirmed in the areas of 15m×0.5km and 4km×2km. Previous analytical data indicates that ore assay were Cu 0.034 % to 0.074 % and Mo 0.002 % to 0.018 %. Short drillings were conducted in mineral showings, but typical mineralizations were not detected. Although high FE anomaly by IP electric survey was also reported in the area, the drilling survey did not report any remarkable mineralization.

### **Geological Survey Results**

Geology in this area is composed of late Permian alkali volcanic rocks, late Triassic to early Jurassic volcanic rocks, Permian to Triassic granites, Jurassic dykes, dykes and quaternary. K-Ar ages of the diorite and the rhyolitic porphyry of the late Triassic ages (T3) indicate 208 Ma and 210Ma, respectively. These ages are close to the radiometric ages, 190 Ma to 210 Ma, of the sericite minerals from the Erdenet mine. Diorite and the rhyolitic porphyry for the K-Ar measurements are adakitic rocks, which indicate their relation to the porphyry copper-molybdenum deposit as it has been recently reported. .

The area is regionally located in the cross junction of the EW trending faults and the NW-SE trending faults. The main faults indicate the dominant NNW-SSE, NW-SE and EW direction in the northern part, the dominant NW-SE and EW direction in the central part and the dominant NE-SW and EW direction in the southern part. The Erdenet ore deposit is also known to be in the junction of the NW-SE and the EW trending structure zones and in this respect, the white silicification zone in the Mogoin gol area is similar to that of the Erdenet deposit.

Mineralization zones, which are silicified zones associated to oxidized copper minerals, are confirmed around the Mt. Shar Chuluut and in the southern part of the mountain. The alteration zoning in the zone located in the north is formed, from the center outwards, by the zones of quartz or quartz-sericite, the sericite-chlorite and chlorite, respectively. This alteration zoning is similar to the one zoning in the Erdenet ore deposit. The center part of alteration zoning in the southern silicified zone belongs to the quartz-sericite alteration group that includes biotite, topaz and andalusite. There

is no alteration zone in its surroundings. These alteration features indicate the epithermal acidic alteration zone in high sulfidation system that develops at the upper part of the mineralizations in the porphyry copper- molybdenum deposit.

The white silicification at the north zone extends about 1.2km along NS direction and 2km along EW. The white silicification at the south zone, characterized by secondary silicified rocks, consists of a small-scale alteration zone extended about 800m along NS direction and over 1400m along EW. The magnetite zone that belongs to another type of alteration zone is produced by liparite and diorite intrusion. In the white silicification zone, azurite and malachite are present as spotty films. The maximum ore grades in some mineralization points are as low as 0.026 %Cu, 0.001 %Mo, 0.021 %Pb, 0.004 %Zn and 12.72 %Fe. Maximum ore grades in a mineralization point located in the south silicified zone are also as low as 0.009 %Cu, < 0.001 %Mo, 0.006 %Pb and 0.002 %Zn. The ore grades in the magnetite zone are also low.

According to the statistical results of the rock chemical analytical data shown in Fig. 16, three factors related to the mineralization were detected as Factor 2 (Mo: the south silicification zone), Factor 4 (Au-(Ag-Ni): the north silicification zone, the rhyolitic porphyry and the southern part of the area) and Factor 5 (Hg-Cu: the north silicification zone and the south silicification zone). High factor scores were confirmed in the north silicified zone. Analytical values of Mo, Au, Ag, Ni, Hg and Cu were relatively high.

### **Geophysical Survey Results**

According to the airborne survey results in first phase as shown in Fig. 17, part of the low magnetic anomalous zone was detected in the Mogoin gol mineral showing area. High potassic contents were not detected in the northern part; however, they were detected in the southern part of the area.

According to TDIP electric survey results in Phase II as shown in Figs. 18 and 19, remarkable IP anomaly zones were detected in the northern and southern alteration zones. Around the southern alteration zone, a zone of low resistivity with high chargeability was detected above the depth of 200m but no anomaly is recognized at deeper part. Around the northern alteration zone, large scale IP anomaly was detected continuously below 100m depth. According to the plane map of 340m in depth, low resistivity zone under 500m extends about 2.0km along NW-SE direction with a width of about 1.5km. High chargeability over 20mV/V together with low resistivity is distributed continuously from east to west with a width of about 2.0km.

As compared to 2D analysis, the 3-D analysis reflects more consistent results of the subsurface structure because the analysis does not make use of the extreme high resistivity or high chargeability value regarded as artifacts in the 2-D analysis. 3-D analysis is shown in Fig. 19 at the stations 32 to 42 on the line MG-6 and the stations 24 to 36 on the MG-12. 3-D analysis results are more



effective in areas such as in Mogoin gol where the assumptions of two dimensional topography and subsurface structure is unsatisfactory when using 2D analysis. Except for places located around the alteration zones, high chargeability was detected at the center part in the west of the survey area (the stations 30 to 40 on the lines MG-1 to MG-3). Intruded diorite accompanied by magnetite is recognized. This anomaly seems to reflect some mineralization, but with a weak intensity of mineralization as indicated by high resistivity values.

### **Drilling Survey Results**

According to the results of the geophysics and geological survey in Phase II, the white silicified zones in the north and south parts, present high potential for finding host porphyry copper-molybdenum deposits. However, it is highly probable that the ore bodies are located at relatively deep levels. In view of these results, it was recommended to conduct the drills in the white silicification zone in the north part. It was also recommended to extend the IP electric survey area to the eastern side of the Phase II survey area because high chargeability zone increases and continues to the eastern deeper zone. More exploration programs are useful to delineate total IP structure related to the mineralization which could make feasible the construction of a mineralization model in more detail.

During Phase II, the drilling survey included two drill holes sited on the western end and the eastern end of the north silicification zone in Sharchuluut Mountain. Phase III, the drilling of two drill holes continued in the central part of the Mountain. The drilling sites are shown in Fig. 20. Drilling depth was 501.80m in MJME-M1, 500.20m in MJME-M2, 501.00m in MJME-M3 and is 501.30m in MJME-M4. Total drilling length was 2004.30m. A geologic section of the Mogoin gol area constructed from the drilling survey results is shown in Fig. 21.

The drilling cores of MJME-M1 indicated that the geology presents volcanic tuff of Permian to Triassic age, granodiorite of Selenge Complex of Triassic age, diorite porphyry and micro-granodiorite of Triassic to Jurassic age and andesite dyke. The alterations related to mineralization are propylite alteration with pyritization, sericite-chlorite type alteration. The alteration shows intermediate to acidic alteration as the hydrothermal alteration overprinting on the diagenesis. The promising mineralization can be found in the rim of the polymetallic-type mineralization consisting of chalcopyrite-sphalerite-galena or the porphyry copper type mineralization.

The drilling cores of MJME-M2 indicated that the geology consists of silicified and argillized volcanic tuff of Permian to Triassic age, micro-granodiorite of Triassic to Jurassic age and andesite dyke. Reverse fault zones were detected around the depths of 160m and 335m of the drill hole. Upper 160m indicated mainly sericite-chlorite type alteration including potassic feldspar and pyrophyllite. The hydrothermal mineralization is thought to be related because of the temperature of 300 degrees C.

Brecciation and many pyrite ore minerals characterize the mineralization found in the MJME-M2 drilling core. The hydrothermal mineralization shows intermediate to acidic alteration. The mineralization is the active pyritization including sulphide vein with pyrite, chalcopyrite and sphalerite, which is polymetallic type or porphyry copper type. In the silicified tuff from 160m to 335m, the quartz-sericite-chlorite type alteration to the quartz-sericite type alteration is confirmed and accompanies of analcite. The hydrothermal alteration seems to be a type of the intermediate to acidic alteration. Activity of mineralization is high pyritization accompany with chalcopyrite and sphalerite. In the silicified tuff from 335m to 500m, quartz-sericite alteration type alteration and propylite alteration with zeolite minerals of laumontite and stilbite are detected together with many gypsum veins. The alteration is thought to be the alteration that hydrothermal alteration is overprinted on the diagenesis alteration. Ore minerals are pyrite, chalcopyrite and sphalerite in the sulphide veins and azurite in the argillized zones. Alteration and mineralization of the silicified tuff between two fault zones at 160m and 335m shows their upper part and the lower limit.

The drill cores of MJME-M3 identified mainly strong pyrite mineralization such as dissemination and network veinlets in Permian to Triassic strong silicified tuff. The geology consists of Permian to Triassic tuff, fine grained, granodiorite dyke and andesite dyke. Faults zones were detected at 250m, 330m, 400m and 440m. In the lower part of the drilling cores, the drilling cores were found frequently crushed and sheared. According to the results of X-ray diffraction analysis, from 19m to 140m, silicified tuff found main alteration minerals, including mainly quartz, plagioclase (albite), sericite, alunite, jarosite, rutile. Mineral assemblage mainly consists of quartz-sericite-alunite- jarosite alteration or quartz-sericite alteration. Other minerals are kaolinite. Secondary enrichment includes jarosite mineral. From 160m~300m, silicified tuff with alteration minerals mainly of quartz, sericite, pyrite, rutile and consisting mainly of alterations of quartz-sericite-pyrite. Other minerals are kaolinite. From 320m to 460m, silicified tuff includes mainly alteration minerals of quartz, plagioclase (albite), chlorite, sericite, laumontite, pyrite, and mainly consisting of quartz-chlorite-sericite-pyrite alteration. Other minerals are laumontite, epi-stilbite, rutile and kaolinite. From 480m to 500m, silicified tuff presents mainly alteration minerals of quartz, potassic feldspar, sericite, pyrite and consists mainly of quartz-potassic feldspar-sericite-pyrite alteration in mineral assemblage. These mineral assemblages are related to acidic alteration type. Microscopic observation detected pyrite, goethite, hematite and magnetite. Analytical ore assay results of silicified tuff indicated that range of ore assay analysis show less than Cu 0.001% to Cu 0.660%, Pb 0.002% to Pb 0.033 %, Zn 0.001 % to Zn 0.120%, S 0.12% to S 10.48%. Average values of assay grade are Cu 0.009%, Pb 0.008 % and Zn 0.010%.

The drill cores of MJME-M4 identified mainly the strong pyrite mineralization such as dissemination and network veinlets in Permian to Triassic strong silicified tuff. The geology consists of Permian to Triassic tuff, fine grained, granodiorite dyke and andesite dyke. Faults zones were

detected at 160m and 335m, which are thought to be reverse faults. X-ray diffraction analysis results of silicified tuff detected altered minerals of quartz, sericite, kaolinite, pyrophyllite, alunite and pyrite and mineral assemblages were mainly quartz-sericite-pyrophyllite-alunite-pyrite. Other minerals are plagioclase (albite), smectite and rutile. This alteration minerals show acidic alteration type to phyllic alteration type. From 80m to 140m, silicified tuff included quartz, sericite, alunite and pyrite and including mainly quartz-sericite-pyrite mineral. Other minerals are kaolinite, calcite and rutile. Alteration minerals show phyllic alteration type. From 160m to 360m, silicified tuff is occurred, alteration is relatively weak and includes quartz, plagioclase (albite), potassic feldspar, chlorite, sericite and pyrite, showing mainly quartz-albite-potassic feldspar-chlorite-sericite-pyrite mineral assemblage. Other minerals are laumontite, calcite and rutile. From 380m to 500m, silicified tuff includes quartz, sericite, kaolinite, alunite, pyrite and rutile, and associated mainly to quartz-sericite-kaolinite alunite-pyrite-rutile mineral assemblage. Other minerals are potassic feldspar and halite. This is phyllic alteration type. Microscopic observation identified ore minerals of pyrite, goethite, hematite, limonite, magnetite, chalcopyrite and sphalerite. Ore assay in the silicified tuff show that ore assay grade are less than Cu 0.001% to Cu0.370%, less than Pb 0.001% to Pb0.012%, Zn 0.001% to Zn 0.320% and S 0.003% to S 10.20%. Average values of ore assay are Cu 0.006%, Pb 0.004% and Zn 0.009%.

### **Discussion**

Based on the results of drilling survey in the white silicified zone of the Sharchuluut mountain, the alteration mineral assemblages consist of quartz-sericite-alunite-jarosite or quartz-sericite alteration, quartz-sericite-pyrite alteration, quartz-chlorite-sericite-laumontite-pyrite alteration and quartz-K-feldspar-sericite-pyrite alteration from upper part to the lower part of drilling hole. Bottom of drillhole consists of alteration with K-feldspar. The genesis temperature is moderate temperature (350°C to 150°C). Pyrophyllite mineral was detected from drilling cores of MJME-M4 and the genesis temperature of pyrophyllite is more than 250°C. The alteration consists partly of pyrophyllite alteration zone of acidic alteration. Generally speaking, these minerals occurred from middle to upper part of the porphyry copper type mineralization structure system.

According to the results of the fluid inclusion test, the homogenization temperatures are 147 degrees C to 165 degree C in the MJME-M1 drilling core and 173 degrees C to 188 degree C in the MJME-M2 drilling core, which are relatively low. The salinity values are NaCl 3.9 % to NaCl 17.3 % in the MJME-M1 and NaCl 1.8 % in the MJME-M2. Maximum homogenization temperature in all data was 191 degrees C. On the other hand, salinity values are less than NaCl 10 % in most data, but show high values of NaCl 28.9 % in a sample from MJME-M1 that included liquid CO<sub>2</sub> inclusions.

Based on the results of surveys, drilling survey with four drillholes has been conducted on

phase II and III exploration program. The drilling holes detected very strong and wide pyritization in strong silicified rock consisting of tuff and granitic rocks; however, copper mineralization was not be detected. Based on the distribution of alteration minerals in the drilling cores, porphyry copper mineralization occurred in the deeper part from surface.

No further exploration work in the future will be recommended for the area.



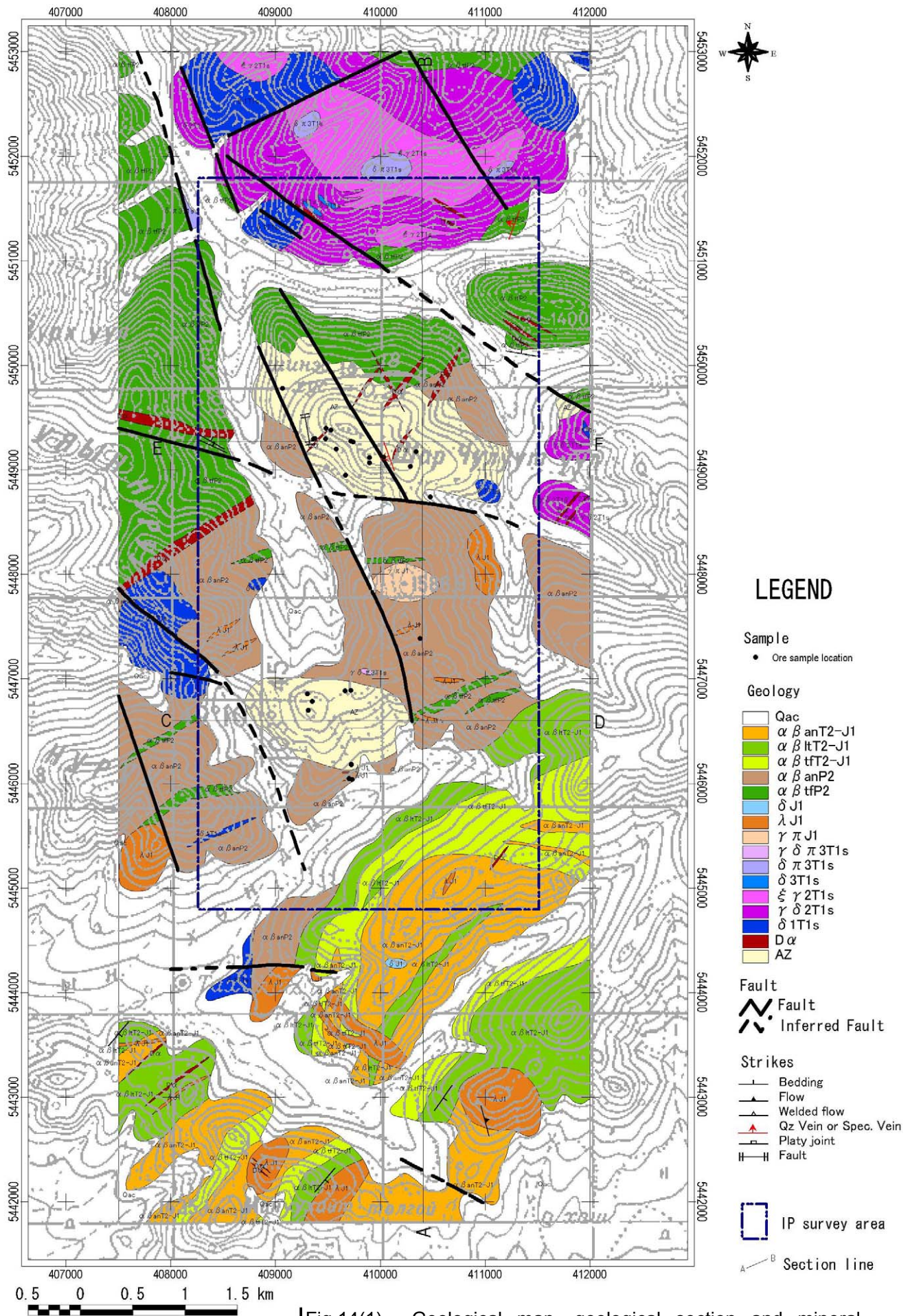


[Fig.14(1) Geological map, geological section and mineral showing of the Mogoin gol area



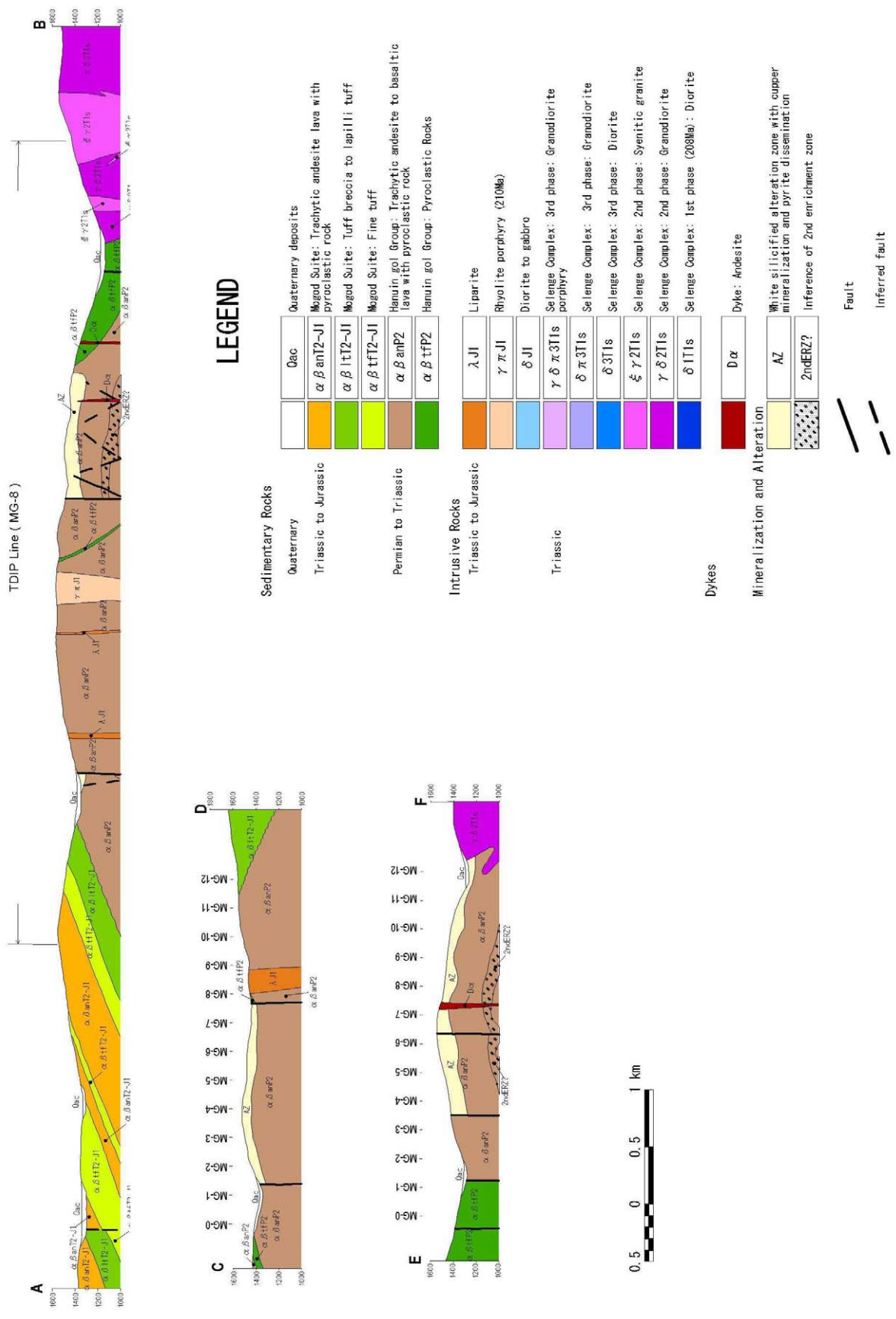


Fig.14(2) Geological map, geological section and mineral showing of the Mogoin gol area



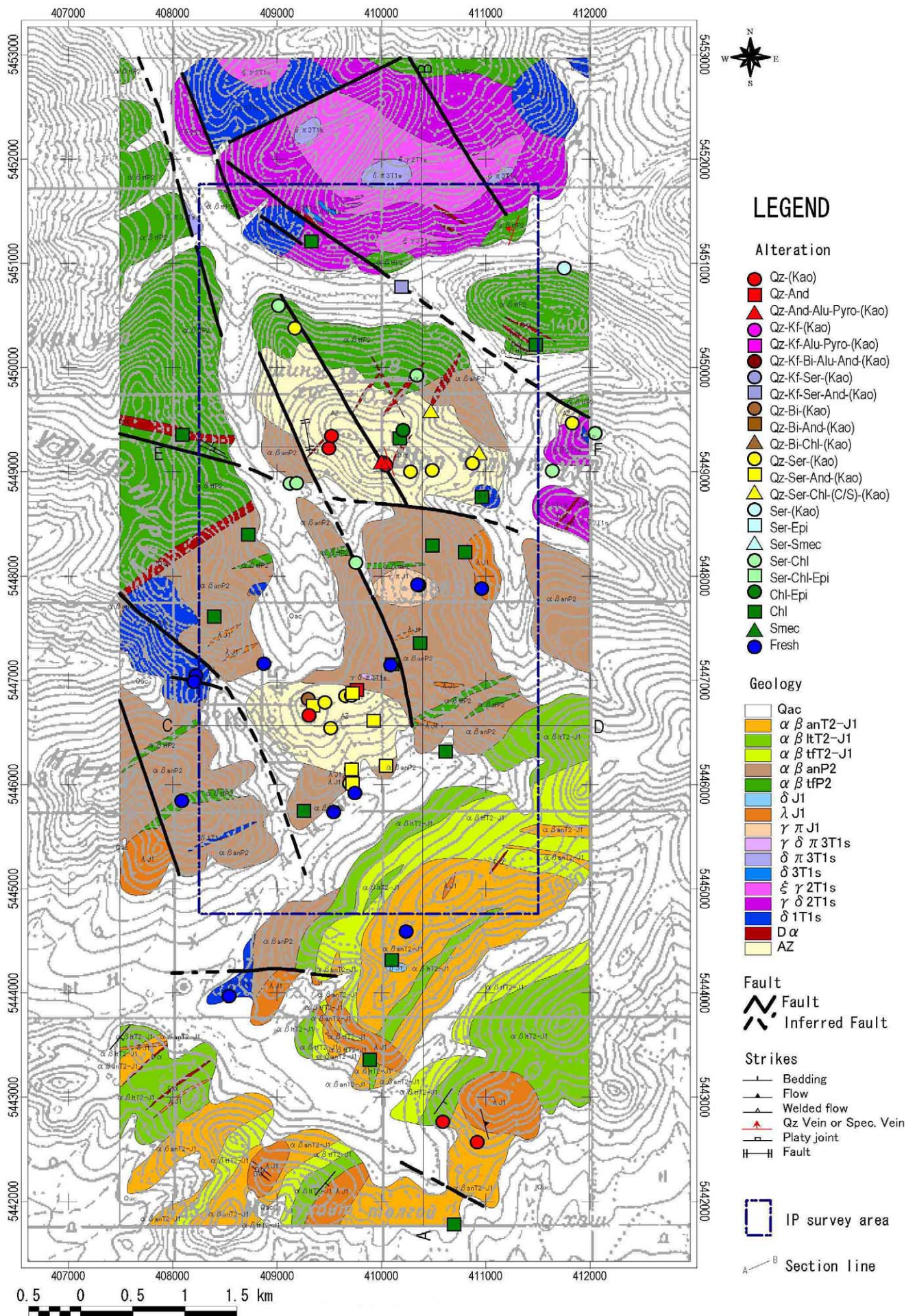


Fig.15 Distribution map of alteration mineral assemblages in the Mogoin gol area



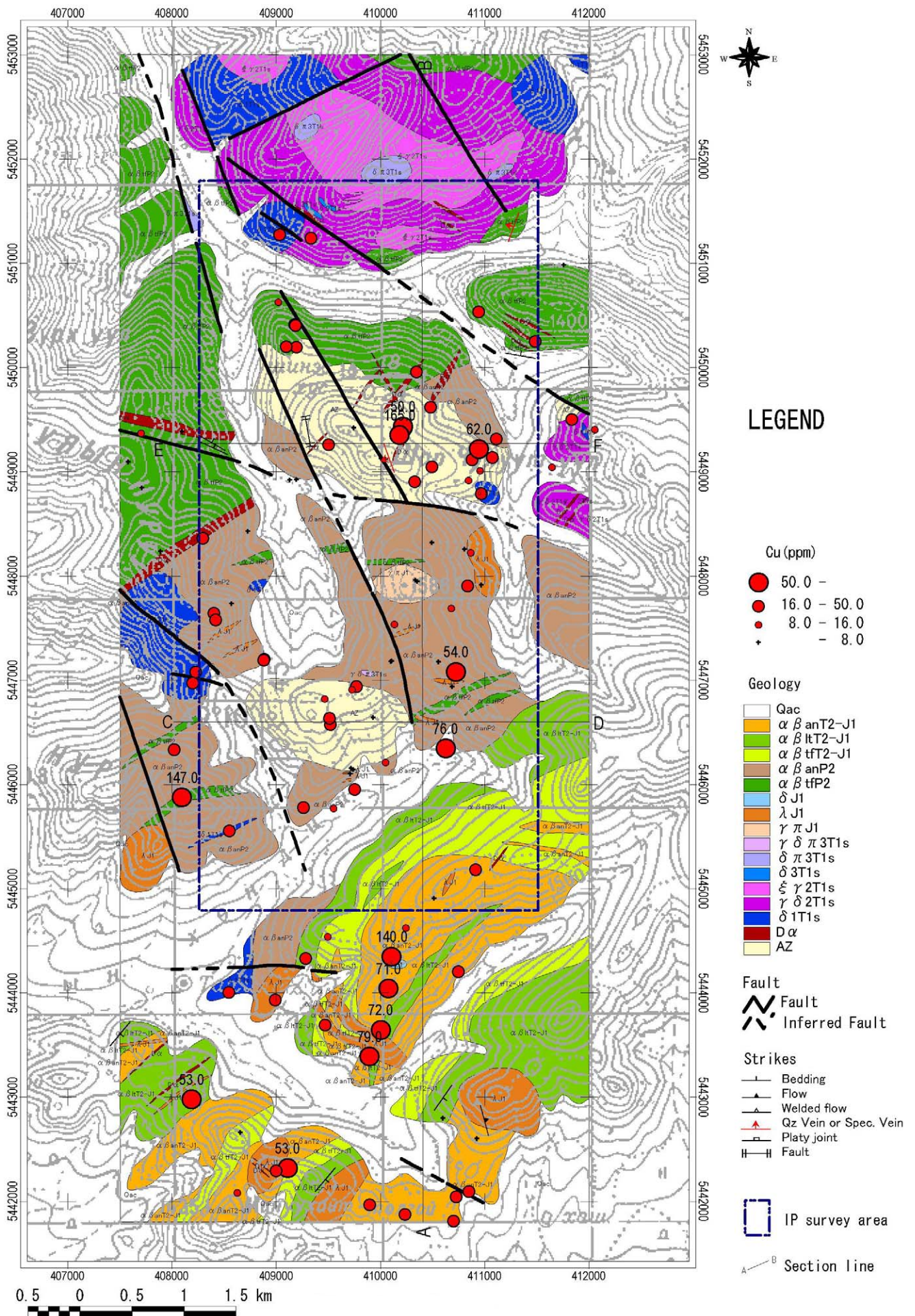


Fig.16 Distribution map of Cu anomaly in the Mogoin gol area



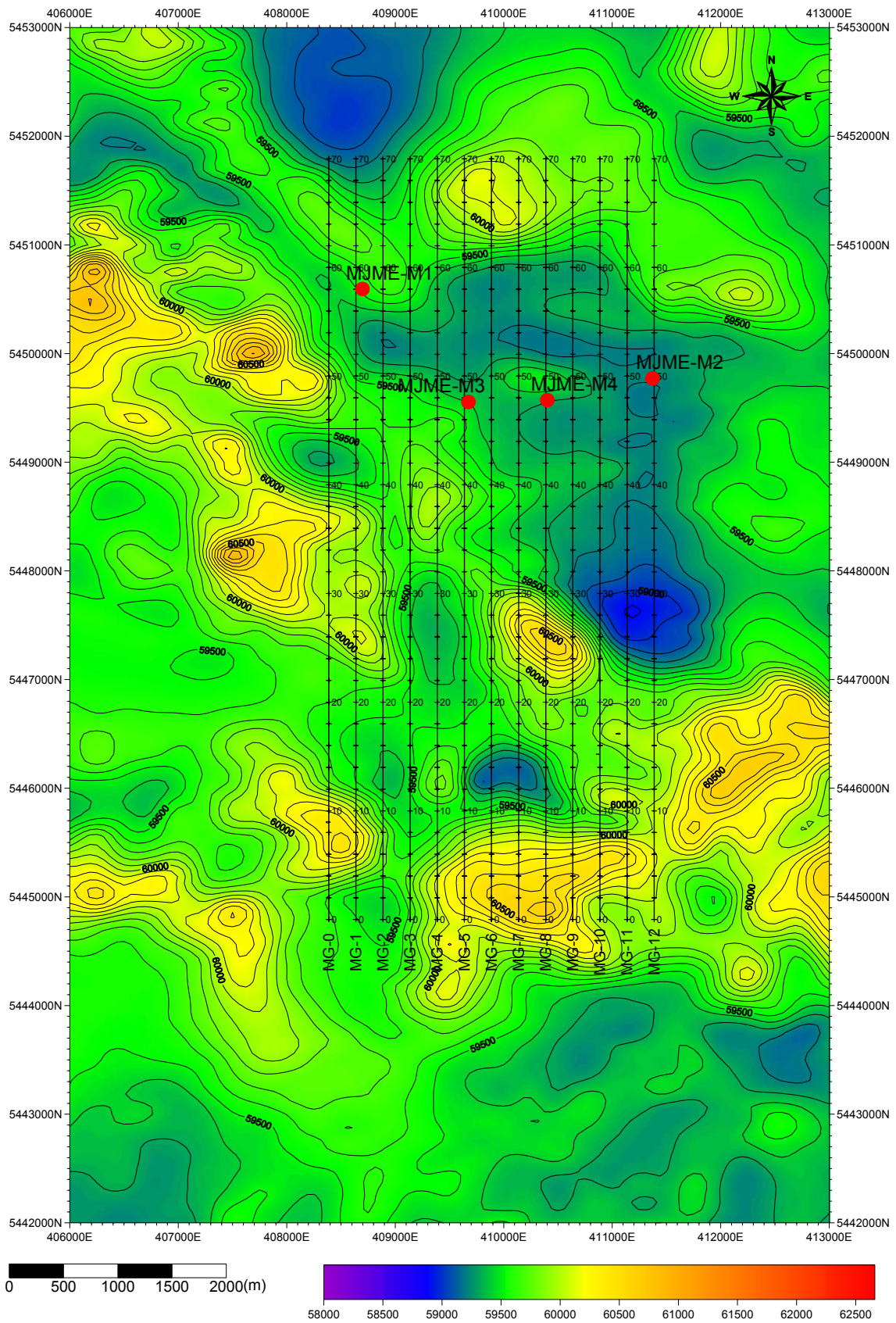


Fig. 17 Magnetic anomaly map (RTP) in Mogoin gol area.

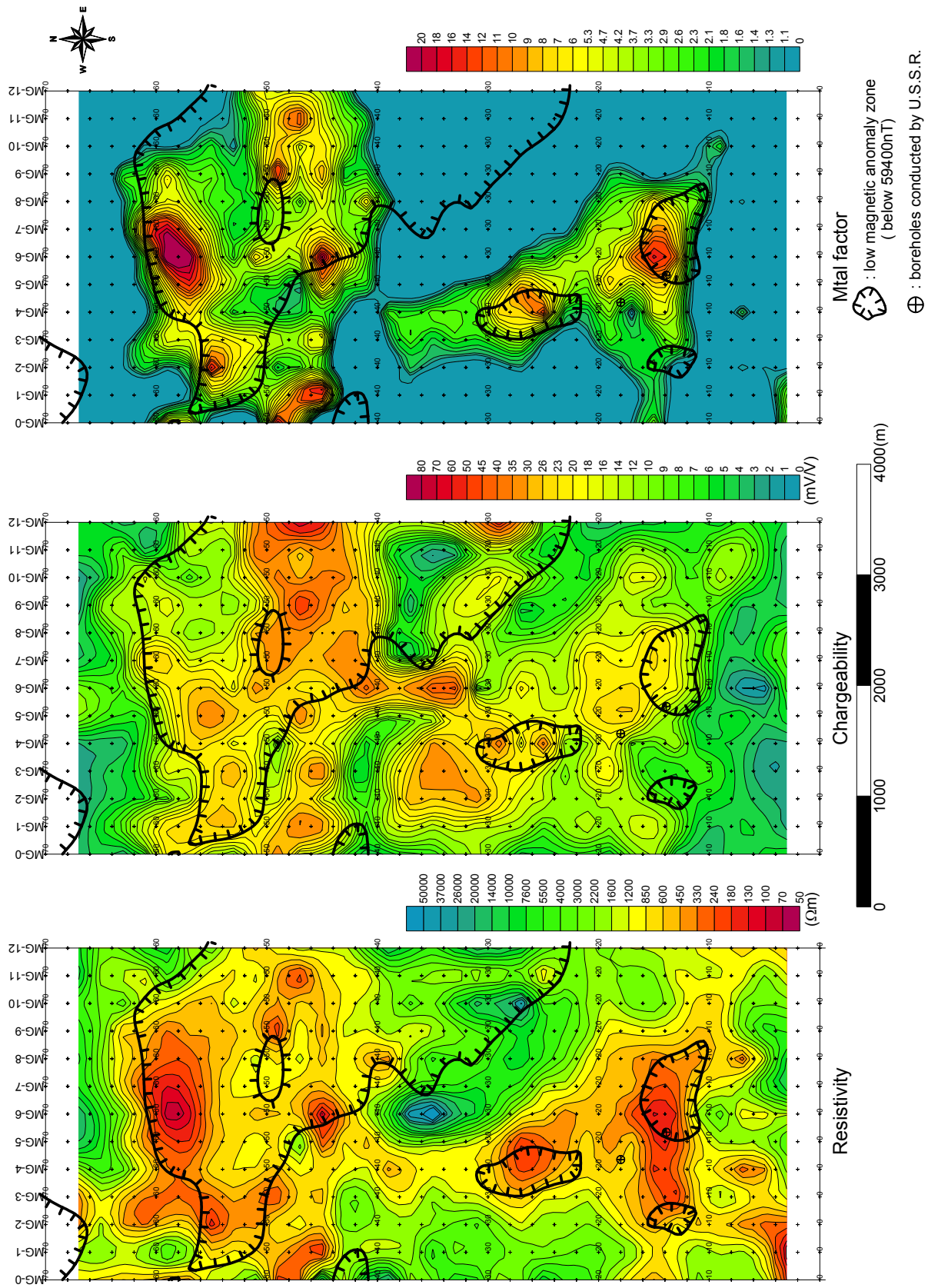


Fig.18 2D analysis plane map at the depth of 170m in Mogoin gol area



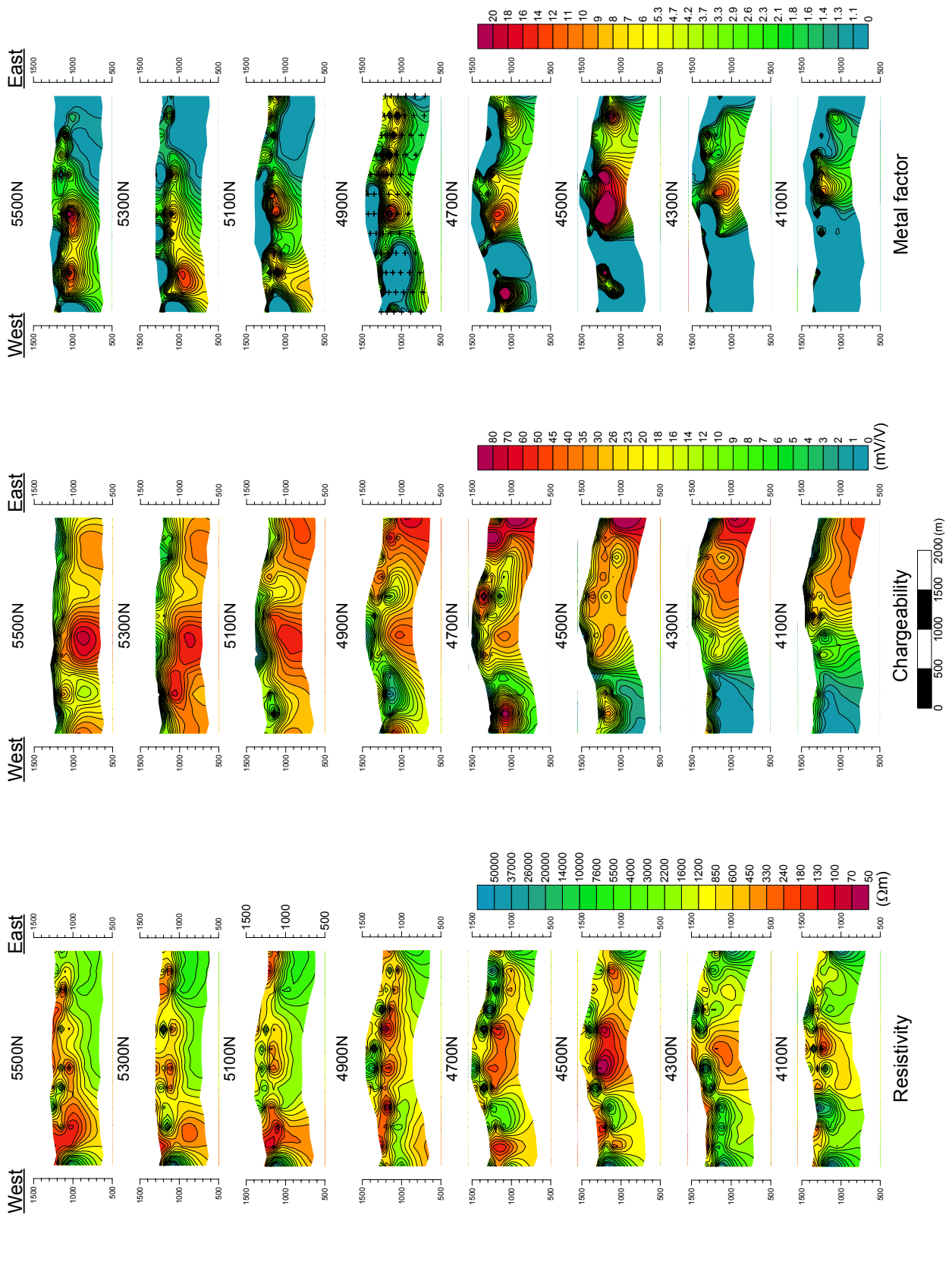


Fig. 19 3D analysis section at the northern part of Mogoin gol area (4100N – 5500N)



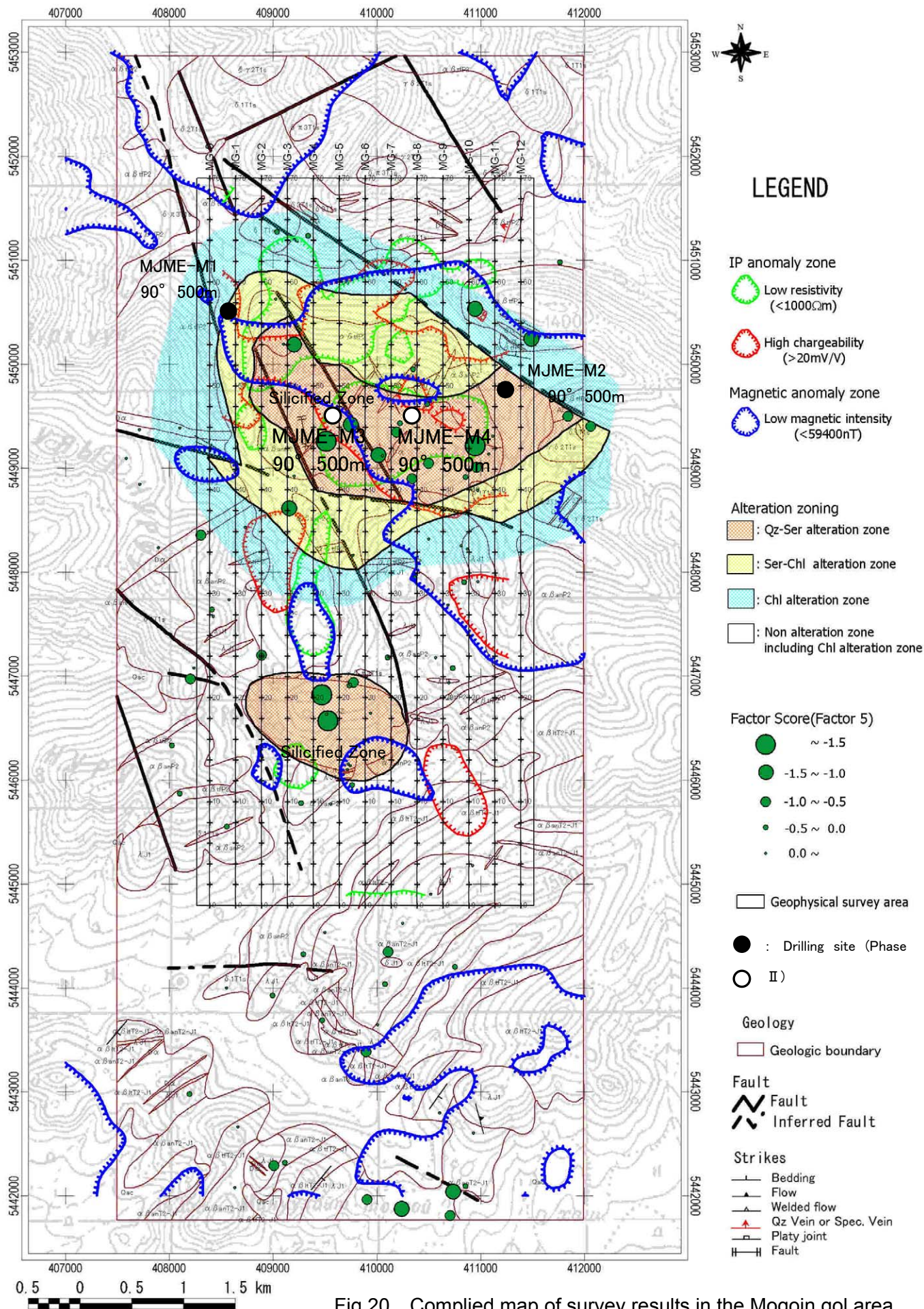


Fig.20 Compiled map of survey results in the Mogoin gol area

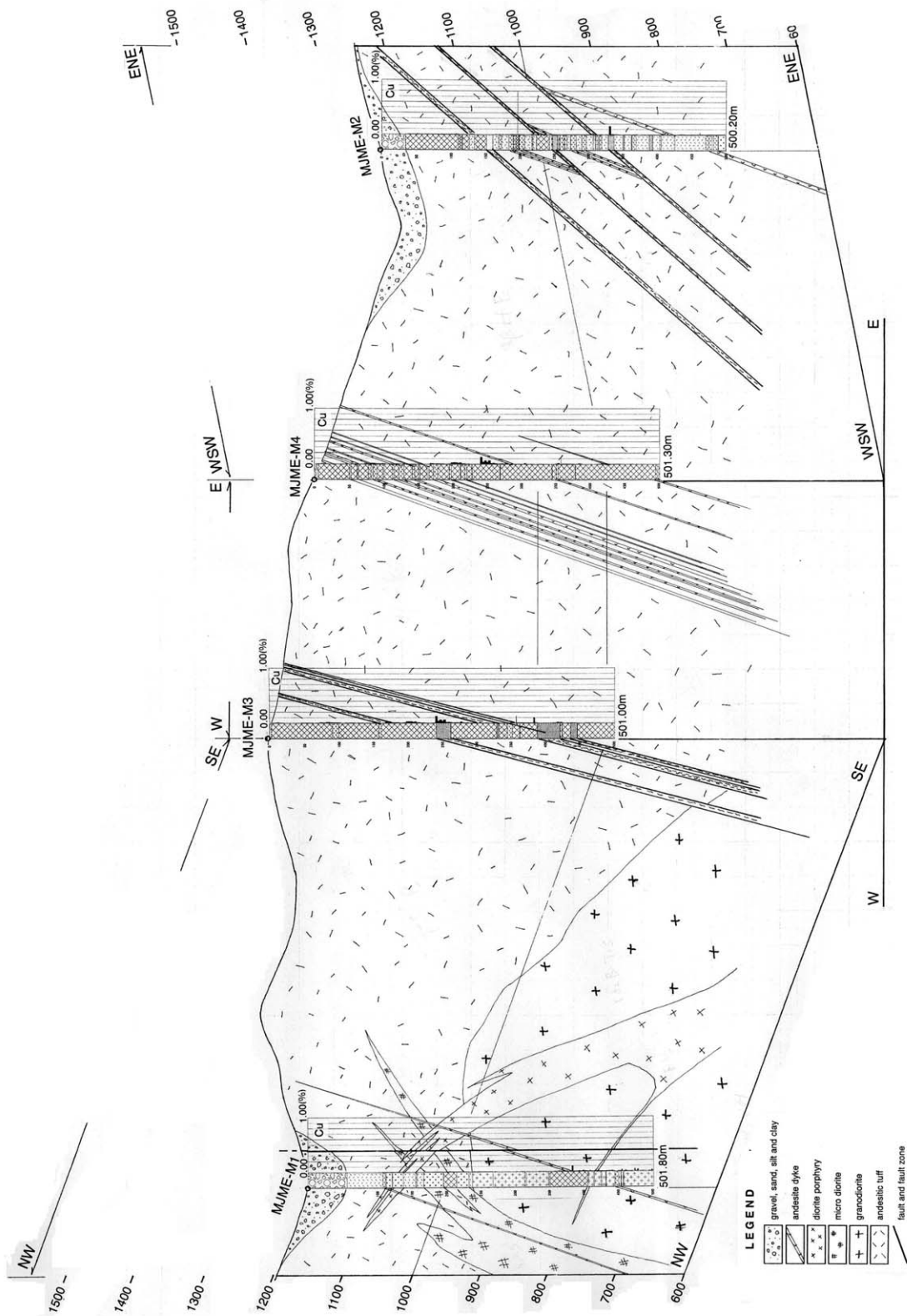


Fig.21 Geologic cross sections and panel diagram by the drilling survey results in the Mogoin gol area.

### **(3) Zuukhiin gol Area**

#### **Introduction**

The area is located 25 km northeast from Erdenet city and at an approximate sea level elevation between 1,100m to 1,400m. The topography shows gently undulating hills. The vegetation in the area is composed of coniferous forests and tall grasses in the hill and valley and low grasses along the streams.

Zuukhiin gol mineralization was discovered in 1966 through a cooperation project between Czech-Slovakia and Mongolia in 1966. The geological survey, geophysical survey and drilling survey that were carried out indicated low potential for porphyry Cu-Mo mineralization.

From 1978 to 1980, the geological survey, the ground magnetic survey, IP electric survey and geobiochemical survey were performed in a wide area around the Erdenet Mine area including the Zuukhiin gol area. According to the results obtained from these surveys, lead minerals were detected in the area of 4.2km<sup>2</sup>. Ore assays were Pb 0.07% to Pb 0.5% and Mo 0.0002% to Mo 0.03%.

From 1981 to 1985, a systematic drilling survey was carried out in the area. Previous drilling survey showed that the analytical values of ore assay results were Cu: 0.006 to 0.2 %, Mo: 0.00 to 0.003%. Drilling data from the Geological Information Center indicated analytical values of Cu: 0.11% to .17% and Mo: 0.003% to 0.007%.

#### **Geological Survey Results**

As shown in Fig. 22, the results of the Phase I survey indicates that the geology of the area presents Permian volcanic rocks, Triassic to Jurassic volcanic rocks and Triassic granites. Fault structures are developed in the area along the NE-SW, WNW-ESE and EW directions. Granitic bodies are elongated north to south. The alteration in the mineralized zone of the area, which is composed of sericite-chlorite type and chlorite type, indicated propylitic alteration. Especially, the center of the Zuukhiin gol mineralized zone as seen from the trench, presents alteration of sericite-chlorite type. The alteration related to the mineralization indicates the same alteration mineral assemblage as the Erdenet mine area. The results of rock chemical analysis indicated that values of more than Cu 50 ppm with Cu 11,740 ppm in maximum are concentrated in the center of the Zuukhiin gol mineralized zone.

In Phase III survey, the geological survey was mainly conducted in the eastern part of the known mineralized area where exploration works had been conducted in the 1980s. Outcrops of quartz veins were observed around rhyolite intrusion and oxide copper minerals were also observed in granodiorite. Because of gentle topography and a few of outcrops, soil sampling at 250m interval was conducted along the hill. Soil geochemistry detected geochemical anomaly zones with more than Cu 100ppm, with a trending that extends from east to west in the southern part of the known



mineralized zone. Oxide copper minerals are observed in outcrops of granodiorite in grand size, but copper minerals are found filled only in fractures. It is concluded that the copper mineralization is epigenetic after emplacement of granodiorite observed in grand. Spotted oxide minerals are seen occurred in altered andesite. Ore assay indicated a maximum of Cu 1.48%.

Therefore, it is considered that porphyry type copper-molybdenum ore deposits probably existed in the Zuukhiin gol area. According to previous survey results, the mineralization is considered to be extended more than 300m in depth.

### **Geophysical Survey Results**

According to the previous survey data, the mineralization is inferred with an extension up to 300 m in depth. The TMI reduced to the pole map and the radiometric potassium count maps of the area are shown in Fig. 23. In the area, a part of the low magnetic anomalous zone could be seen but high potassic content was not detected.

According to resistivity analysis of TDIP electric survey in Phase III program, the low resistivity zone is distributed within an area underlain by Quaternary sediments, whereas the high resistivity is distributed in the mountain area. Low resistivity is conspicuously distributed in the ridge around the Stations 16 to 20 on the lines F and K. Below the depth of 150m, low resistivity can not be further detected due to the influence of the Quaternary sediments. At the depth from 200m to 400m, low resistivity zone extends from the Station 10 on the line L to the station 20 on the line J along the direction of WSW-ENE.

The analyzed chargeability value ranges between 0.4 ~ 70.6mV/V with an average of 14.3mV/V. High chargeability zone is distributed widely in the western part of the area. The extension of this high chargeability zone becomes broader at the deeper part with high chargeability values 20mV/V that extends about 4km along E-W, and 2km along N-S direction at the depth of 200m. It seems that the high chargeability zone consists three parts. According to the plane map at the depth of 200m, high chargeability zones over 30mV/V are recognized around the Stations 10 to 18 on the lines F to I, the Stations 20 to 28 on the lines G to F and the Stations 12 to 18 on the lines L to K. The low resistivity zone above mentioned is surrounded by these three high chargeability zones. There is a positive correlation between the grade of sulfur and chargeability, and it is considered that high chargeability reflects large amount of sulfide in this area. The presence of metallic minerals such as iron and copper, are thought to decrease the resistivity, but there is no remarkable correlation between the grade of iron or copper and resistivity.

### **Drilling Survey Results**

Survey results that lead to decision to conduct the drilling survey in the Phase III in Zuukhiin gol area can be mentioned as follows:



- Analysis of existing data previous to Phase I. Previous geochemical surveys as well as geophysical surveys, such as ground magnetic and IP electrical survey, were able to detect anomalies.
- Low magnetic zones were detected during the aeromagnetic survey of Phase I
- The geological survey results of Phase I, detected on the ground copper mineralization zones including malachite and chalcopyrite as well as rock geochemical anomalies of Cu, Pb and Zn.
- In Phase III, soil geochemical anomalies of more than Cu 200ppm and Zn 100ppm to Zn 200ppm were found concentrated in the area. High ore grade values of Cu, Zn, and Ag were found distributed along a east to west trending in the central part of the area.
- Also in Phase III, TDIP geophysical survey detected very high IP anomalies in the area

Drilling survey with three drill holes was conducted in the area. The drill hole locations are shown in Fig. 28. Depths of holes were 502.10m in MJME-Z1 hole, 500.45m in MJME-Z2 hole and 502.0m in MJME-Z1 hole, and total length of drillholes was 1504.55m. The schematic geologic section was made as shown in Fig. 29.

The geology of MJME-Z1 drilling cores consists mainly of Triassic granodiorite, andesite dykes and Quaternary deposits. Main alterations were chloritization, silicification and sericitization. Mineralizations were disseminations of chalcopyrite, sulphide veinlets of chalcopyrite and bornite and veinlets of chalcopyrite and molybdenite. Alteration mineral assemblage consists mainly of chlorite-sericite-calcite-pyrite, and propylite to phyllic alterations. Other minerals consist of kaolinite, pyrophyllite and alunite. Ore minerals in granodiorite consist of pyrite, goethite, hematite, limonite, magnetite, chalcopyrite, malachite, sphalerite and galena. Ore assay results indicated Cu values in the range from < Cu 0.008% to Cu 0.784%, with an average value of Cu 0.086%. Ranges of ore assay were Pb 0.003% to Pb 2.270 %, Zn 0.003% to Zn 0.828%. Maximum values of other elements were Au 80.8g/t and S 4.97%.

The geology of MJME-Z2 drilling cores consists mainly of Triassic granodiorite, fine-grained diorite to gabbro, medium grained diorite, rhyolite dyke, andesite dykes and Quaternary deposits. Alteration consists of weak chloritization, silicified veins and sericitization around the silicified veins. Mineralizations were dissemination of chalcopyrite, sulphide veinlets of chalcopyrite and bornite and veinlets to dissemination of chalcopyrite and molybdenite. Alteration mineral assemblage consists mainly of quartz-sericite-chlorite. Other alteration minerals were epidote, secondary biotite, calcite and pyrite. These minerals are observed in the phyllic alteration and propylitic alteration. Ore minerals consist mainly of pyrite, goethite, hematite, magnetite, chalcopyrite, chalcocite, sphalerite and molybdenite. Paragenesis of chalcopyrite and sphalerite can be observed in the entire core.

The geology of MJME-Z2 drilling cores consists mainly of Triassic granodiorite, andesite dykes and Quaternary deposits. Alterations consist of chloritization, epidotization, carbonatization,

sericitization and silicified vein. Mineralizations are dissemination of chalcopyrite, sulphide veinlets with chalcopyrite and veinlets with chalcopyrite and molybdenite. Analytical results by X-ray diffraction analysis indicated that the alteration minerals consist mainly of quartz, plagioclase (albite), potassic feldspar, hornblende, biotite, chlorite-sericite, calcite, dolomite and pyrite and rarely of talc, laumontite. Dolomite mineral was detected at depths deeper than 420m. Mineralization and alteration are generally weak and consisting mainly of sericite-chlorite in mineral assemblage. Mineralization consists mainly of chalcopyrite including pyrite and formed porphyry type chalcopyrite ore deposits type. The hydrothermal activity is approximately neutrality to acidic alteration. Ore minerals were pyrite, goethite, magnetite, chalcopyrite and sphalerite. Paragenesis of chalcopyrite and sphalerite was seen in the whole cores. Ore assay values were less than Cu 0.005% to Cu 0.455%, and copper average values of Cu 0.039%. Other assay values were less than Pb 0.01% to Pb 0.375% and Zn 0.003% to Zn in range. Gold value is Au 0.07g/t and Sulfur is S 2.39%.

Homogeneous temperatures of fluid inclusions in quartz veins were 167°C to 197°C in MJME-Z1 core, 187°C to 267°C in MJME-Z2 core and 160°C to 237°C in MJME-Z3. The temperatures show a tendency to increase toward MJME-Z2. On the other hand, salinities were estimated from 1.2‰ to 12.0‰ in MJME-Z1 cores, 1.3‰ to 10.1‰ in MJME-Z2 cores and 1.9‰ to 2.9‰ in MJME-Z3 cores. These salinity values show a tendency to increase toward western side.

The drilling survey in the Zuukhiin gol area results shows that mineralization is porphyry type copper ore deposits.

## **Discussion**

Copper mineralization in the Zuukhiin gol area was discussed as follows:

These mineral assemblages consist of phyllic alteration to propylitic alteration of porphyry copper type mineralization system. At 163m depth in MJME-Z1 hole, pyrophyllite mineral was detected and the genesis temperature of pyrophyllite was estimated in more than 250°C. At 160m depth of MJME-Z2 hole, abundant biotite minerals were detected. At 260m in depth, quartz index of biotite mineral was 10 in maximum. If this biotite is secondary biotite, the genesis temperature is more than 300°C. The detection of K-feldspar implies that the alteration is probably related to potassic alteration zone in parts. Alteration of MJME-Z3 drilling cores consists of quartz-chlorite-pyrite-calcite and quartz-chlorite-sericite-pyrite and related to propylite alteration. In the deeper part of MJME-Z3 hole, the detection of dolomite minerals suggests that the alteration is caused probably by neutral hydrothermal alteration. The alteration in the Zuukhiin gol area indicated that phyllic alteration to propylitic alteration appeared widely in the granitic rocks and high temperature water passed along the fractures in the granitic rock in parts.

The analytical results of homogenization temperature of fluid inclusion in quartz vein show 160°C to 267°C in average. The temperature of MJME-Z2 hole is relatively high, 231°C to 312°C at 428m depth and 267°C in average. The salinity in the three holes is 1.21% to 12.00%. The salinity is relatively high, 12.00% at 263m depth of MJME-Z1 hole and 10.10% at 248m depth of MJME-Z2 hole.

Homogeneous temperatures of fluid inclusions in quartz veins were 167°C to 197°C in MJME-Z1 core, 187°C to 267°C in MJME-Z2 core and 160°C to 237°C in MJME-Z3. The temperatures show a tendency to increase toward MJME-Z2. On the other hand, salinities were ranging from 1.2% to 12.0% in MJME-Z1 cores, 1.3% to 10.1% in MJME-Z2 cores and 1.9% to 2.9% in MJME-Z3 cores. The salinities show a tendency to increase toward western side. It is considered that original hydrothermal fluid presented high temperature and high salinity and that temperature and salinity of fluid became probably low in the diffusion process.

As shown in figure of  $\delta^{18}\text{O}$  vs.  $\delta\text{D}$  diagram by Taylor(1979), analytical data of oxygen and hydrogen isotopes in sericite minerals collected from drilling cores in Zuukhiin gol area was plotted near the kaolinite line and marked under the distribution range of the Climax ore deposit shown in isotope figure of porphyry copper deposits.

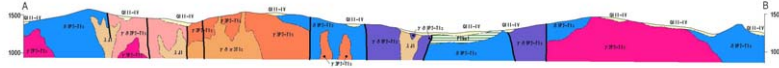
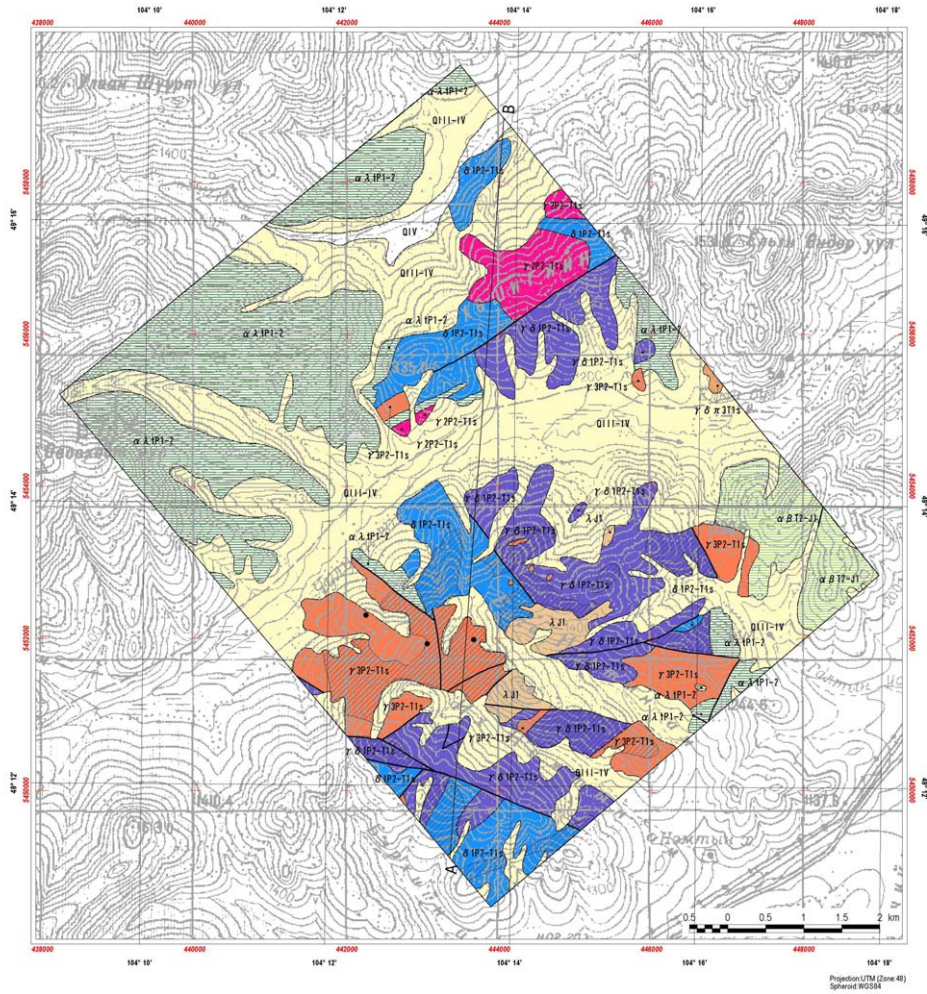
Based on the fact that quartz veins in granodiorite and sericite minerals in the host rock required silicification and sericitization around quartz veins in materials made at the same time, isotope ratio values of ore solution can be calculated from values of oxygen and hydrogen isotopes by using the homogeneous temperature of fluid inclusion in quartz veins. Also, since isotope values of oxygen and hydrogen estimated by temperature correction were marked in the central range of epithermal deposits in the western part of Nevada, primary magma water is suggested to receive the influence of meteoric water which is approximately  $\delta\text{D} = -150\text{‰}$  and which resulted probably from highland water.

Re/Os isotope dating analysis using a sample with molybdenum mineralization was conducted. As shown Fig. 12, the age of Re/Os dating was  $240.60 \pm 0.8\text{Ma}$ . The Re-Os age of the Erdenet Mine is 10Ma in difference and older than the Zuukhiin gol area.

The Re/Os dating ages, the K-Ar dating ages and the results of natural remanent magnetization were shown in Fig. 12. The K-Ar dating ages of granodiorite and syenite porphyry show  $224.8 \pm 5.9\text{Ma}$  and  $208.0 \pm 5.4\text{Ma}$  and are younger than the Re/Os dating ages of molybdenite. The process indicates probably that original magma melting made firstly, that molybdenite was crystallized during rising or emplacing of magma in next and that magma completed finally to emplace in situ.

Based on the above results, the drilling survey in the Zuukhiin gol area shows that the mineralization is porphyry type copper ore deposits. It is recommended to carry out further exploration works in future to clarify the extension of the copper mineralization toward southwestern

area including its geological and mineralogical features. Copper grades estimated in drill hole number MJME-Z2 show increasing values from north toward southwest. Homogeneous temperatures of fluid inclusions also show increasing values toward southwest from north. It is expected that extension of copper mineralization toward southwest will be clarified by detailed TDIP geophysical survey and drilling survey in the future.



**LEGEND**

|                          |  |
|--------------------------|--|
| <b>Sedimentary Rocks</b> |  |
| Quaternary               | QIV Recent sediments: alluvial deposits: gravels, sand, silt and clay  |
|                          | QII-IV Upper - Recent sediments: alluvial and colluvial deposits: gravels, sand, silt and clay                           |
| Jurassic                 | J1 Mogod suite: volcanic rocks and dykes: microdiorite, andesite, porphyry, lipante, dacite and tuffaceous conglomerate. |
| Triassic to Jurassic     | T3-J2 Mogod suite: volcanic rock and dyke of lipante, dacite, andesite and their tuff.                                   |
| Permian                  | P1-2 Lower Hanaigol Formation: volcanic rock and dyke of basalt, andesite, dacite and lipante.                           |
| <b>Plutonic Rocks</b>    |  |
| Triassic                 | S1 Selenge Complex: Lower Triassic: fine grained granodiorite porphyry.  |
| Permian to Triassic      | S2 Selenge Complex: granite.   |
|                          | S3 Selenge Complex: granite.   |
|                          | S4 Selenge Complex: granodiorite.  |
|                          | S5 Selenge Complex: diorite.   |
| <b>Structure</b>         |  |
|                          | Fault  |
| <b>Alteration</b>        |  |
|                          | Alteration Zone: silicification, sericitization, chloritization  |
| <b>Mineralization</b>    |  |
|                          | Mineral showing  |
|                          | Section line   |

Fig. 22 Geological map, geologic section and mineral showings in the Zuukhiin gol area.



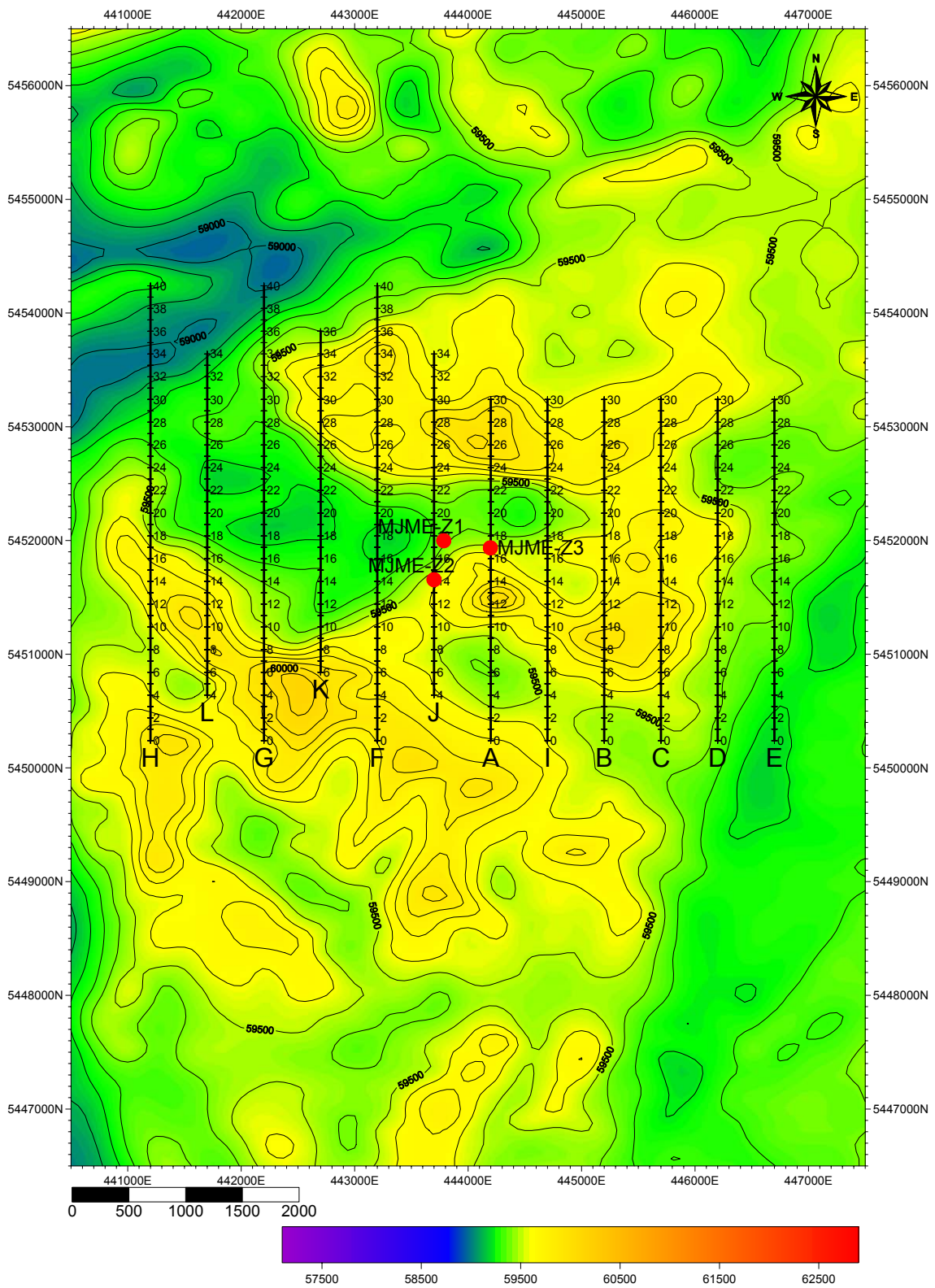


Fig. 23 Magnetic anomaly map (RTP) in Zuukhin gol area

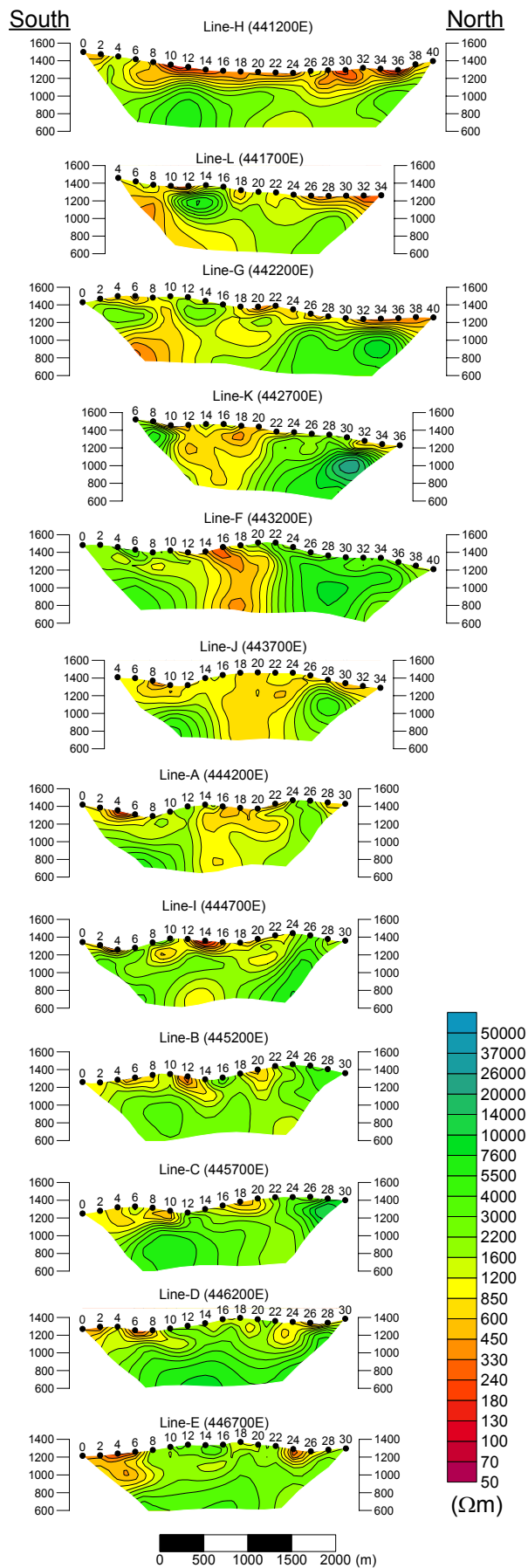


Fig.24 2D analysis sections for resistivity in the Zuukhiin gol area.

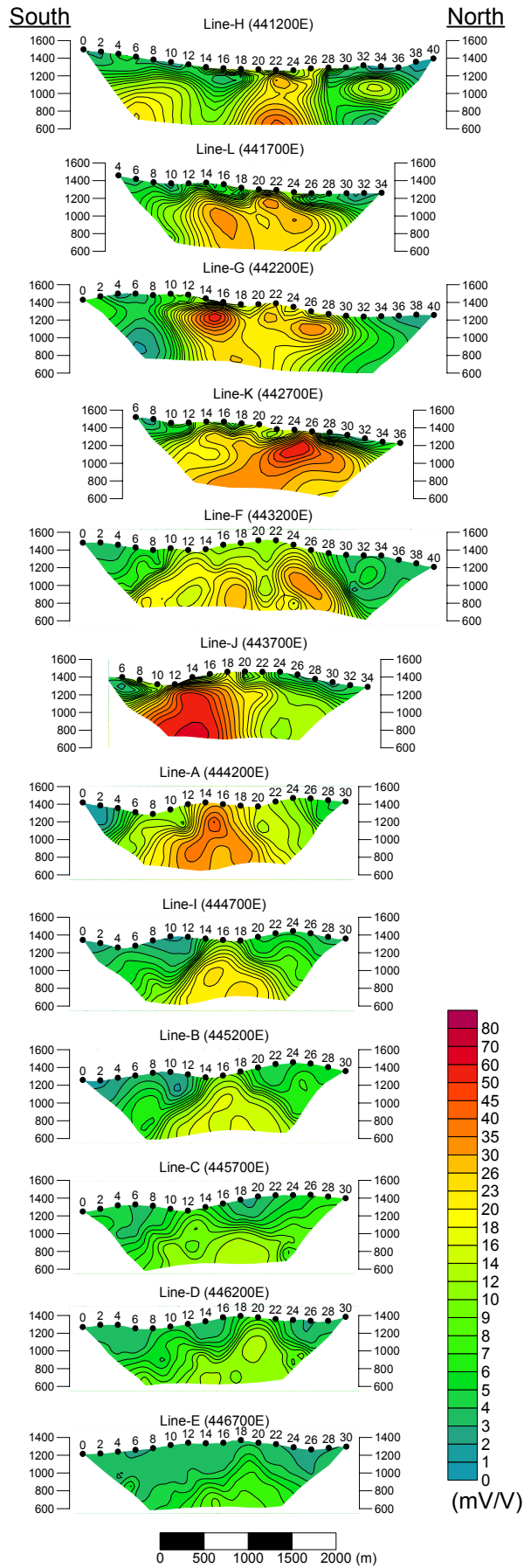


Fig.25 2D analysis sections for chargeability in the Zuukhiin gol area.

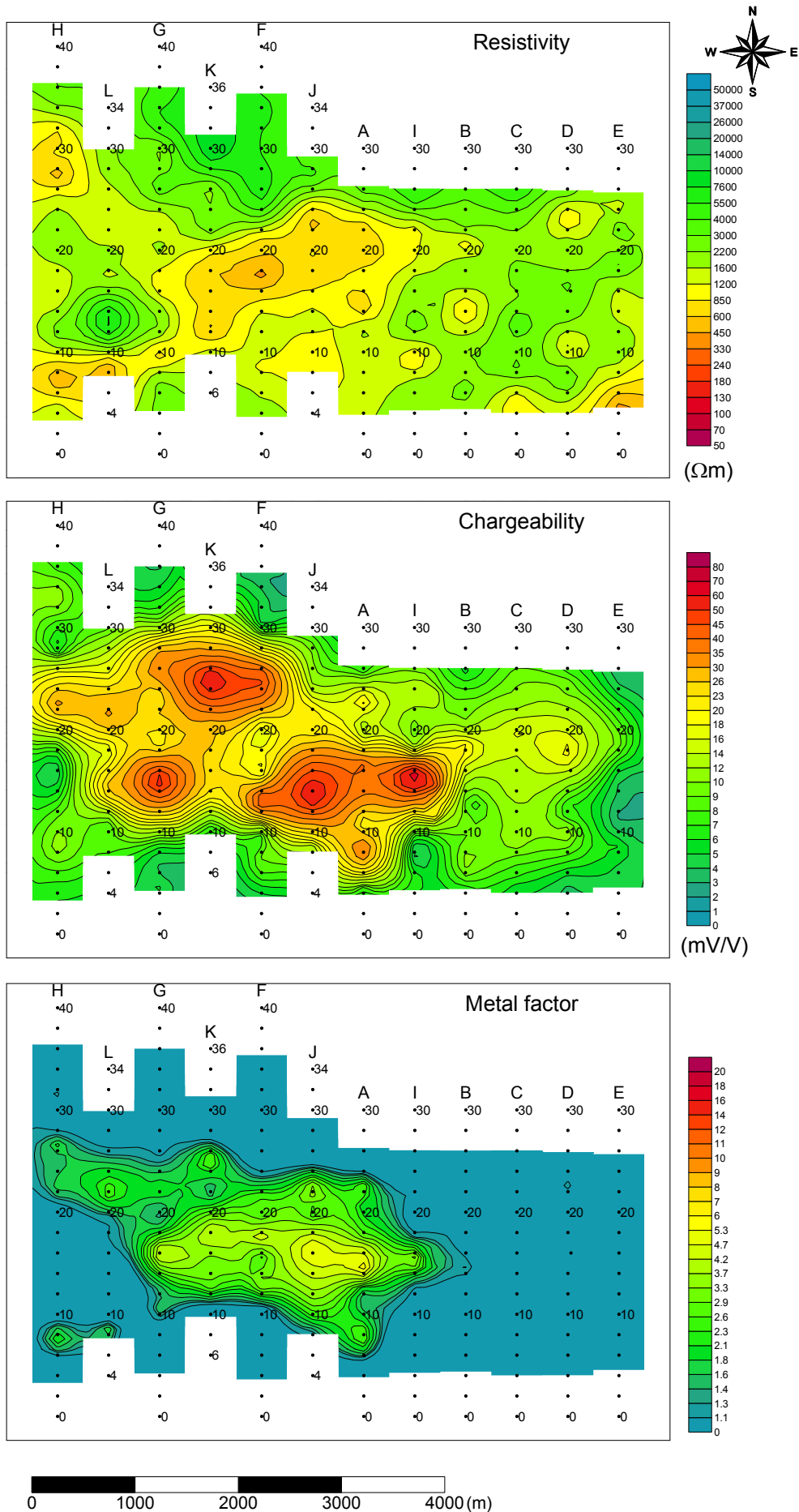


Fig.26 2D analysis plane at the depth of 200m in the Zuukhiin gol area.



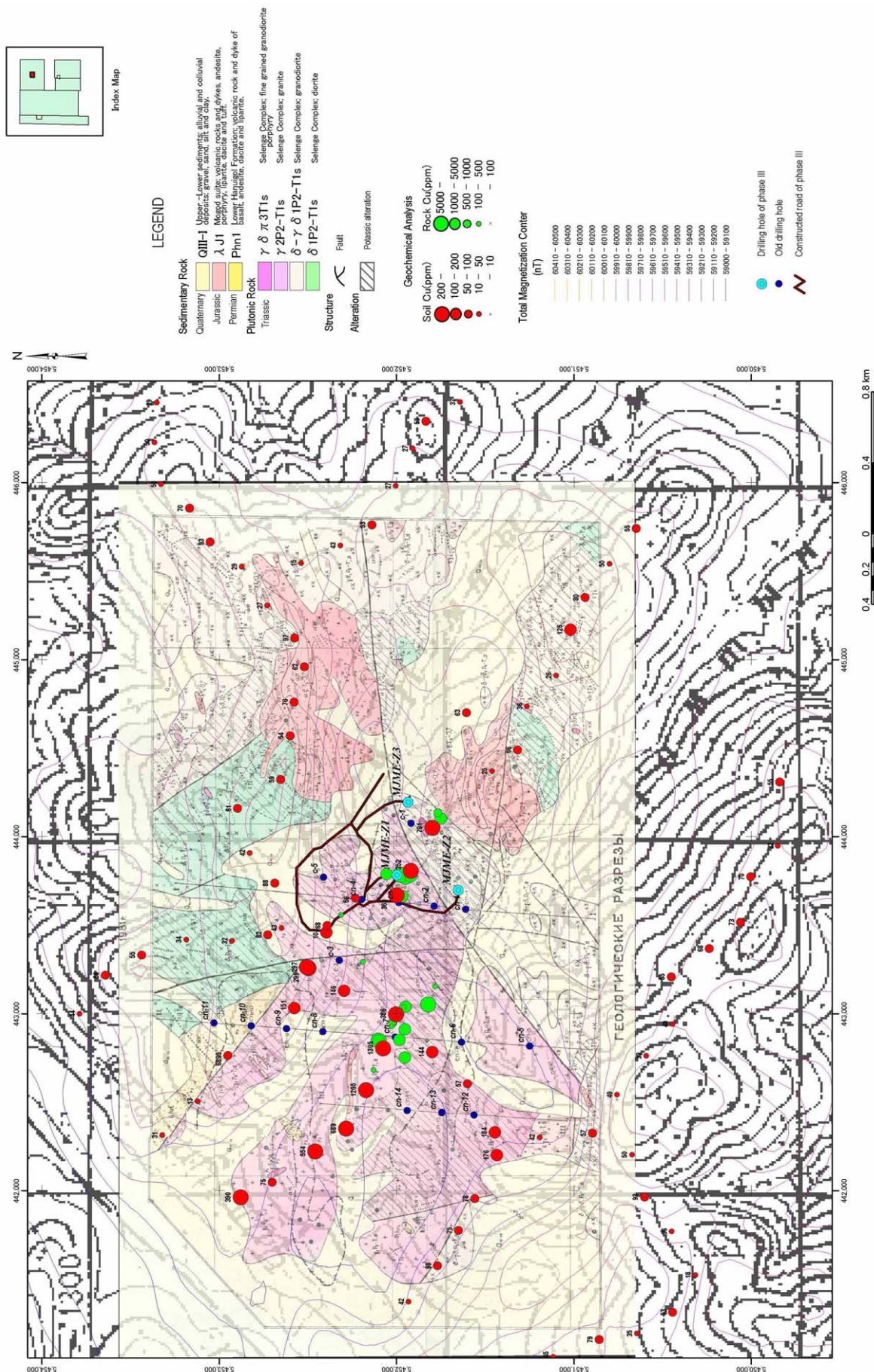


Fig. 27 Geological map and compiled map in the Zuukhiin gol area.



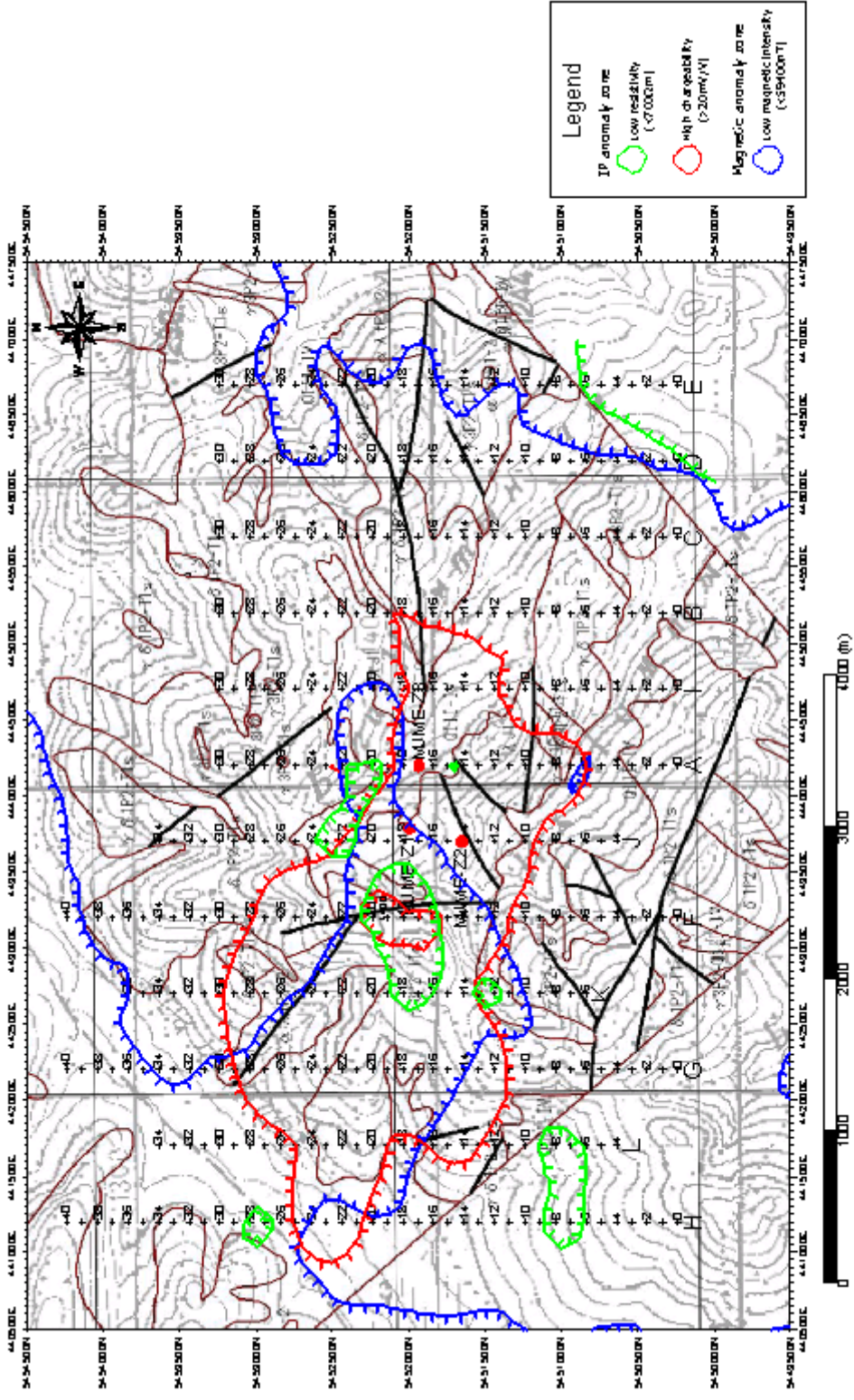


Fig.28 Compiled map in the Zuukhiin gol area.

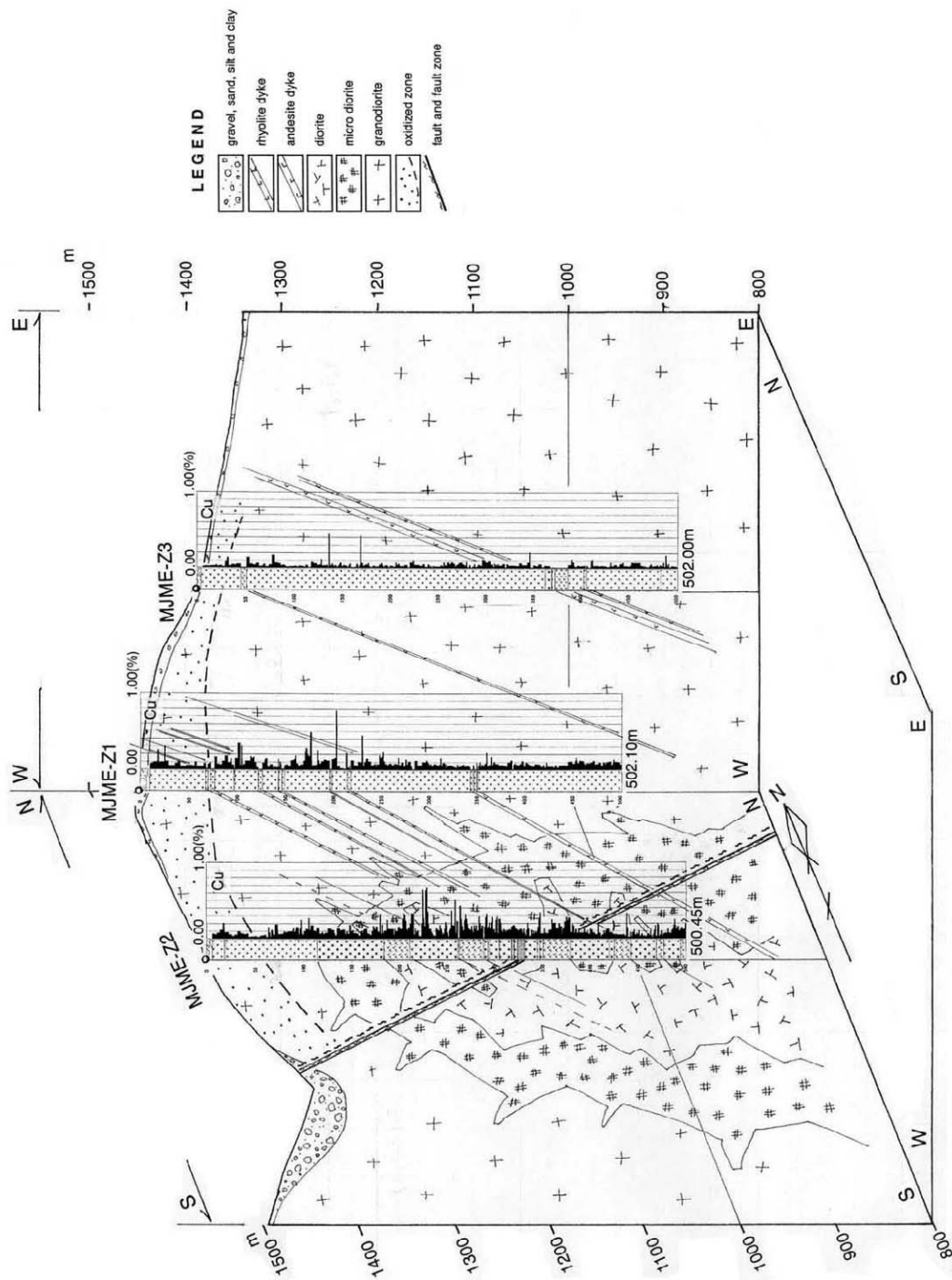


Fig. 29 Schematic geologic section by the drilling results on the topographic map of the Zuukhiin gol area

#### **(4) Khujiriin gol Area**

##### **Introduction**

The area is located approximately 25 km northwest from Erdenet city and about 1,240m to 1,700masl. The topography consists of steep to gentle hills. The vegetation in the area is composed of coniferous forests and tall grass in the hill and valley and low grass along streams. Outcrop studies are difficult because of the high and abundant grass.

It takes about 1.5 hours to go from Erdenet city to the Khujiriin gol mineral showing. Accessibility is good. The height is 1,195 m ASL. Copper oxide minerals are observed in the mineral showing. The direction of the mountain ridge and the streams is along the WSW-ENE direction. Topography becomes low towards the ENE direction.

##### **Geological Survey Results**

As shown in Fig. 30, the geology of the area present Permian volcanic rocks, Triassic to Jurassic volcanic rocks, Permian to Triassic granites, Jurassic stocks, dykes and Quaternary deposits. Fault structures are developed EW direction in the area. The granitic bodies are arranged along the directions NW-SE in the eastern area and EW in the western area.

According to the geological survey results of phase I survey in the Khujiriin gol area, the alteration mineral assemblage of sericite-(smectite) type, sericite-chlorite-(smectite) type and chlorite type are distributed in the area. The distribution of the alteration mineral assemblages is same as the Erdenet mine area. In relation to the results of the rock chemistry, high copper vales of more than Cu 50 ppm and Cu 5,5072 ppm in maximum is concentrated in the central part of the Khujiriin gol mineralization zone. Factor 2 scores of more than 0.5 are also concentrated in the center of the Khujiriin gol mineralization zone. The ore samples with copper oxides show high values of: Cu 11.13 %, Pb 5.78 %, Zn 2.64 %, Mo 0.269 % and Ag 221 ppm in maximum. Mineralization type of the Khujiriin gol mineralization zone may be not only the porphyry copper type mineralization but also the poly-metallic mineralization. The results from fluid inclusion presented an average temperature of 244.2 °C to 289.0 °C and salinity of 3.0 % to 4.0% which means that the low temperatures of porphyry copper type mineralization system indicates epithermal mineralization.

According to the geological survey results of Phase III survey, pale red colored, medium grained granite was distributed widely in the area. In the northern part of the area, pale blue to white granodiorite is exposed. Oxide copper minerals occur in the central eastern part and southeastern parts of the area. Licensed mine area registered by other owner is located in the eastern side of the survey area. According to existing data, mineralized zone including copper minerals extends east to west. The geological survey of this phase was conducted in the western side of the licensed area and



soil sampling survey was done by grid sampling method consisting of sampling at 500m intervals along lines spaced 250m. Quarts veins trending east to west were confirmed in southeastern part of the area with mineralization showing analytical values of more than Cu 0.1%. The mineralization probably continues toward the licensed area. Copper mineralization occurred locally in the southwestern part of the area, however, copper mineralization could not be observed in the northeastern part of the area.

### **Geophysical Survey Results**

According to geophysical survey results of Phase I survey, relative high magnetic anomalous zones and high potassium content zones were detected in the Khujiriin gol area.

In the Phase III survey, TDIP electric survey was conducted in the area as shown in Fig. 31. As indicated in Fig. 32 and Fig. 33, the plane maps below the depth of 150m show high resistivity values distributed widely in the east part of the area. The resistivity structure changes greatly along the east and west of the stream running through the eastern part of the area from north to south. At depth levels below 300m, the high resistivity extends westward around the stations 14 to 16 on each line. The resistivity section of the line A shows a high resistivity zone oriented north. High chargeability anomaly zone oriented also towards north distributes continuously to deeper part below the depth of 200m around the stations 12 to 16 on the lines A and E. This high chargeability zone is seemed to continue eastward, but on the lines C and B, the center of high chargeability is located at the depth of 300 to 400m around the stations 14 to 18, but continuity to deeper part is not recognized. High chargeability is also distributed at the deep part of the stations 24 to 26 on the line A.

The IP anomaly corresponding to the quartz vein is not clear because the dipole length is too long to detect vein with suitable resolution. It is considered generally that a range of anomaly distribution caused by vein is smaller than that by porphyry copper ore. Therefore, a detailed survey using shorter length dipole can be effective to detect vein in more detail.

The geophysical survey results are compiled in Fig. 34.

Since the mineral potential in the area has not yet been evaluated, it is expected that detailed TDIP geophysical survey and soil geochemical survey will be useful to clarify even more the geology and mineralization in the area.

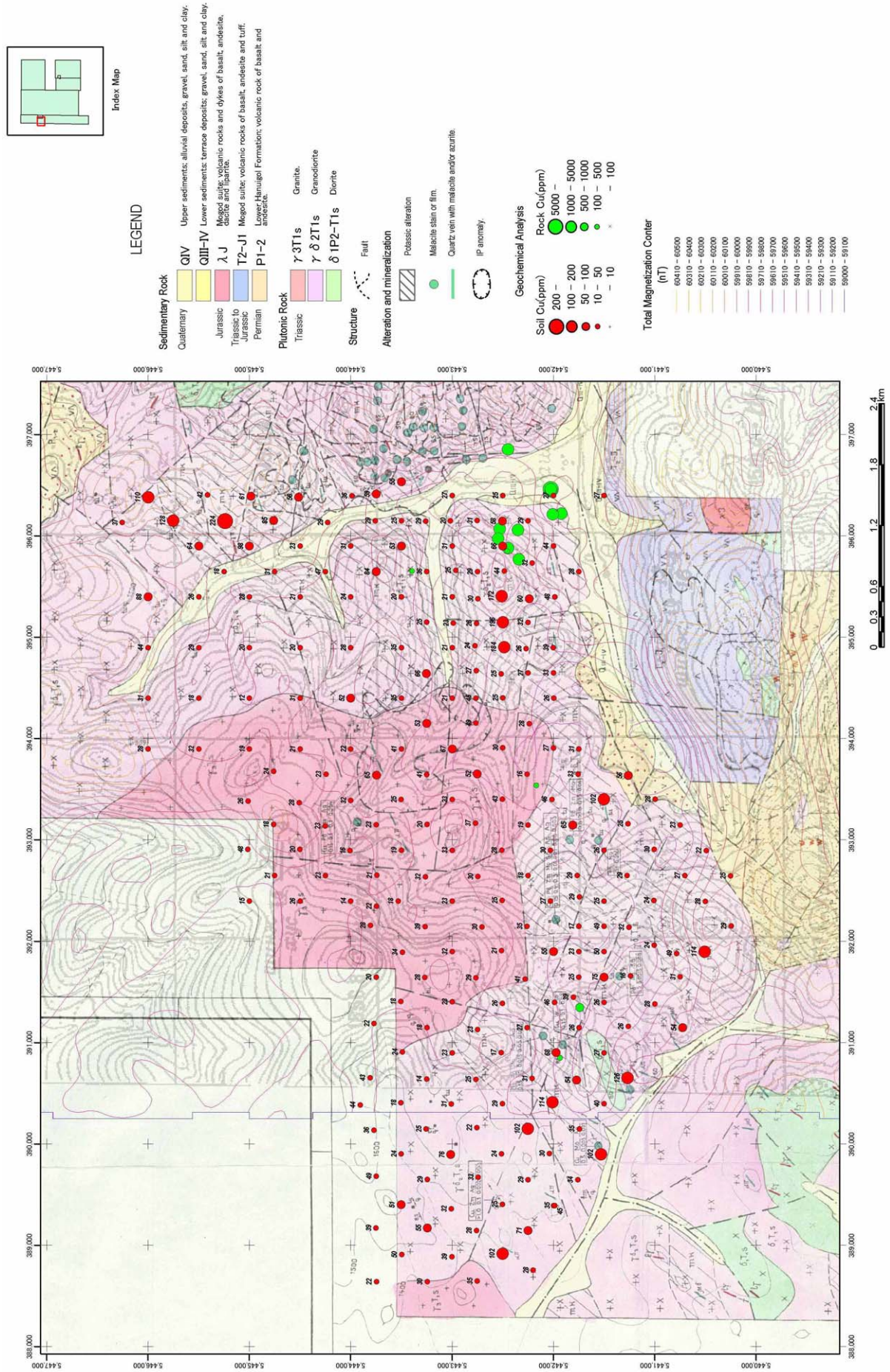


Fig. 30 Geological map and compiled map in the Khujiiriin gol area



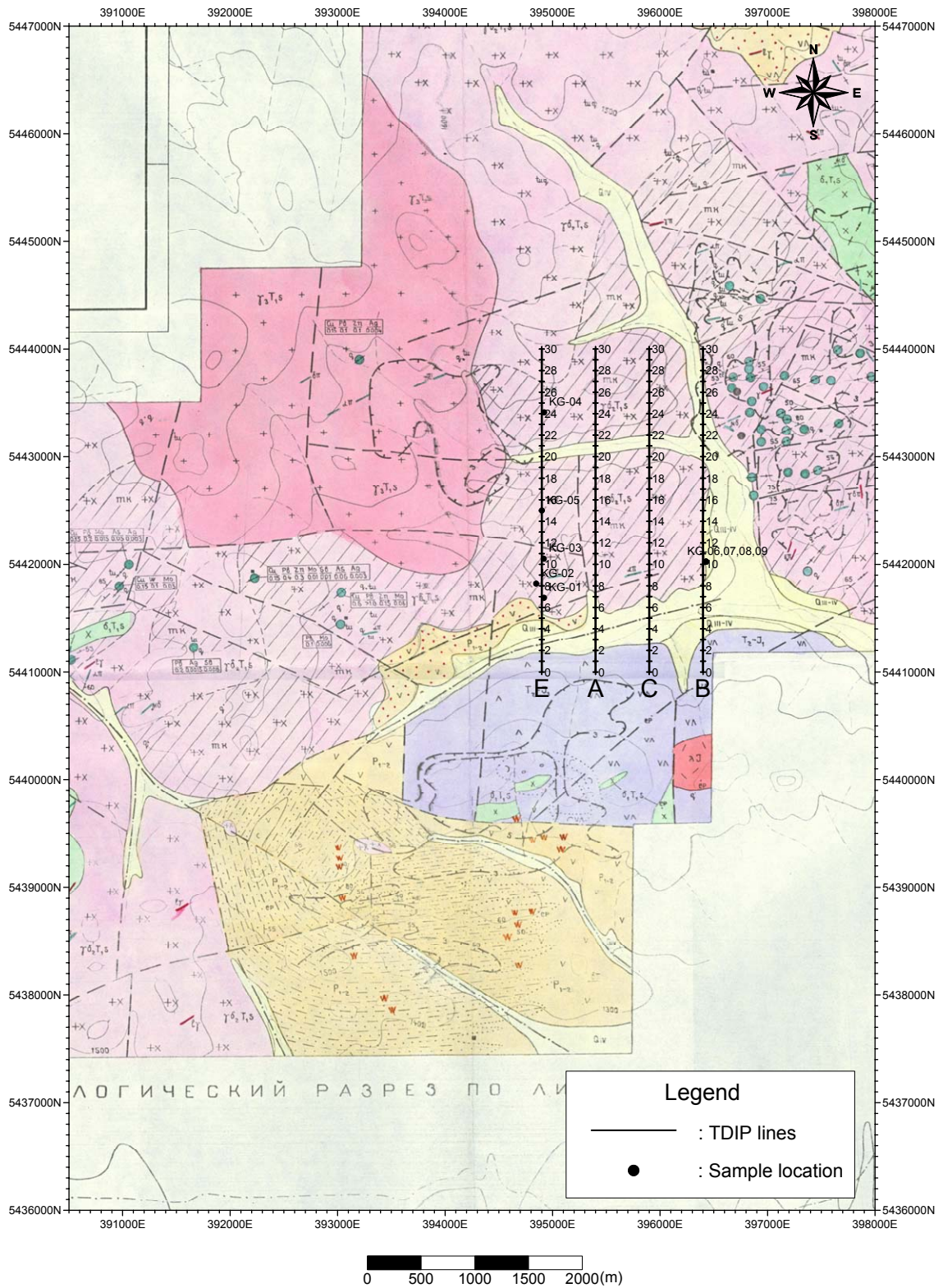


Fig.31 Geophysical survey location in the Khujiriin gol area.

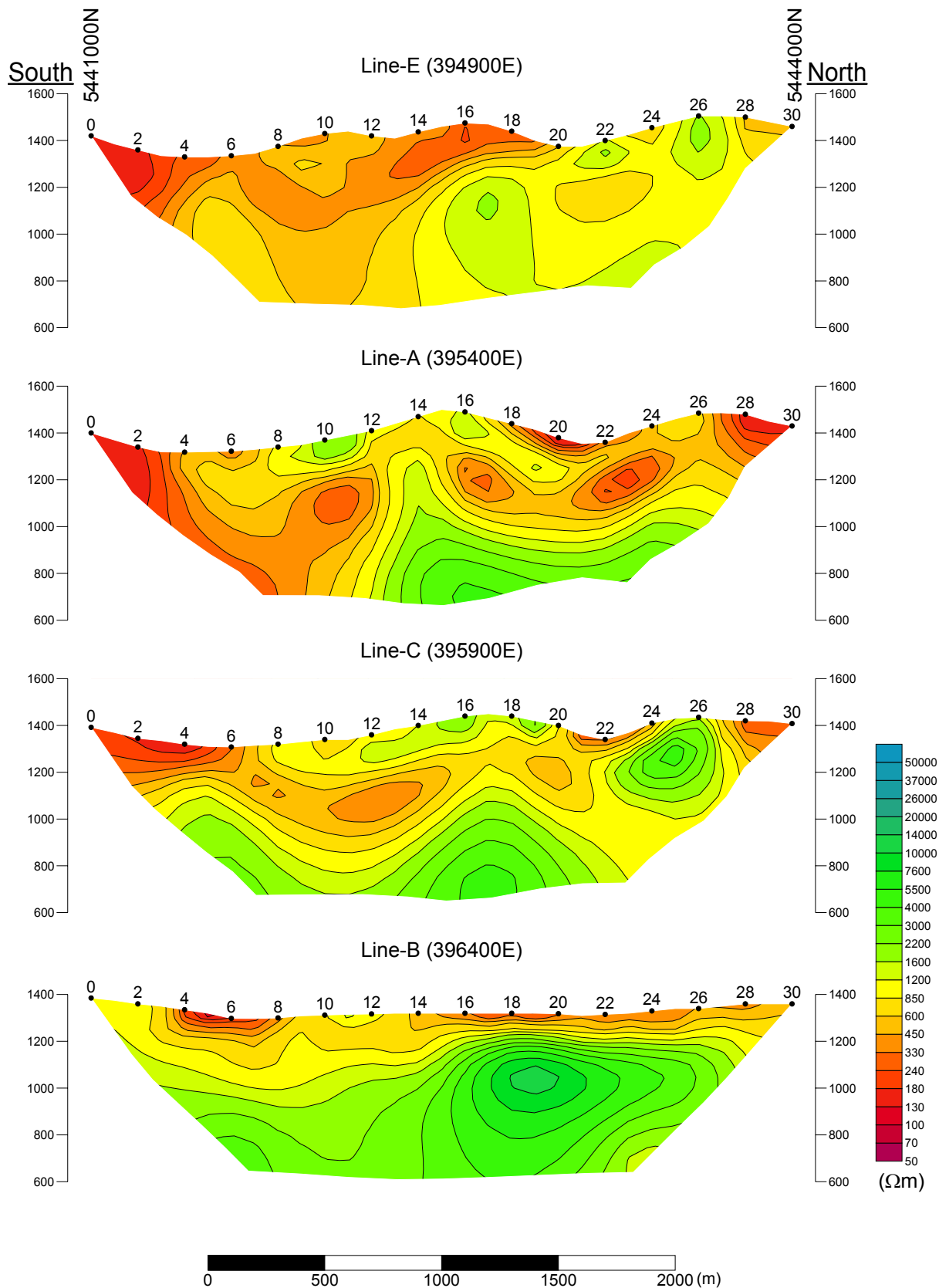


Fig.32(1) 2D analysis sections for resistivity in Khujiriin gol area



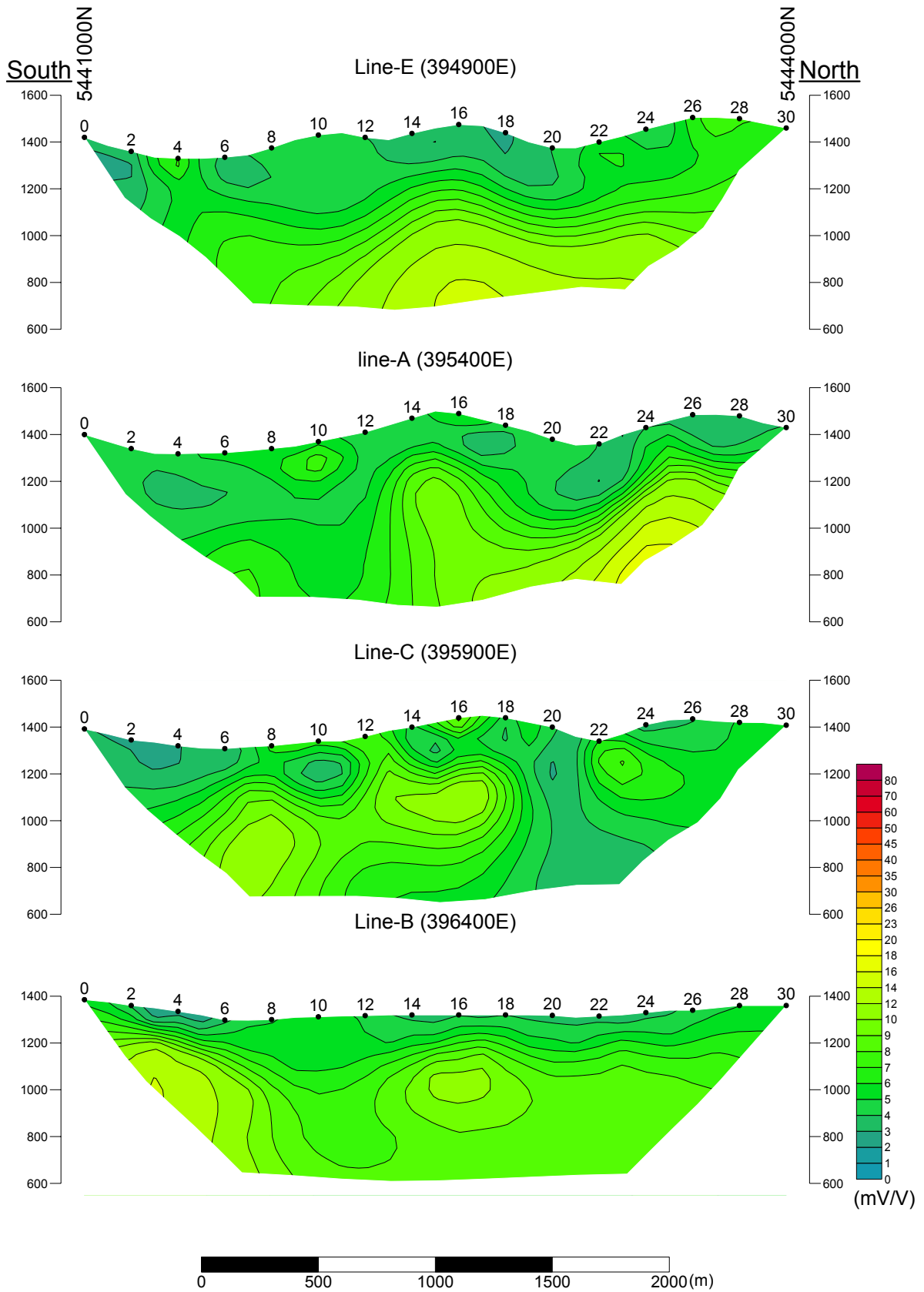


Fig.32(2) 2D analysis sections for chargeability in Khujiirin gol area

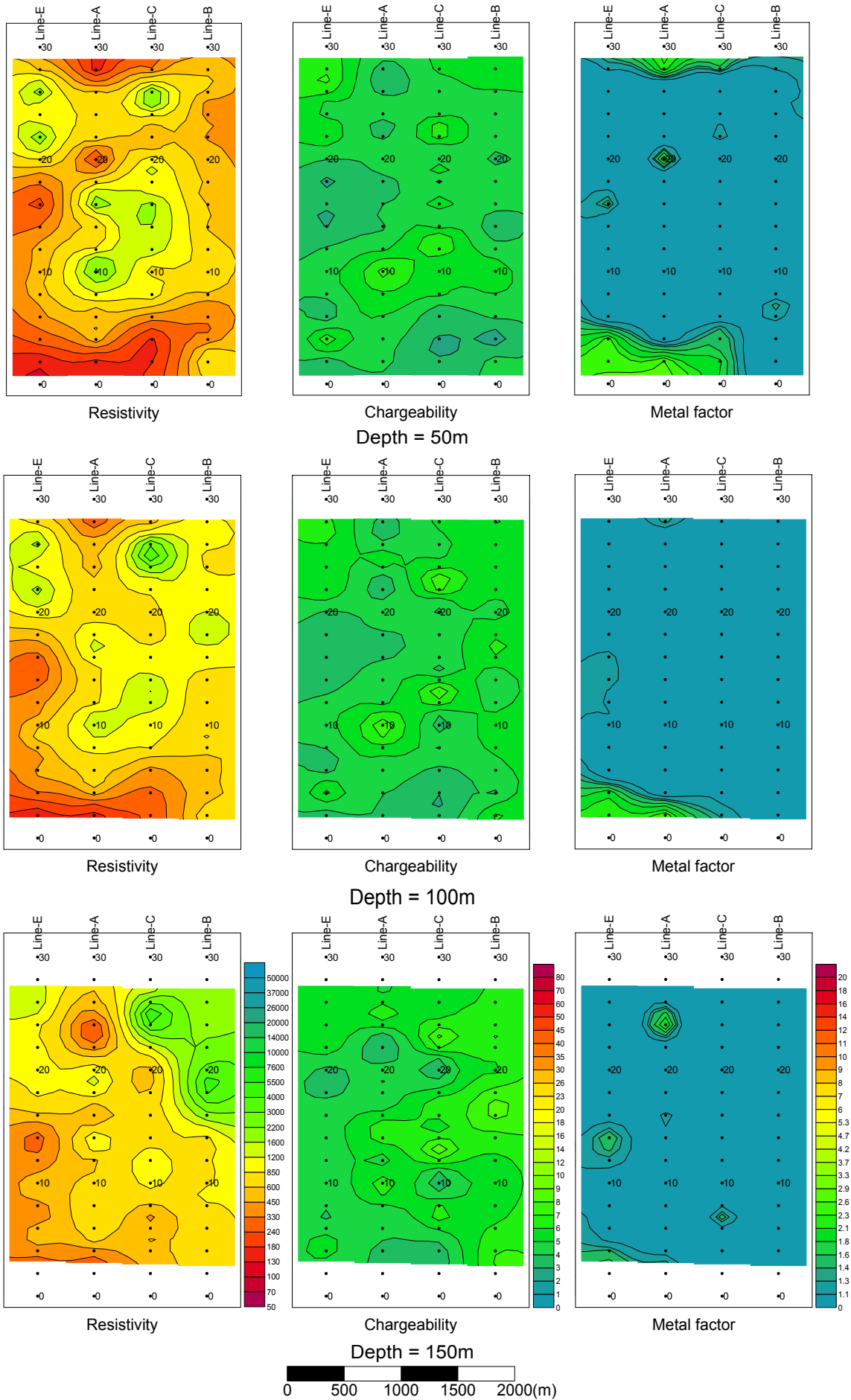


Fig.33 2D analysis plane at the depth of 200m in the Khujiriin gol area.

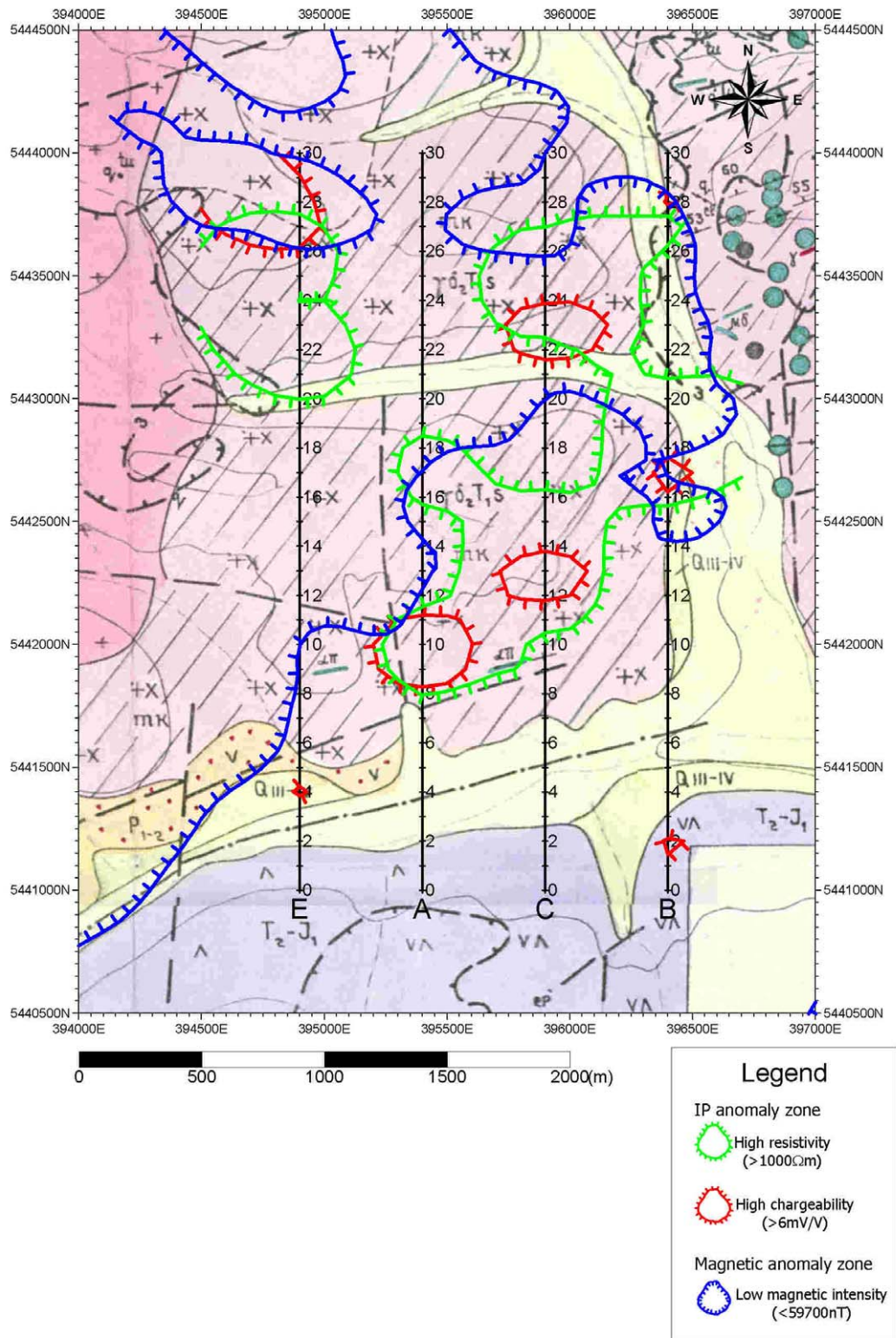


Fig.34 Compiled map of geophysical survey in Khujirjin gol area



## **(5) Under/Shand Area**

### **Introduction**

As shown in Fig. 2, the area is located 25km southeast from Erdenet City at approximately 1,050m to 1,600mASL. Geographic features in the area are classified as low land (1,050 to 1,200 m) and hillside (1,200 to 1,600 m). Grass cover the ground in almost all the area.

In this area, two prospects were studied : the Under prospect in the Under/Shand1 area and the Shand prospect in the Under/Shand3 area.

In the Under prospect, geological mapping at a scale of 1/200,000, 1/10,000 and 1/50,000 and geophysical surveys were conducted. IP and ground magnetics detected several anomalies. In the Shand prospect, several surveys were carried out: geological mapping at a scale of 1/200,000 and 1/2,500, geochemical exploration, geophysical survey and drilling program.

Judging from above investigations and existing geological map at a scale of 1/50,000, geochemical anomalies coincided well with the IP anomalies in the area. Silicified, sericite and potassic alteration were found at surface. A porphyry type Cu-Mo mineralization was delineated in the Shand area by a drilling program of 17 drillholes. The geological resources were estimated 500,000t at 0.2%Cu and 5,000t at 0.001%Mo.

### **Geological Survey Results**

As shown in Fig. 35, the geology consists of the late Permian volcanic rocks, the quaternary sediment rocks, the Selenge complex intrusion, the late Permian granitic rocks, and dykes in this area. Ages of the granodiorite and the granodiorite porphyry indicate 235 Ma (medium Triassic; T3) and 239 Ma (medium Triassic; T3) respectively.

Main geological structures are the NW-SE, the NS and the NE-SW trending faults. From the distributions of the syenite porphyry, which are arranged along the NW-SE direction, trending potential fracture zones are estimated in the southern part of the area along NW-SE where lineaments along NW-SE are seen predominantly distributed. From satellite imagery results, NS and the NE-SW trending lineaments are seen predominantly distributed in the northern part.

The Under mineral showing is located on the NS trending lineament and the Shand mineral showing exists on the cross junction of the NS and the NW-SE trending lineaments.

At the center of the acidic alteration zone in the Under mineral showing, quartz-sericite alteration is present and the sericitization spread outwards. Alteration mineral assemblages are considered the results of the acidic hydrothermal alteration. The size of the mineralization is small scale around 100m X 100m with ore grades indicate low values such as 0.002 %Cu, less than 0.001 %Mo, 0.003 %Pb, less than 0.001 %Zn and 0.83 %Fe.

The Shand mineral showing is a blind deposit covered by quaternary deposits. Mineral

assemblage of sericite-chlorite around the showing is widely distributed. It is possible that this alteration assemblage indicates a part of alteration assemblages in relation with the porphyry copper-molybdenum deposit in the Erdenet mine.

The greenish oxidized copper minerals of the film-like malachite and azurite are observed in the potassium metasomatized medium-grained granodiorite. Maximum ore grades estimated are 0.119 %Cu, 0.036 %Pb, 0.116 %Zn and 24 ppm Ag.

The pyrite dissemination zone with the silicified zone in the western central part of the area is the oxidized zone, which is composed mainly of limonite. Quartz, K-feldspar, biotite, alunite, andalusite and kaolin that is present in the central part of the mineralization. Chloritization occur outward. Ore minerals such as spotty azurite and chalcopyrite, the disseminated pyrite, goethite, hematite and limonite were observed. Ore grades resulted in 0.001 to 0.014 %Cu, < 0.001 to 0.003 %Mo, 0.003 to 0.005 %Pb, <0.001 to 0.002 %Zn and 0.40 to 8.55 %Fe.

Green oxidized copper, malachite and azurite films were observed at western and northwestern part within granodiorite with moderate to strong potassic alteration. Green oxidized copper is associated with quartz vein elongated along northwest direction. Identified alteration minerals are silicification, quartz veinlets or stockwork, chlorite and epidote. Ore grades values are 0.018% to 0.119%Cu, <0.001%Mo, 0.018% to 0.036%Pb, 0.009% to 0.116%Zn and 2.21% to 5.04%Fe. The only silver analytical result was 24ppm.

### **Geophysical Survey Results**

Resulting from the Phase I program, 3 low magnetic zones were extracted as shown in Fig. 36.

As shown in Fig. 37, TDIP electric survey of phase II survey can be described as follows:

In the Under/Shand 1 area, a weak IP anomaly zone was detected at the northeast part. High chargeability continues from shallow to deep part, while resistivity shows relatively low value at shallow part (100 to 200m depth), and high value at deeper part (below 240m). Based on the results and the declination disturbance on the compass, this anomaly is estimated to reflect weak mineralization of magnetite. This anomaly zone is located between 2 high magnetic anomaly zones detected by airborne magnetic survey. The low magnetic anomaly zone is located at the low resistivity zone in the direction of NE-SE. The results of 3-D analysis are almost same as that of 2-D analysis.

In the Under/Shand 2 area, low resistivity anomaly zone is detected along the direction of E-W below the depth of 170m. It is estimated that some alteration affecting to resistivity exists but the alteration is not related to sulphide because the chargeability shows low value. The low resistivity anomaly zone at the deep part is distributed along the south edge of low magnetic anomaly zone. The results of 3-D analysis are almost same as that of 2-D analysis.

In the Under/Shand 3 area as shown in Fig. 38, remarkable IP anomaly is detected. This

anomaly shows high chargeability (maximum is 58mV/V) and low resistivity, and is considered to reflect the mineralization of sulphide minerals. This IP anomaly zone shows ring-shaped pattern at the depth of 100m to 200m, and continues to deeper part. The anomaly zone extends horizontally 1200m from east to west and 1000m from north to south. It corresponds to the low magnetic anomaly zone detected by airborne magnetic survey.

IP anomaly overlapped by small-scale low resistivity and high chargeability was detected in the Shand mineral showing, the Under/ Shand\_3 area. The characteristics of the mineralization combined with above interpreted geophysical structures were intersected and well clarified by the results of the existing 17 drillholes.

A porphyry type Cu-Mo mineralization was delineated in the Shand area by a drilling program of 17 drillholes. Its geological resources were already estimated 500,000t at 0.2%Cu and 5,000t at 0.001%Mo.

The results of geological survey and geophysical survey were compiled in Fig. 39.

No further exploration is recommended for the Under/Shand area.



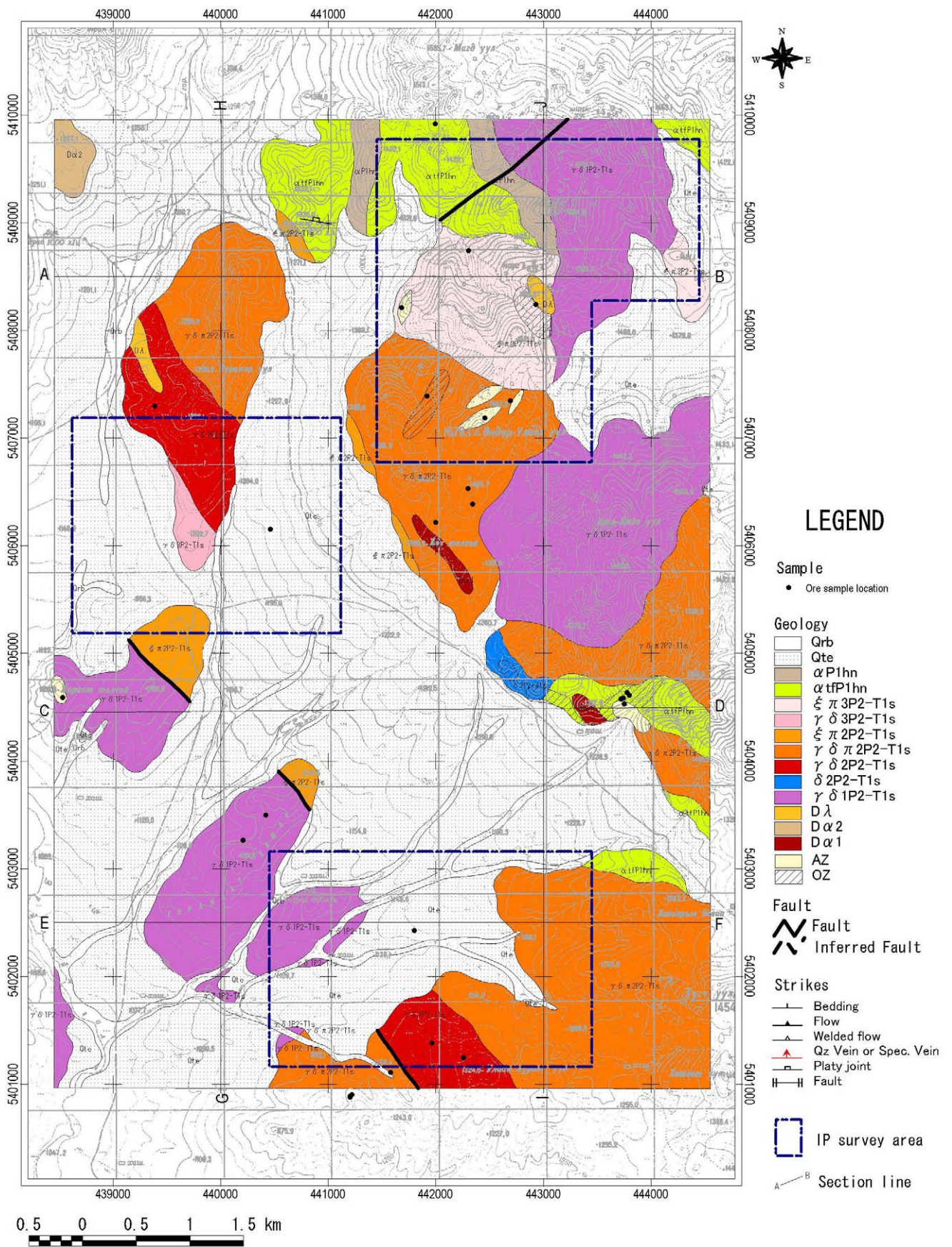
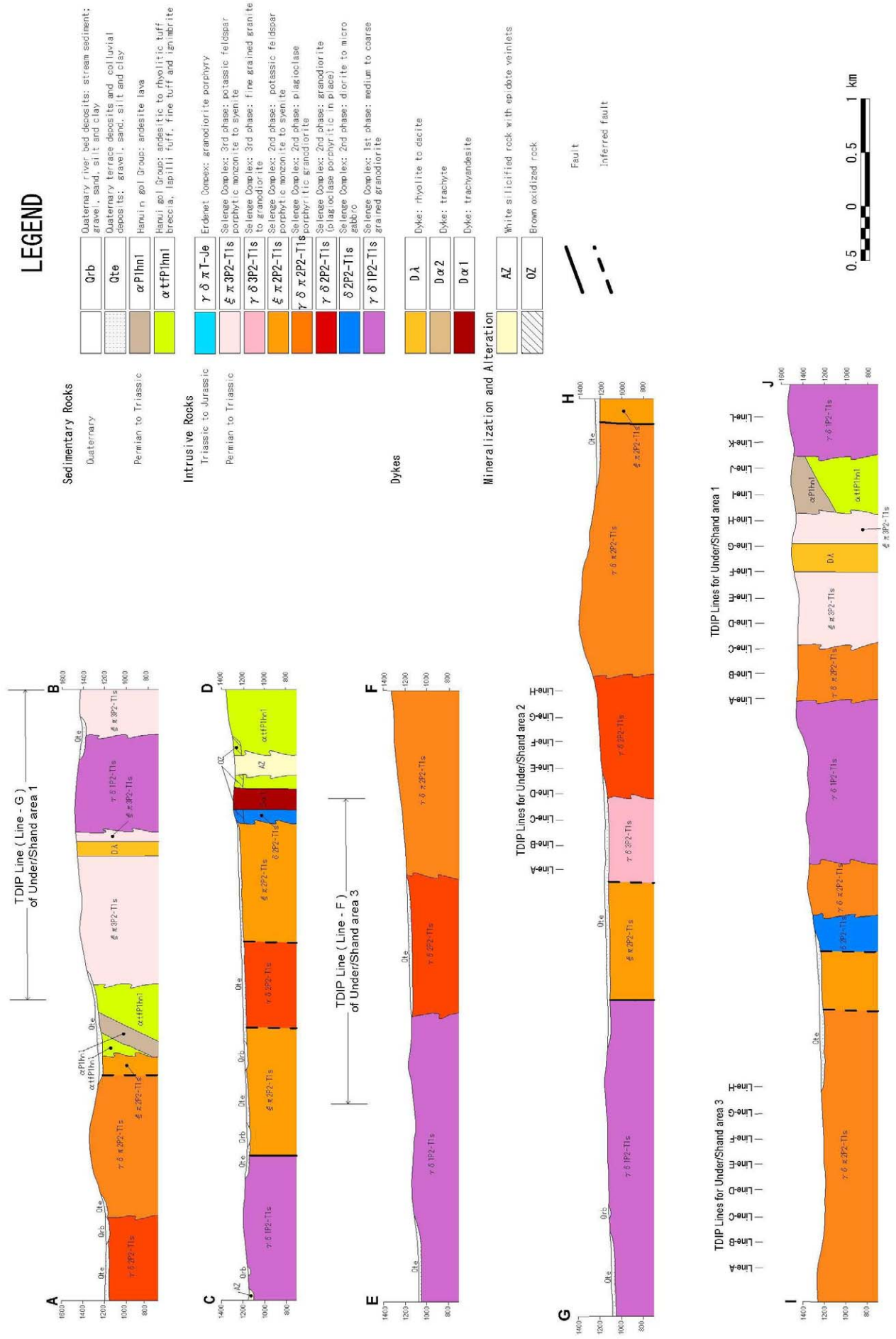


Fig.35(1) Geological map, geological section and mineral showing of the Under/Shand area



# LEGEND

- Sedimentary Rocks**
- Quaternary
    - Qrb: Quaternary river bed deposits; stream sediment; gravel, sand, silt and clay
    - Qte: Quaternary terrace deposits and colluvial deposits; gravel, sand, silt and clay
  - Permian to Triassic
    - αP1hm1: Hanlin gōl Group; andesite lava
    - αtP1hm1: Hanlin gōl Group; andesitic to rhyolitic tuff breccia, lapilli tuff, fine tuff and ignimbrite
- Intrusive Rocks**
- Triassic to Jurassic
    - γ δ π T-Je: Erdem; Complex: granodiorite porphyry
    - ξ π 3P2-T1s: Selenge Complex; 3rd phase: potassic feldspar porphyritic monzonite to syenite
    - γ δ 3P2-T1s: Selenge Complex; 3rd phase: fine grained granite to granodiorite
    - ξ π 2P2-T1s: Selenge Complex; 2nd phase: potassic feldspar porphyritic monzonite to syenite
    - γ δ 2P2-T1s: Selenge Complex; 2nd phase: plagioclase porphyritic granodiorite
    - γ δ 2P2-T1s: Selenge Complex; 2nd phase: granodiorite (plagioclase porphyritic in place)
    - δ 2P2-T1s: Selenge Complex; 2nd phase: diorite to micro gabbro
    - γ δ 1P2-T1s: Selenge Complex; 1st phase: medium to coarse grained granodiorite
- Dykes**
- Dλ: Dyke: rhyolite to dacite
  - Dα2: Dyke: trachyte
  - Dα1: Dyke: trachyandesite
- Mineralization and Alteration**
- AZ: White silicified rock with epidote veinlets
  - OZ: Brown oxidized rock

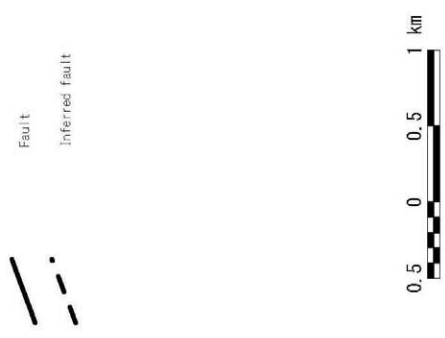


Fig. 35(2) Geological map, geological section and mineral showing of the Under/Shand area



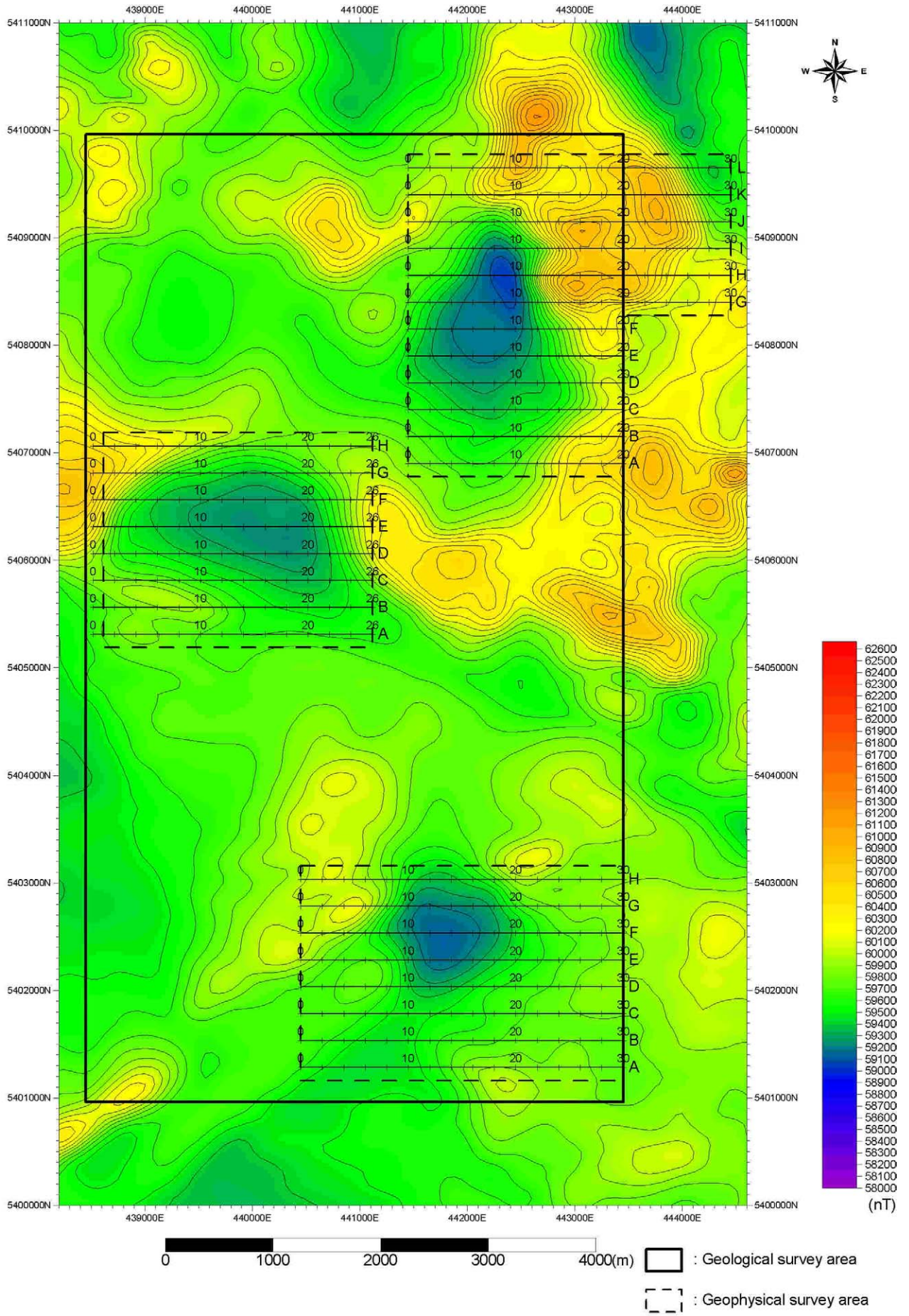


Fig.36 Airborne magnetic intensity map in the Under/Shand area on Phase I survey



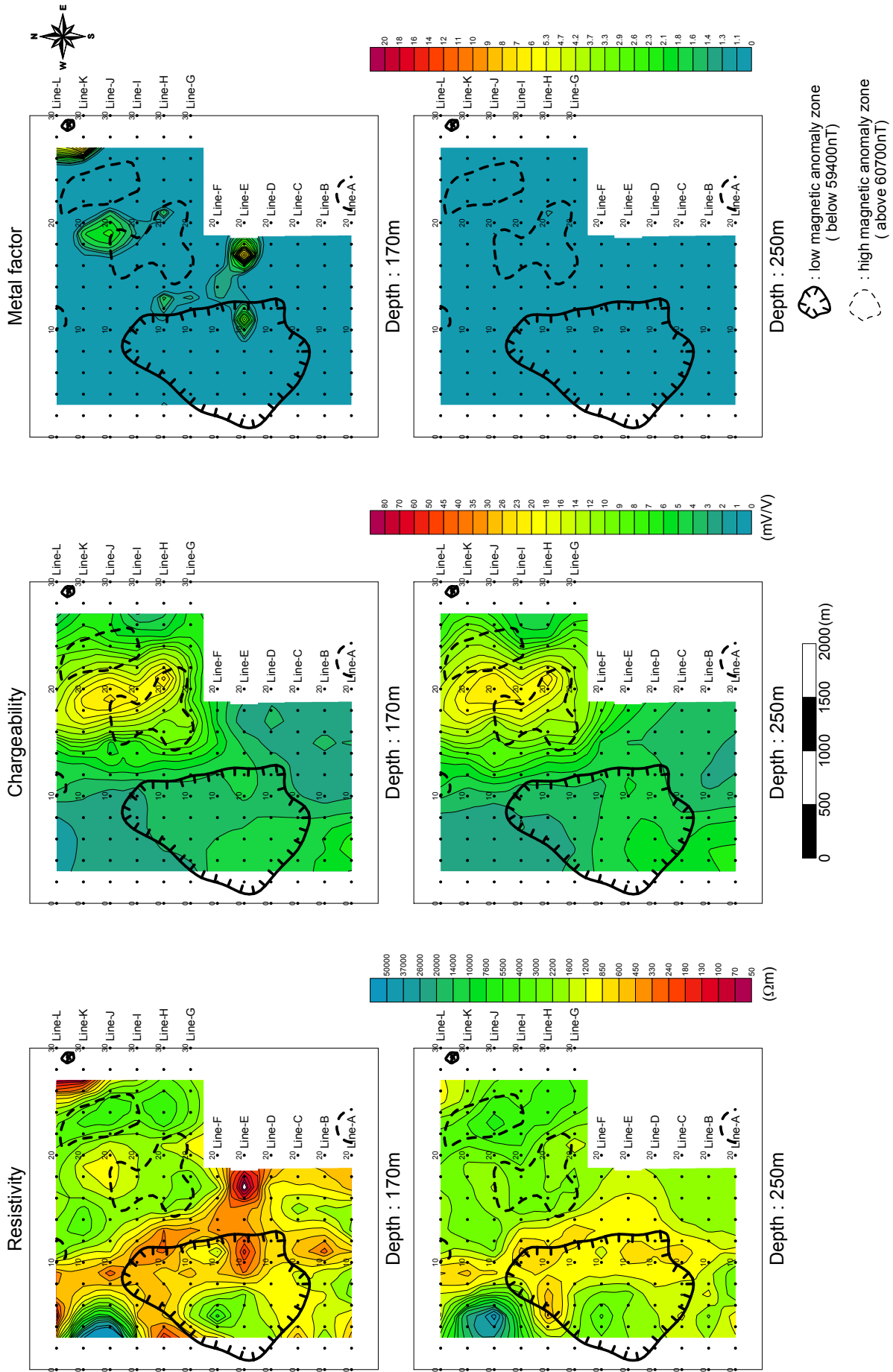


Fig. 37 2D analysis plane map at the depth of 170m and 250m in Under/Shand\_1 area

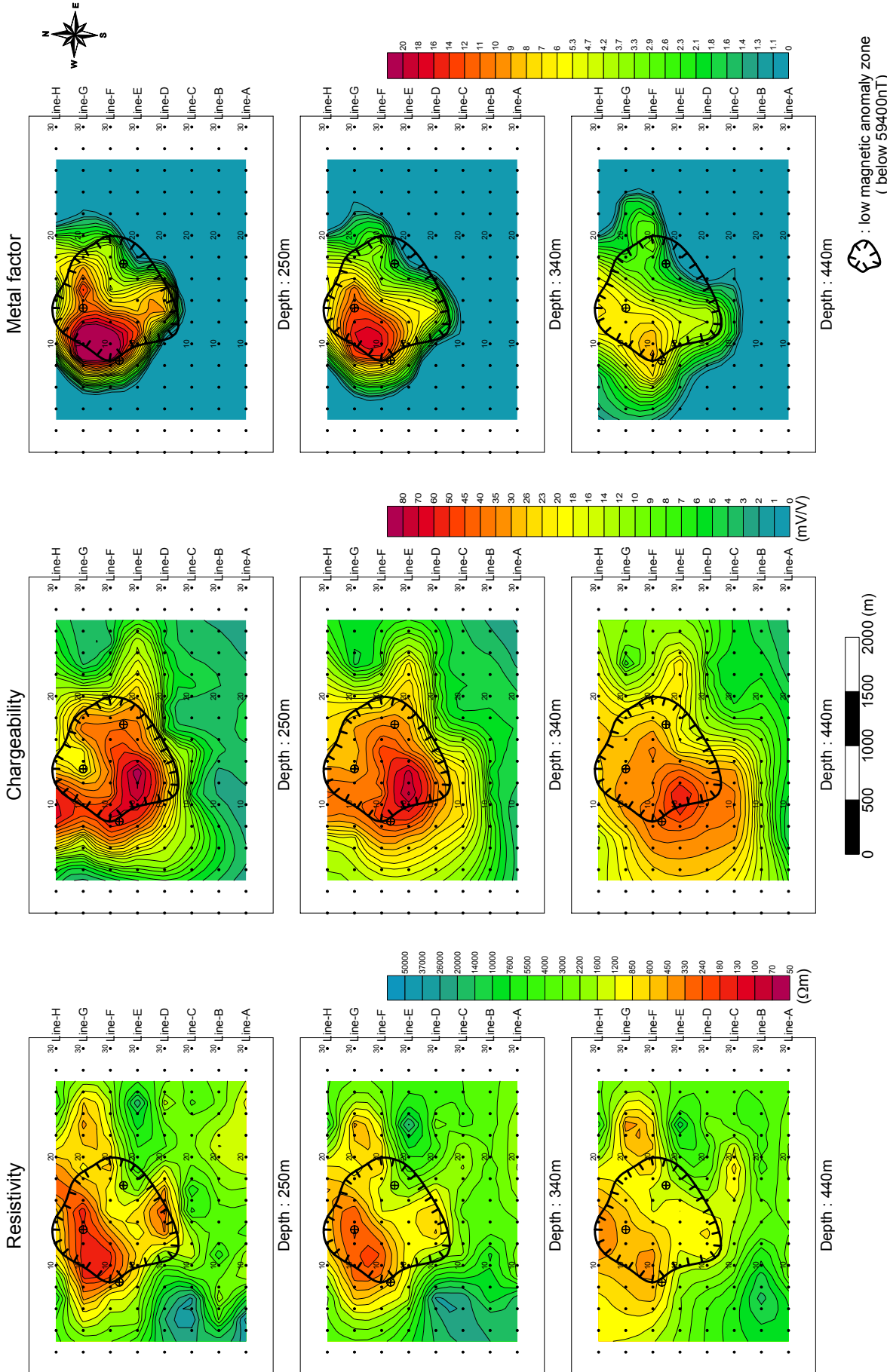


Fig.38 2D analysis plane map at the depth of 250m, 340m and 440m in Under/Shand\_3 area



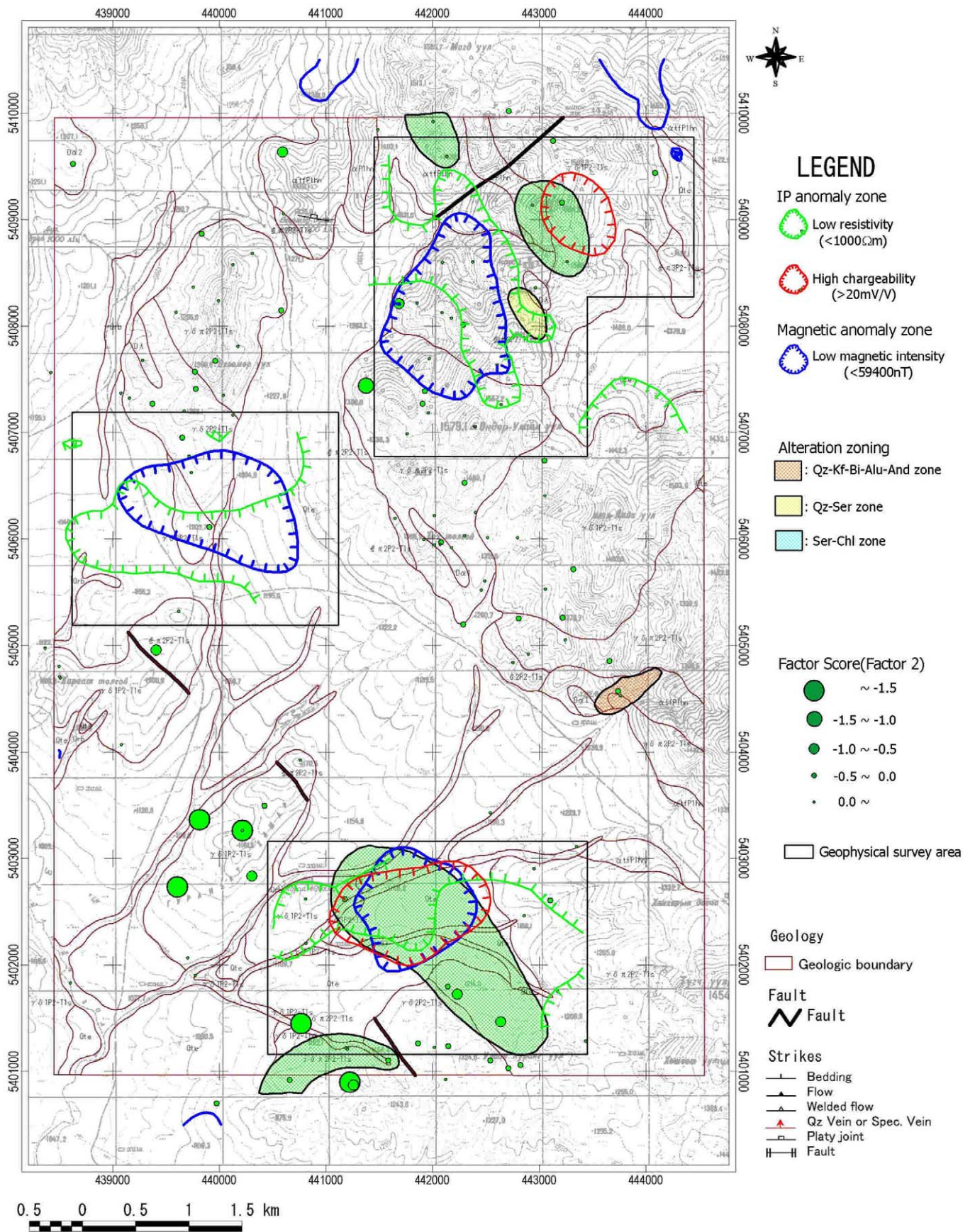


Fig.39 Compiled map in the Under/Shand area

## **(6) Erdenet SE Area**

### **Introduction**

The area is located 12km southeast of Erdenet City (Fig.2) and mainly grassland in lowland at an approximately 1,300m ASL. Geographic features in north and south of the area indicates hillsides over 1,400m ASL. The Erdenet SE area detected low magnetic anomalies by airborne magnetic and radiometric surveys in Phase I and recognized as a prospective area. Early Permian volcanic rocks and late Permian granitic rocks are distributed in the area and Quaternary sediments covering a vast area. Alteration zones are recognized in the granitic rocks. The NW-SE fault system and the N-S system cross in the area.

### **Geological Survey Results**

Geology is composed of the late Permian volcanic rocks, the quaternary sediment rocks, the Selenge complex intrusion, the late Permian granitic rocks, and dykes in this area. K-Ar age of the granodiorite of granitic rocks in the Selenge complex indicate 196Ma, the early Jurassic. Diorite is adakitic rock and indicates the same feature as the granodiorite observed in the Erdenet mine in the Selenge complex. The main geological structures indicate the NE-SW direction of the dykes and the NS and NE-SW directions of the fault structures. The NW-SE trending faults are dominant along the river in the southern part of the area.

The mineral showing with the white silicification zone including quartz veins is confirmed in the northeastern part of the area. This alteration zone was formed by acidic hydrothermal alteration composed of quartz, plagioclase, K-feldspar, kaolin and sericite. Ore is of low grade.

In this area, though alterations are composed of quartz-K-feldspar-sericite-(kaolin), quartz-sericite-(kaolin), quartz-sericite-andalusite-(kaolinite), sericite-chlorite-epidote, and chlorite-epidote and chlorite, the alteration zones related to larger scale mineralization was not detected. Resulting from single-element and multi-element factor analysis of the rock geochemical values, geochemical anomalies related to the mineralization was not detected. However, it is estimated that the adakitic diorite, which is equivalent to suitable igneous rock for generating porphyry Cu-Mo deposits like the Erdenet deposit, is distributed in the area but that there is no mineralization accompanied with the porphyry copper-molybdenum deposit.

### **Geophysical Survey Results**

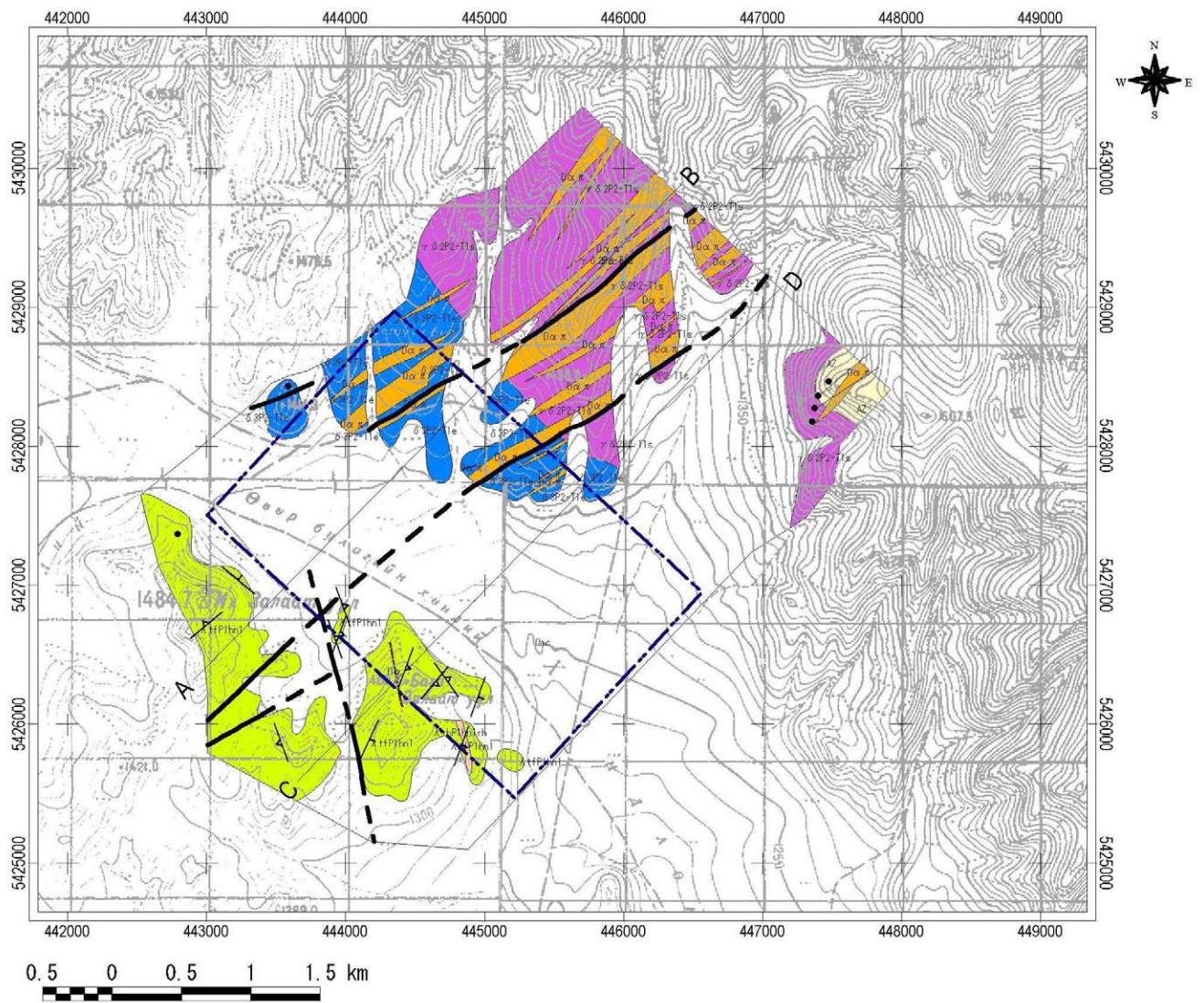
Based on the results of airborne geophysical survey of phase I survey, as shown in Fig. 41, low magnetic anomaly was detected in the area covered widely by Quaternary deposits. Adakitic diorite is distributed in the northern part of the area. The diorite may be reversely magnetized. Silicified zone was detected in the northeastern part of the area where low rock magnetic anomaly is detected..



According to the results of the geophysical survey (TDIP electric method), the Fig. 42 shows the low resistivity widely distributed at the center part of this area, and it corresponds to the area underlain by Quaternary sediments. Remarkable high resistivity is detected at the south of the area, and it is considered to reflect dacite and rhyolitic tuff. No chargeability anomaly is detected. Though there is no good correlation between low magnetic anomaly zone and resistivity or chargeability, chargeability is relatively high at the margin of the low magnetic anomaly zone. If the low magnetic anomaly is caused by intrusive rock, the chargeability anomaly is possible to reflect some weak mineralization. Low resistivity anomaly is detected at the southeast of the area, and it extends from shallow to deep part below the depth of 150m. This anomaly is located at the northwestern edge of high magnetic anomaly zone, and it is estimated that conductive intruded rock exists.

The low magnetic anomaly detected by the airborne magnetic surveys carried out last year recognized to be the result of existence of adakitic diorite but it is concluded that there does not exist igneous intrusions.

The mineralization relating to the porphyry copper-molybdenum deposit could not be detected in the area by geological and geophysical surveys. Therefore, it is considered not necessary to continue explorations in the area.



## LEGEND

**Sample**  
• Ore sample location

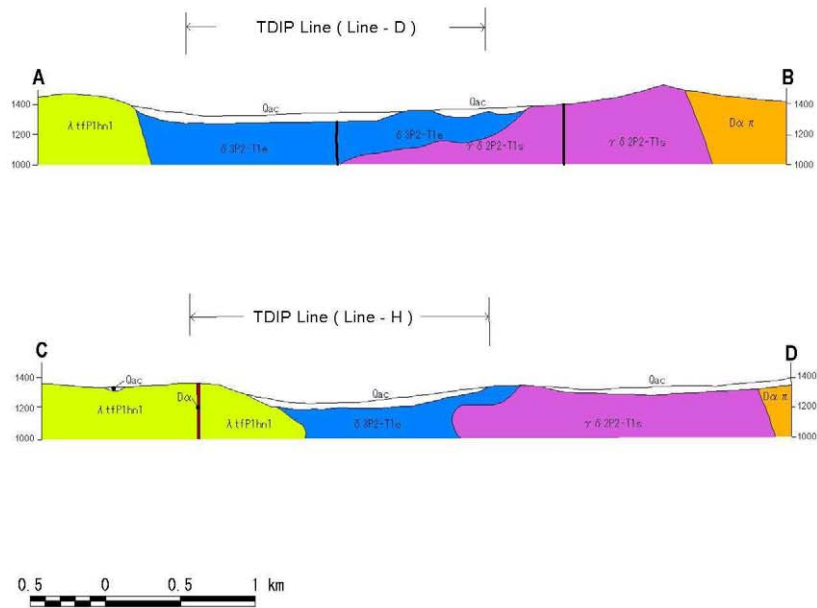
**Geology**  
 □ Qac  
 □ λ tfP1hn1  
 □ λ rhP1hn1rh  
 □ δ 3P2-T1e  
 □ γ δ 2P2-T1s  
 □ Dα π  
 □ Dα  
 □ AZ

**Fault**  
 — Fault  
 - - - Inferred Fault

**Strikes**  
 — Bedding  
 — Flow  
 — Welded flow  
 ▲ Qz Vein or Spec. Vein  
 □ Platy joint  
 —|— Fault

□ IP survey area  
 A—B Section line

Fig.40(1) Geological map, geological section and mineral showings of the Erdenet SE area



## LEGEND

### Sedimentary Rocks

Quaternary

|  |     |  |
|--|-----|--|
|  | Qac | Quaternary deposits: stream sediment, colluvial deposits |
|--|-----|--|

Permian to Triassic

|  |                   |   |
|--|-------------------|---|
|  | $\lambda$ tfP1hn1 | Hanuin gol Formation: Dacitic to rhyolitic welded tuff, lapilli tuff, fine tuff, sandy tuff |
|--|-------------------|---|

|  |                     |                                     |
|--|---------------------|-------------------------------------|
|  | $\lambda$ rhP1hn1rh | Hanuin gol Formation: Rhyolite lave |
|--|---------------------|-------------------------------------|

### Intrusive Rocks

Triassic to Jurassic

|  |                  |   |
|--|------------------|---|
|  | $\delta$ 3P2-T1e | Erdenet Complex: 3rd phase: Fine grained, heterogeneous diorite with granodiorite xenoliths |
|--|------------------|---|

|  |                           |  |
|--|---------------------------|--|
|  | $\gamma$ $\delta$ 2P2-T1s | Selenge Complex: 2nd phase(196Ma): Medium grained, hornblende - biotite granodiorite |
|--|---------------------------|--|

### Dykes

|  |                  |                                    |
|--|------------------|------------------------------------|
|  | D $\alpha$ $\pi$ | Andesite to andesite porphyry dyke |
|--|------------------|------------------------------------|

|  |            |               |
|--|------------|---------------|
|  | D $\alpha$ | Andesite dyke |
|--|------------|---------------|

### Mineralization and Alteration

|  |    |   |
|--|----|---|
|  | AZ | White silicified rock with epidote veinlets |
|--|----|---|

|  |                |
|--|----------------|
|  | Fault          |
|  | Inferred fault |

Fig.40(2) Geological map, geological section and mineral showings of the Erdenet SE area



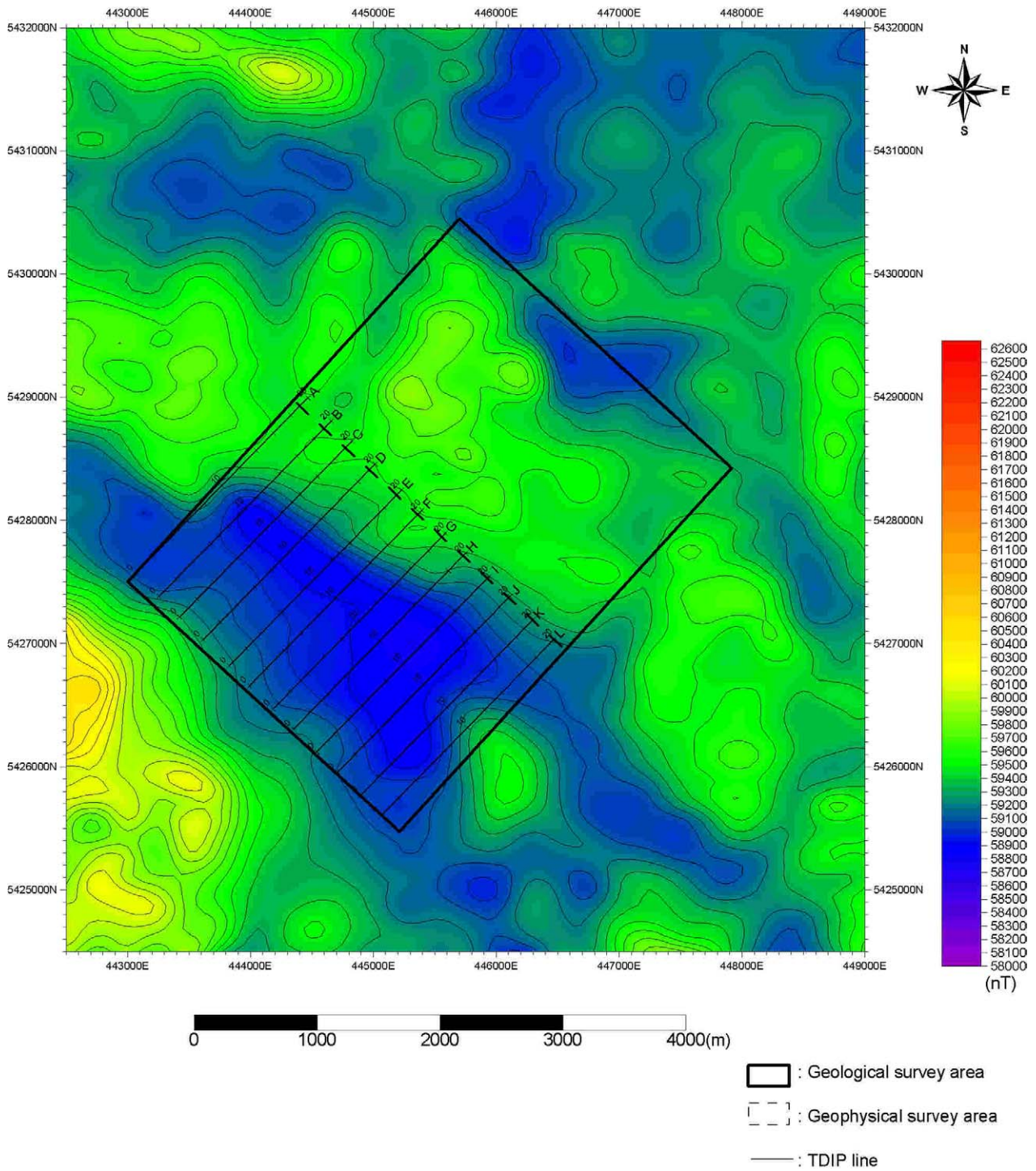
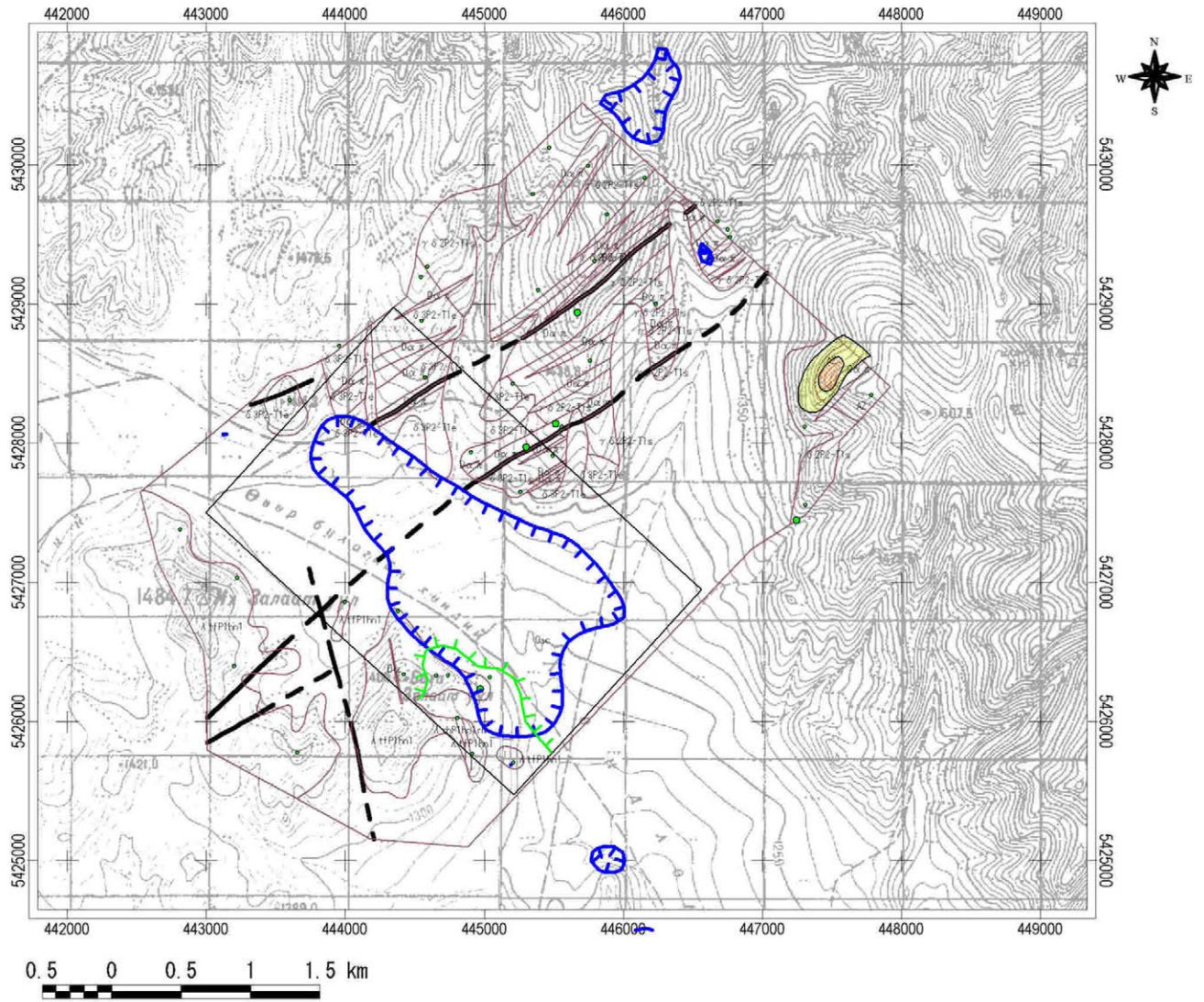


Fig.41 Airborne magnetic intensity map in the Erdenet SE area on Phase I survey





- IP anomaly zone
- Low resistivity (<math><1000\Omega\cdot m</math>)
  - High chargeability (>20mV/V)
- Magnetic anomaly zone
- Low magnetic intensity (<math><59000\text{nT}</math>)
- Geophysical survey area

- Alteration zoning
- Qz-Kf-Ser alteration zone
  - Qz-Ser alteration zone
- Factor Score(Factor 2)
- ~ -1.5
  - 1.5 ~ -1.0
  - 1.0 ~ -0.5
  - 0.5 ~ 0.0
  - 0.0 ~

## LEGEND

- Geology
- Geologic boundary
- Fault
- Fault
  - Inferred Fault
- Strikes
- Bedding
  - Flow
  - Welded flow
  - Qz Vein or Spec. Vein
  - Platy joint
  - Fault

Fig.42 Compiled map in the Erdenet SE area

## **(7) Other areas**

### **The Tsagaan chuluut Area and Tsagaan chuluut West Area**

According to the geological survey results of the Tsagaan Chuluut Mountain, as shown in Fig. 43, the area presents Permian volcanic rocks, Permian to Triassic granites, Triassic to Jurassic volcanic rocks and stocks, dykes and Quaternary deposits. In the southwestern part of the Tsagaan Chuluut Mountain, the granodiorite of Selenge complex is distributed and was covered widely by the Triassic to Jurassic volcanic rocks. Fault structures are developed in the area. The main directions of the faults are NW-SE to NS and other is EW and NE-SW. The granitic bodies are elongated to the NW-SE direction.

The alteration mineral assemblage of quartz-(jarosite)-(kaolinite) type and quartz-alunite-(pyrophyllite)-(kaolinite) type is distributed in the white argillized and silicified zone in and around the Tsagaan Chuluut Mountain. The alteration zone belongs to the advanced argillic alteration zone of the porphyry Cu/Au type alteration system. The expected porphyry Cu-Mo mineralization is inferred to exist in the deeper part from the ground surface.

According to the results of airborne survey of Phase I indicated in Fig. 44, the white alteration zone occurred in the high magnetic anomaly but potassium anomaly was not detected in the area.

Previous geophysical survey results indicated that the white argillized and silicified zone are located in the magnetic the IP anomaly zone.

### **Danbatseren Area and Danbatseren east Area**

According to the geological survey results of the Danbatseren area, as shown in Fig. 43, the area presents Permian volcanic rocks, Triassic to Jurassic volcanic rocks, Permian granites, stocks, dykes and Quaternary deposits. Fault structures are developed in the area along the main directions NW-SE to WNW-ESE. The granitic bodies are distributed trending north to south direction.

The alteration mineral assemblage of quartz-jarosite-kaolinite type is observed in the white argillized and silicified zone. The mineral assemblage shows the deeper part of the litho-cap and the path of the hydrothermal water with high temperature. Previous geochemical exploration were not able to detect any geochemical anomaly, but the previous geophysical survey detected anomalies with high chargeability zones of small scale.

The TMI reduced to the pole map and the radiometric potassium count map of the area is shown in Fig. 46. In the area, a part of the low magnetic anomalous zone and high potassic content was not confirmed.

According to the TDIP electric survey results as shown in Fig. 47 and Fig. 48, no remarkable IP anomalies was detected.

## **Undrakh Area**

According to the geological survey results of the Tsagaan Chuluut Mountain, as shown in Fig. 49, the area presents early Paleozoic granite, Devonian granite, Permian to Triassic granites, stocks, dykes, Quaternary volcanic rocks and Quaternary deposits. Fault structures are developed in the area along the main directions NW-SE.

The mineralized zone in the UndraK-Area consists of porphyry type copper mineralization. But the scale of the mineralization is small and with a weak intensity. The analytical value of ore assay is Cu 0.011% and very low. The previous geophysical survey did not detect any geophysical anomaly.

Previous geophysical surveys were carried out around the mineral showing in the Undrakh area indicated the following IP characteristics

The TMI reduced to the pole map and the radiometric potassium count map of the area is shown in Fig. 50. The area is located in the high magnetic anomalous zone and high potassic content is not confirmed.

## **Tsookher mert Area**

According to the geological survey results of the Tsagaan Chuluut Mountain, as shown in Fig. 51, the area presents Devonian volcanic rocks, Permian to Triassic granites, Triassic to Jurassic volcanic rocks, stocks, dykes, Quaternary volcanic rocks and Quaternary deposits. Fault structures are developed in the area along main directions of NE-SW in the central to eastern area, NW-SE in the western area and EW in southern area. The distribution of granitic bodies shows EW direction or NS direction.

According to the results of the geological survey, the scale of the Tsookher Mert mineral showing is 1.5m in width and 700 m in EW length. The ore assay grade is Au1.49g/t, Ag538g/t, Cu0.247%, Pb6.737%, Zn0.682% and Bi0.017% in maximum. The rock geochemical vales are widely ranging and low.

The scale of the Hatan hoshuu mineal showing is as small as 50m X 50m. The ore grade shows vales of Cu0.006%, Pb0.005% and Zn0.004%. In the two mineral showings, the ore assay grades are widely changing. The scale of the mineralization was also very small.

The TMI reduced to the pole map and the radiometric potassium count map of the area is shown in Fig. 52. The high magnetic anomalous zone cannot be seen in the area but high potassic content is widely confirmed in the area. The high potassic content zone is located in the syenite rock, which include many potassic feldspars.

Consequently, further survey works for mineral exploration should not be conducted in this area.



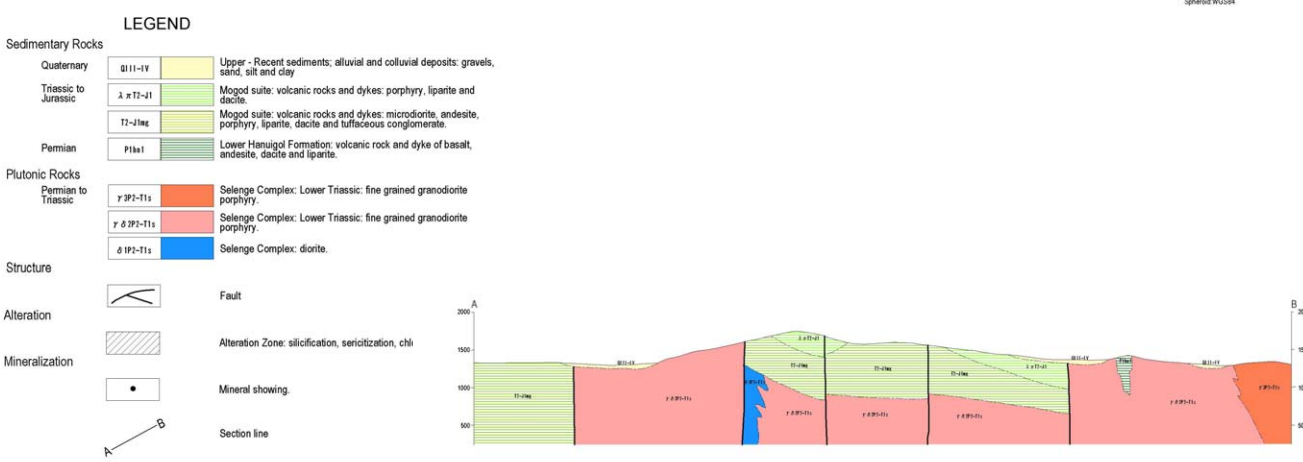
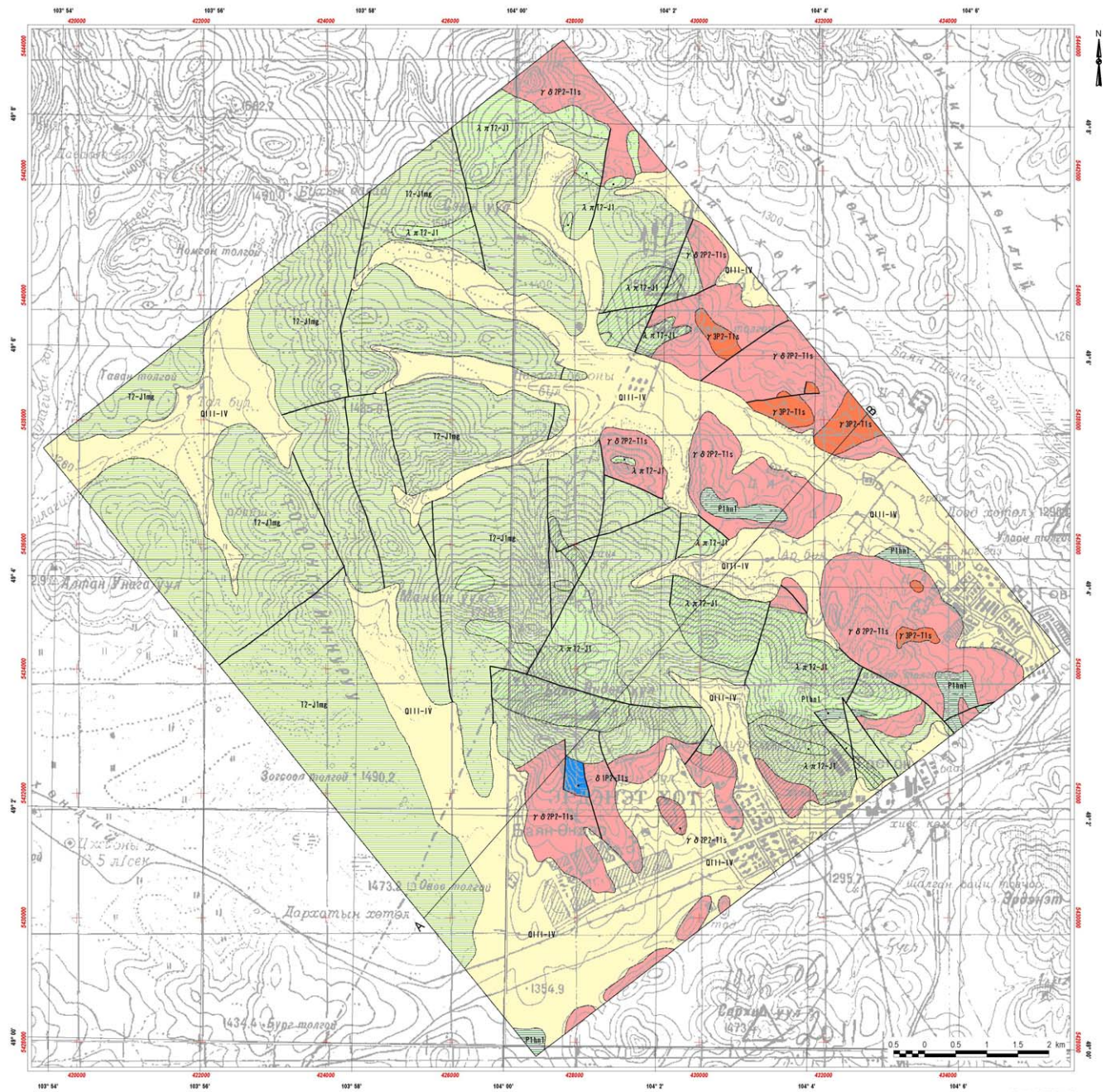


Fig.43 Geological map. Geological section and mineral showings in the Tsagaan Chuluut area.



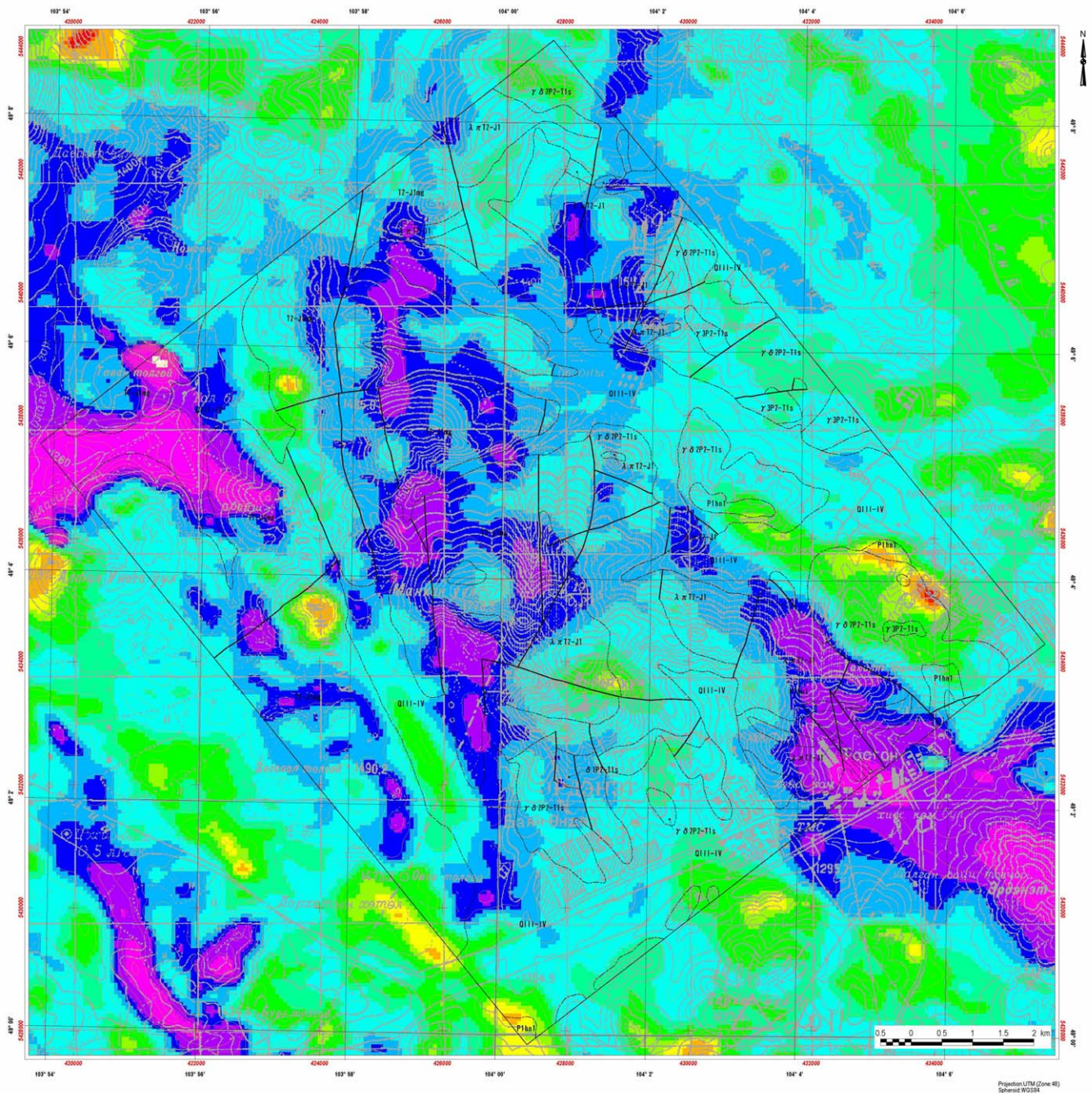


Fig.44 Total magnetic intensity of air borne survey in the Tsagaan Chuluut area.

**LEGEND**

**Sedimentary Rocks**

- Quaternary: Q111-IV Upper - Recent sediments; alluvial and colluvial deposits: gravels, sand, silt and clay
- Triassic to Jurassic: λ π T2-J1 Mogod suite: volcanic rocks and dykes: porphyry, lipante and dacite.
- T2-lmg Mogod suite: volcanic rocks and dykes: microdiorite, andesite, porphyry, lipante, dacite and tuffaceous conglomerate.
- Permian: P1ha1 Lower Harsgal Formation: volcanic rock and dyke of basalt, andesite, dacite and lipante.

**Plutonic Rocks**

- Permian to Triassic: γ δ TP2-T1s Selenge Complex: Lower Triassic: fine grained granodiorite porphyry.
- γ δ TP2-T1s Selenge Complex: Lower Triassic: fine grained granodiorite porphyry.
- δ IP2-T1s Selenge Complex: diorite.

**Structure**

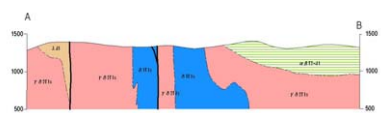
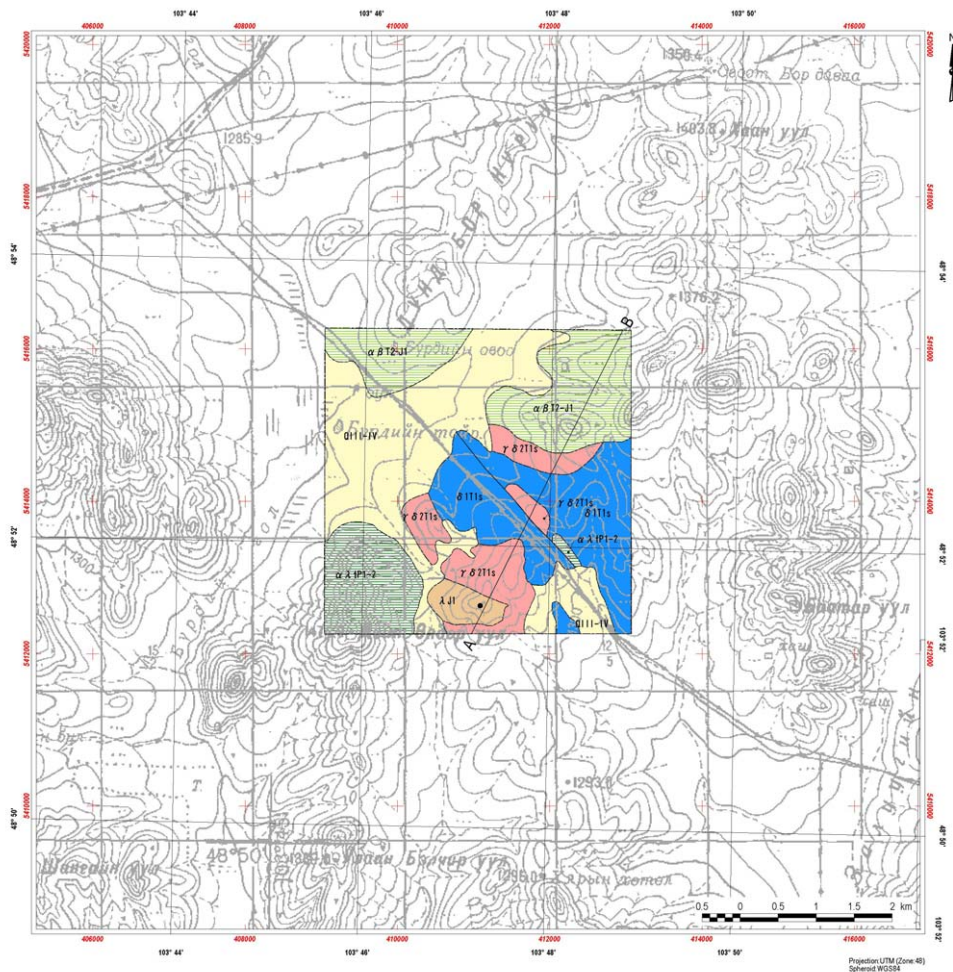
- Fault

**Airborne survey**

Reduced to Pole Magnetic Field (nT)

- 60500 - 62395
- 60400 - 60500
- 60300 - 60400
- 60200 - 60300
- 60100 - 60200
- 60000 - 60100
- 59900 - 60000
- 59800 - 59900
- 59700 - 59800
- 59600 - 59700
- 59500 - 59600
- 59400 - 59500
- 59300 - 59400
- 59200 - 59300
- 59100 - 59200
- 59000 - 59100
- 58900 - 59000
- 58800 - 58900



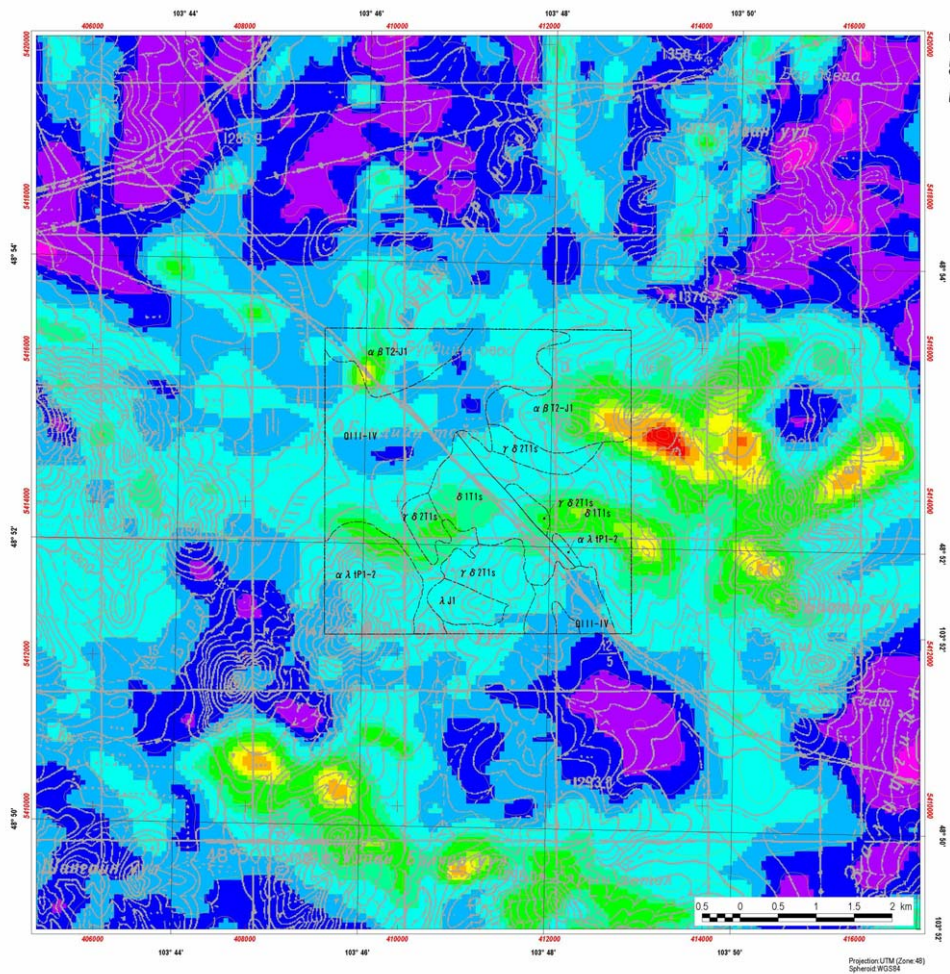


**LEGEND**

|                          |           |  |
|--------------------------|-----------|--|
| <b>Sedimentary Rocks</b> |           |  |
| Quaternary               | Q111-IV   | Upper - Recent sediments; alluvial and colluvial deposits; gravels, sands, silt and clay                               |
| Triassic to Jurassic     | α δ 71-21 | Mogod suite; volcanic rocks and dykes; microdiorite, andesite, porphyry, liparite, dacite and tuffaceous conglomerate. |
| Permian                  | α λ 1P1-2 | Lower Hanuigol Formation; volcanic rock and dyke of basalt, andesite, dacite and liparite.                             |
| <b>Plutonic Rocks</b>    |           |  |
| Jurassic                 | λ. J1     | Granite, granite-porphyry, syenit-porphyry, diorite, and granodiorite.   |
| Triassic                 | γ δ 711s  | Selenge Complex; granodiorite.   |
|                          | δ 111s    | Selenge Complex; diorite.  |
| <b>Structure</b>         |           |  |
|                          |           | Fault  |
| <b>Mineralization</b>    |           |  |
|                          |           | Mineral showing.   |
|                          |           | Section line   |

Fig.45 Geological map, geological section and mineral showings in the Danbatseren area.





**LEGEND**

|                          |                                     |  |
|--------------------------|-------------------------------------|--|
| <b>Sedimentary Rocks</b> |                                     |  |
| Quaternary               | Q11-IV                              | Upper - Recent sediments; alluvial and colluvial deposits: gravels, sand, silt and clay                                |
| Triassic to Jurassic     | α β 17-11                           | Mogod suite: volcanic rocks and dykes: microdiorite, andesite, porphyry, liparite, dacite and tuffaceous conglomerate. |
| Pemian                   | α λ 191-2                           | Lower Hanuigol Formation: volcanic rock and dyke of basalt, andesite, dacite and liparite.                             |
| <b>Plutonic Rocks</b>    |                                     |  |
| Jurassic                 | λ 41                                | Granite, granite-porphyry, syenit-porphyry, diorite, and granodiorite.   |
| Triassic                 | γ δ 211s                            | Selenge Complex: granodiorite.   |
|                          | δ 111s                              | Selenge Complex: diorite.  |
| <b>Structure</b>         |                                     |  |
|                          |                                     | Fault  |
| <b>Airborne survey</b>   |                                     |  |
|                          | Reduced to Pole Magnetic Field (nT) |  |
|                          |                                     |  |

Fig.46 Total magnetic intensity of air borne survey in the Danbatseren area.

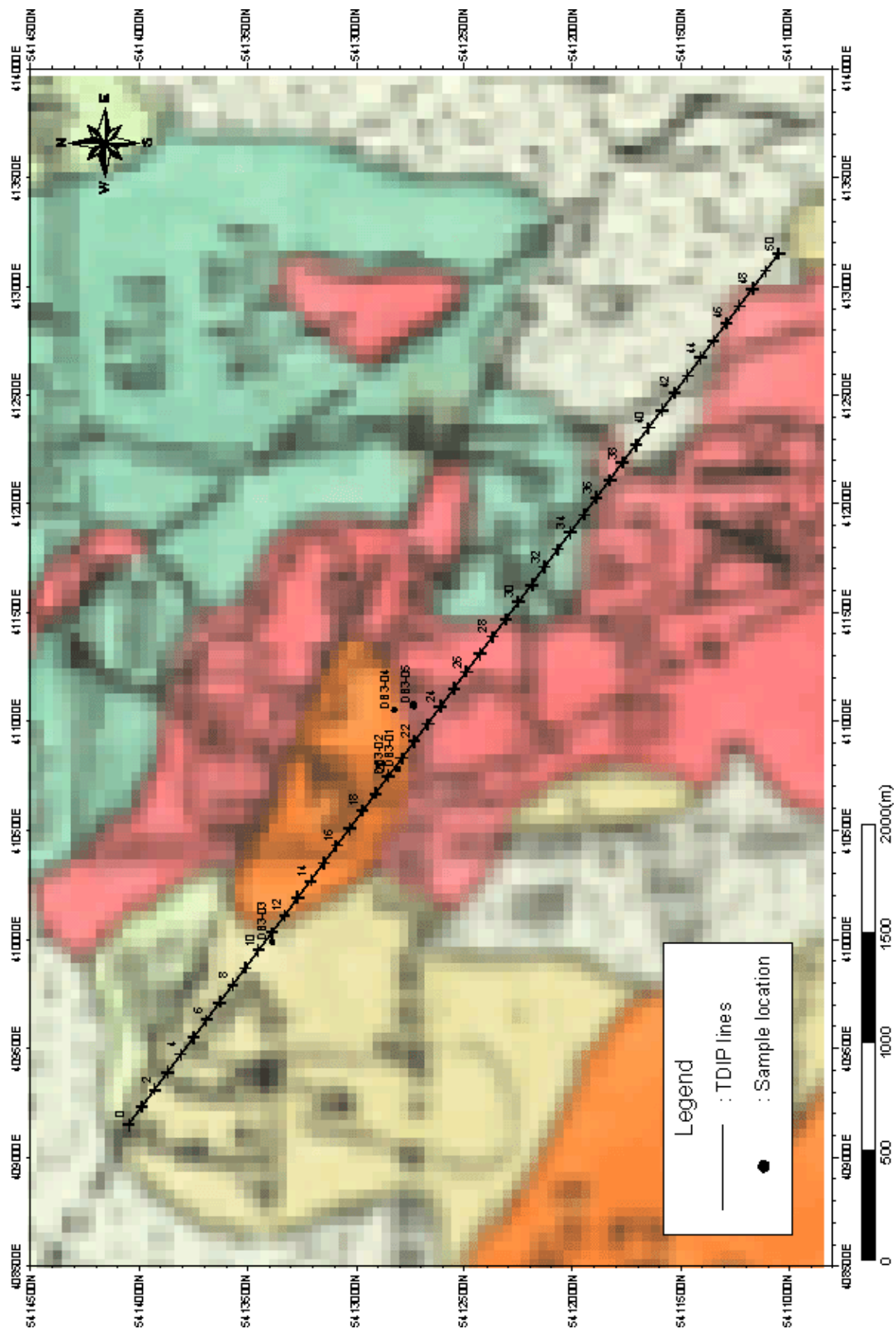


Fig.47 Geophysical survey location in the Danbatseren -3 area.

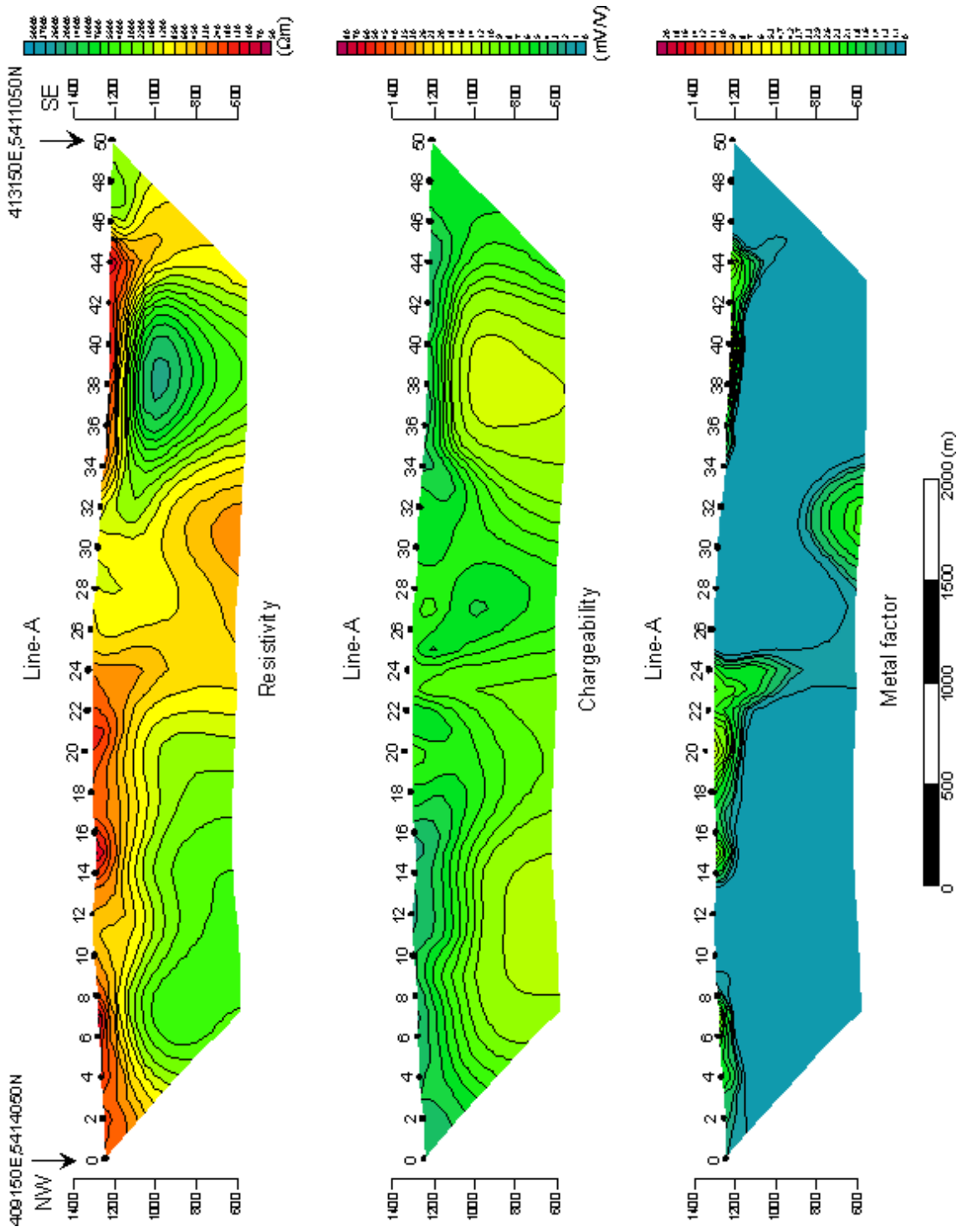
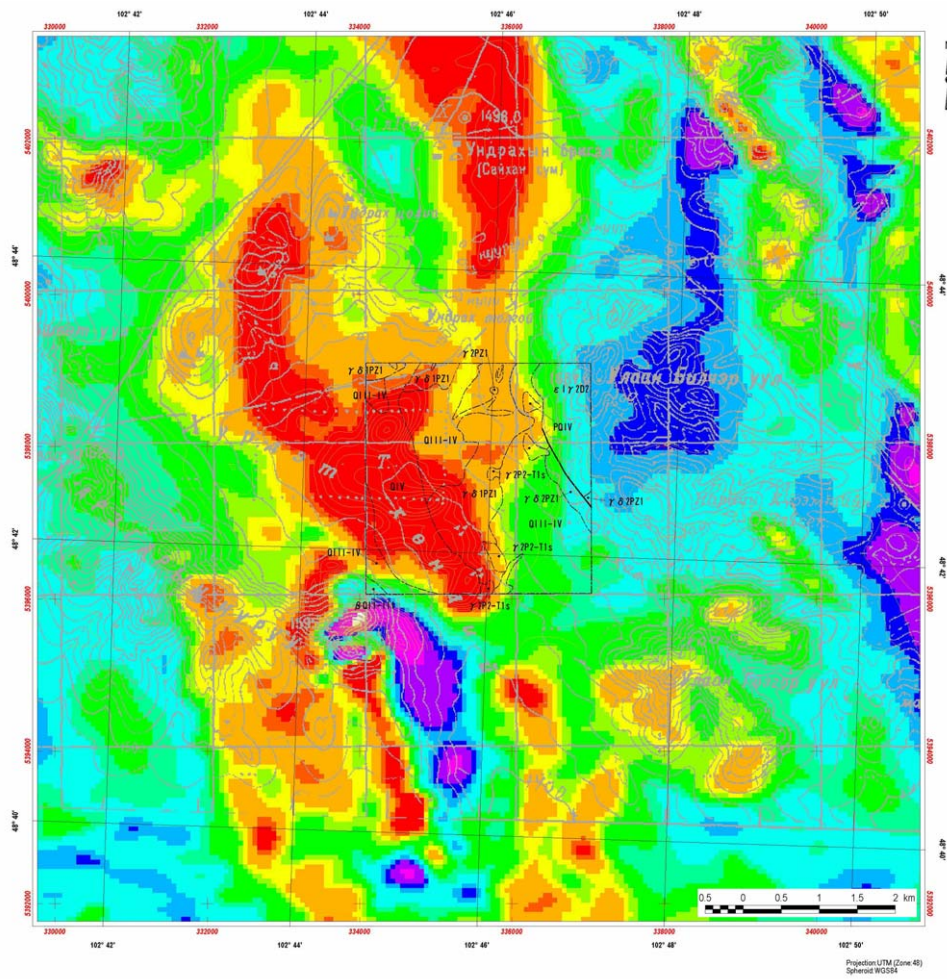


Fig.48 2D analysis section in the Danbatseren east - 3 area.





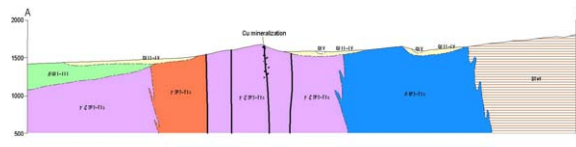
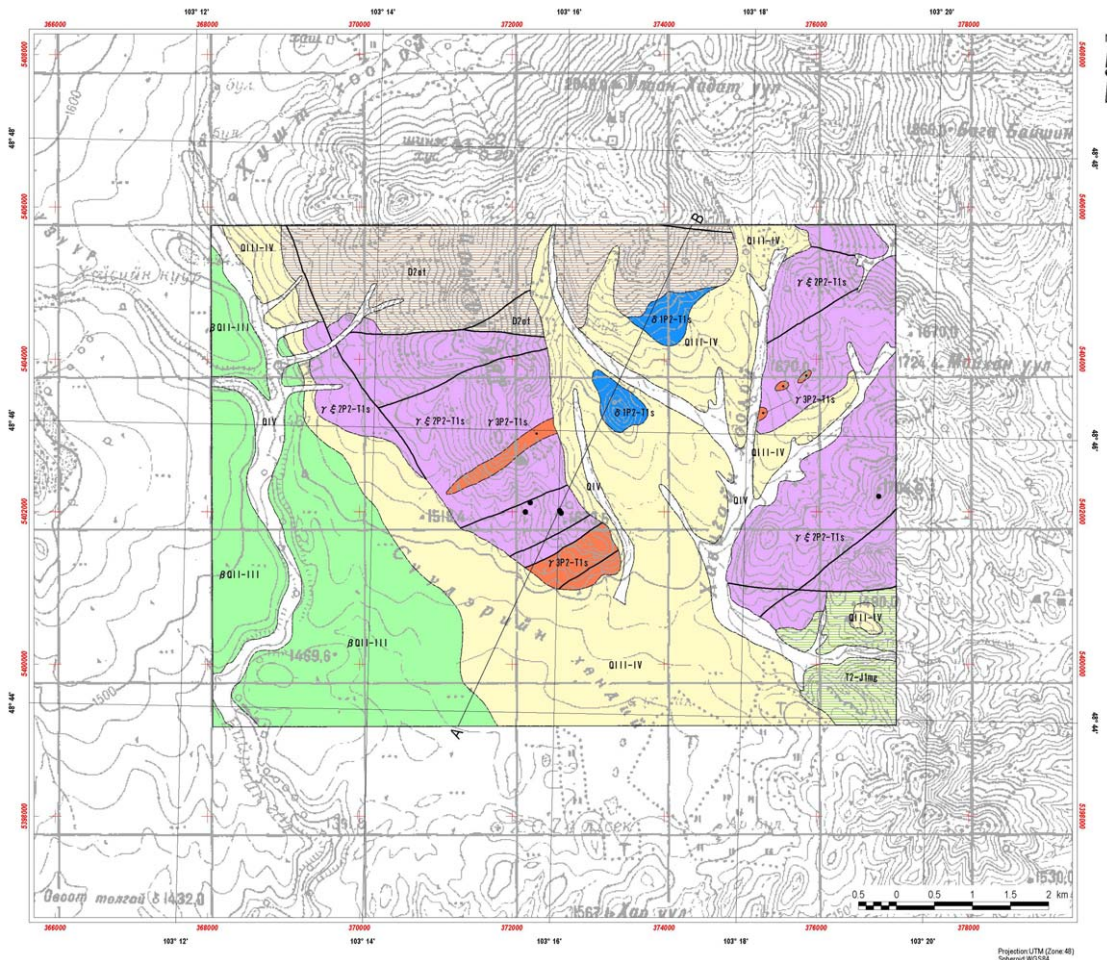


**LEGEND**

|                                     |   |                                     |  |             |   |          |   |           |                               |  |               |  |               |  |               |  |               |  |               |  |               |  |               |  |               |  |               |  |               |  |               |  |               |  |               |  |               |  |               |
|-------------------------------------|---|-------------------------------------|--|-------------|---|----------|---|-----------|-------------------------------|--|---------------|--|---------------|--|---------------|--|---------------|--|---------------|--|---------------|--|---------------|--|---------------|--|---------------|--|---------------|--|---------------|--|---------------|--|---------------|--|---------------|--|---------------|
| <b>Sedimentary Rocks</b>            |   |                                     |  |             |   |          |   |           |                               |  |               |  |               |  |               |  |               |  |               |  |               |  |               |  |               |  |               |  |               |  |               |  |               |  |               |  |               |  |               |
| Quaternary                          | <table border="0"> <tr> <td>QIV</td> <td>Recent sediments: alluvial deposits: gravels, sand, silt and clay</td> </tr> <tr> <td>PQIV</td> <td>Non segmented sediments; conglomerate, gravel, sand, loam</td> </tr> <tr> <td>QIII-IV</td> <td>Upper - Recent sediments; alluvial and colluvial deposits: gravels, sand, silt and clay</td> </tr> <tr> <td>βQIII-III</td> <td>basalt with olivine-pyroxene.</td> </tr> </table>  | QIV                                 | Recent sediments: alluvial deposits: gravels, sand, silt and clay        | PQIV        | Non segmented sediments; conglomerate, gravel, sand, loam | QIII-IV  | Upper - Recent sediments; alluvial and colluvial deposits: gravels, sand, silt and clay | βQIII-III | basalt with olivine-pyroxene. |  |               |  |               |  |               |  |               |  |               |  |               |  |               |  |               |  |               |  |               |  |               |  |               |  |               |  |               |  |               |
| QIV                                 | Recent sediments: alluvial deposits: gravels, sand, silt and clay   |                                     |  |             |   |          |   |           |                               |  |               |  |               |  |               |  |               |  |               |  |               |  |               |  |               |  |               |  |               |  |               |  |               |  |               |  |               |  |               |
| PQIV                                | Non segmented sediments; conglomerate, gravel, sand, loam   |                                     |  |             |   |          |   |           |                               |  |               |  |               |  |               |  |               |  |               |  |               |  |               |  |               |  |               |  |               |  |               |  |               |  |               |  |               |  |               |
| QIII-IV                             | Upper - Recent sediments; alluvial and colluvial deposits: gravels, sand, silt and clay   |                                     |  |             |   |          |   |           |                               |  |               |  |               |  |               |  |               |  |               |  |               |  |               |  |               |  |               |  |               |  |               |  |               |  |               |  |               |  |               |
| βQIII-III                           | basalt with olivine-pyroxene.   |                                     |  |             |   |          |   |           |                               |  |               |  |               |  |               |  |               |  |               |  |               |  |               |  |               |  |               |  |               |  |               |  |               |  |               |  |               |  |               |
| <b>Plutonic Rocks</b>               |   |                                     |  |             |   |          |   |           |                               |  |               |  |               |  |               |  |               |  |               |  |               |  |               |  |               |  |               |  |               |  |               |  |               |  |               |  |               |  |               |
| Permian to Triassic                 | <table border="0"> <tr> <td>γ TP2-T1s</td> <td>Selenge Complex: granite.</td> </tr> <tr> <td>γ ε TP2-T1s</td> <td>Selenge Complex: granite to syenite.</td> </tr> </table>  | γ TP2-T1s                           | Selenge Complex: granite.  | γ ε TP2-T1s | Selenge Complex: granite to syenite.                      |          |   |           |                               |  |               |  |               |  |               |  |               |  |               |  |               |  |               |  |               |  |               |  |               |  |               |  |               |  |               |  |               |  |               |
| γ TP2-T1s                           | Selenge Complex: granite.   |                                     |  |             |   |          |   |           |                               |  |               |  |               |  |               |  |               |  |               |  |               |  |               |  |               |  |               |  |               |  |               |  |               |  |               |  |               |  |               |
| γ ε TP2-T1s                         | Selenge Complex: granite to syenite.  |                                     |  |             |   |          |   |           |                               |  |               |  |               |  |               |  |               |  |               |  |               |  |               |  |               |  |               |  |               |  |               |  |               |  |               |  |               |  |               |
| Devonian                            | <table border="0"> <tr> <td>ε I γ 10I</td> <td>Medium grained biotite granite, alkaline alkasite, granite. Second phase</td> </tr> </table>   | ε I γ 10I                           | Medium grained biotite granite, alkaline alkasite, granite. Second phase |             |   |          |   |           |                               |  |               |  |               |  |               |  |               |  |               |  |               |  |               |  |               |  |               |  |               |  |               |  |               |  |               |  |               |  |               |
| ε I γ 10I                           | Medium grained biotite granite, alkaline alkasite, granite. Second phase  |                                     |  |             |   |          |   |           |                               |  |               |  |               |  |               |  |               |  |               |  |               |  |               |  |               |  |               |  |               |  |               |  |               |  |               |  |               |  |               |
| Paleozoic                           | <table border="0"> <tr> <td>γ TP2I</td> <td>Biotite granite, plagioclase-granite.</td> </tr> <tr> <td>γ δ TP2I</td> <td>Adamellite, granodiorite, tonalite,</td> </tr> <tr> <td>γ δ 1P2I</td> <td>Adamellite, granodiorite, tonalite,</td> </tr> </table>   | γ TP2I                              | Biotite granite, plagioclase-granite.                                    | γ δ TP2I    | Adamellite, granodiorite, tonalite,                       | γ δ 1P2I | Adamellite, granodiorite, tonalite,   |           |                               |  |               |  |               |  |               |  |               |  |               |  |               |  |               |  |               |  |               |  |               |  |               |  |               |  |               |  |               |  |               |
| γ TP2I                              | Biotite granite, plagioclase-granite.   |                                     |  |             |   |          |   |           |                               |  |               |  |               |  |               |  |               |  |               |  |               |  |               |  |               |  |               |  |               |  |               |  |               |  |               |  |               |  |               |
| γ δ TP2I                            | Adamellite, granodiorite, tonalite,   |                                     |  |             |   |          |   |           |                               |  |               |  |               |  |               |  |               |  |               |  |               |  |               |  |               |  |               |  |               |  |               |  |               |  |               |  |               |  |               |
| γ δ 1P2I                            | Adamellite, granodiorite, tonalite,   |                                     |  |             |   |          |   |           |                               |  |               |  |               |  |               |  |               |  |               |  |               |  |               |  |               |  |               |  |               |  |               |  |               |  |               |  |               |  |               |
| Structure                           | <table border="0"> <tr> <td></td> <td>Fault</td> </tr> </table>   |                                     | Fault  |             |   |          |   |           |                               |  |               |  |               |  |               |  |               |  |               |  |               |  |               |  |               |  |               |  |               |  |               |  |               |  |               |  |               |  |               |
|                                     | Fault   |                                     |  |             |   |          |   |           |                               |  |               |  |               |  |               |  |               |  |               |  |               |  |               |  |               |  |               |  |               |  |               |  |               |  |               |  |               |  |               |
| Airborne survey                     | <table border="0"> <tr> <td colspan="2">Reduced to Pole Magnetic Field (nT)</td> </tr> <tr> <td></td> <td>60000 - 62000</td> </tr> <tr> <td></td> <td>60400 - 60500</td> </tr> <tr> <td></td> <td>60700 - 60800</td> </tr> <tr> <td></td> <td>60100 - 60300</td> </tr> <tr> <td></td> <td>60100 - 60200</td> </tr> <tr> <td></td> <td>60000 - 60100</td> </tr> <tr> <td></td> <td>59900 - 60000</td> </tr> <tr> <td></td> <td>59800 - 59900</td> </tr> <tr> <td></td> <td>59700 - 59800</td> </tr> <tr> <td></td> <td>59600 - 59700</td> </tr> <tr> <td></td> <td>59500 - 59600</td> </tr> <tr> <td></td> <td>59400 - 59500</td> </tr> <tr> <td></td> <td>59300 - 59400</td> </tr> <tr> <td></td> <td>59200 - 59300</td> </tr> <tr> <td></td> <td>59100 - 59200</td> </tr> <tr> <td></td> <td>59000 - 59100</td> </tr> <tr> <td></td> <td>58900 - 59000</td> </tr> <tr> <td></td> <td>58800 - 58900</td> </tr> </table> | Reduced to Pole Magnetic Field (nT) |  |             | 60000 - 62000   |          | 60400 - 60500   |           | 60700 - 60800                 |  | 60100 - 60300 |  | 60100 - 60200 |  | 60000 - 60100 |  | 59900 - 60000 |  | 59800 - 59900 |  | 59700 - 59800 |  | 59600 - 59700 |  | 59500 - 59600 |  | 59400 - 59500 |  | 59300 - 59400 |  | 59200 - 59300 |  | 59100 - 59200 |  | 59000 - 59100 |  | 58900 - 59000 |  | 58800 - 58900 |
| Reduced to Pole Magnetic Field (nT) |   |                                     |  |             |   |          |   |           |                               |  |               |  |               |  |               |  |               |  |               |  |               |  |               |  |               |  |               |  |               |  |               |  |               |  |               |  |               |  |               |
|                                     | 60000 - 62000   |                                     |  |             |   |          |   |           |                               |  |               |  |               |  |               |  |               |  |               |  |               |  |               |  |               |  |               |  |               |  |               |  |               |  |               |  |               |  |               |
|                                     | 60400 - 60500   |                                     |  |             |   |          |   |           |                               |  |               |  |               |  |               |  |               |  |               |  |               |  |               |  |               |  |               |  |               |  |               |  |               |  |               |  |               |  |               |
|                                     | 60700 - 60800   |                                     |  |             |   |          |   |           |                               |  |               |  |               |  |               |  |               |  |               |  |               |  |               |  |               |  |               |  |               |  |               |  |               |  |               |  |               |  |               |
|                                     | 60100 - 60300   |                                     |  |             |   |          |   |           |                               |  |               |  |               |  |               |  |               |  |               |  |               |  |               |  |               |  |               |  |               |  |               |  |               |  |               |  |               |  |               |
|                                     | 60100 - 60200   |                                     |  |             |   |          |   |           |                               |  |               |  |               |  |               |  |               |  |               |  |               |  |               |  |               |  |               |  |               |  |               |  |               |  |               |  |               |  |               |
|                                     | 60000 - 60100   |                                     |  |             |   |          |   |           |                               |  |               |  |               |  |               |  |               |  |               |  |               |  |               |  |               |  |               |  |               |  |               |  |               |  |               |  |               |  |               |
|                                     | 59900 - 60000   |                                     |  |             |   |          |   |           |                               |  |               |  |               |  |               |  |               |  |               |  |               |  |               |  |               |  |               |  |               |  |               |  |               |  |               |  |               |  |               |
|                                     | 59800 - 59900   |                                     |  |             |   |          |   |           |                               |  |               |  |               |  |               |  |               |  |               |  |               |  |               |  |               |  |               |  |               |  |               |  |               |  |               |  |               |  |               |
|                                     | 59700 - 59800   |                                     |  |             |   |          |   |           |                               |  |               |  |               |  |               |  |               |  |               |  |               |  |               |  |               |  |               |  |               |  |               |  |               |  |               |  |               |  |               |
|                                     | 59600 - 59700   |                                     |  |             |   |          |   |           |                               |  |               |  |               |  |               |  |               |  |               |  |               |  |               |  |               |  |               |  |               |  |               |  |               |  |               |  |               |  |               |
|                                     | 59500 - 59600   |                                     |  |             |   |          |   |           |                               |  |               |  |               |  |               |  |               |  |               |  |               |  |               |  |               |  |               |  |               |  |               |  |               |  |               |  |               |  |               |
|                                     | 59400 - 59500   |                                     |  |             |   |          |   |           |                               |  |               |  |               |  |               |  |               |  |               |  |               |  |               |  |               |  |               |  |               |  |               |  |               |  |               |  |               |  |               |
|                                     | 59300 - 59400   |                                     |  |             |   |          |   |           |                               |  |               |  |               |  |               |  |               |  |               |  |               |  |               |  |               |  |               |  |               |  |               |  |               |  |               |  |               |  |               |
|                                     | 59200 - 59300   |                                     |  |             |   |          |   |           |                               |  |               |  |               |  |               |  |               |  |               |  |               |  |               |  |               |  |               |  |               |  |               |  |               |  |               |  |               |  |               |
|                                     | 59100 - 59200   |                                     |  |             |   |          |   |           |                               |  |               |  |               |  |               |  |               |  |               |  |               |  |               |  |               |  |               |  |               |  |               |  |               |  |               |  |               |  |               |
|                                     | 59000 - 59100   |                                     |  |             |   |          |   |           |                               |  |               |  |               |  |               |  |               |  |               |  |               |  |               |  |               |  |               |  |               |  |               |  |               |  |               |  |               |  |               |
|                                     | 58900 - 59000   |                                     |  |             |   |          |   |           |                               |  |               |  |               |  |               |  |               |  |               |  |               |  |               |  |               |  |               |  |               |  |               |  |               |  |               |  |               |  |               |
|                                     | 58800 - 58900   |                                     |  |             |   |          |   |           |                               |  |               |  |               |  |               |  |               |  |               |  |               |  |               |  |               |  |               |  |               |  |               |  |               |  |               |  |               |  |               |

Fig.50 Total magnetic intensity of air borne survey in the Undrakh area.



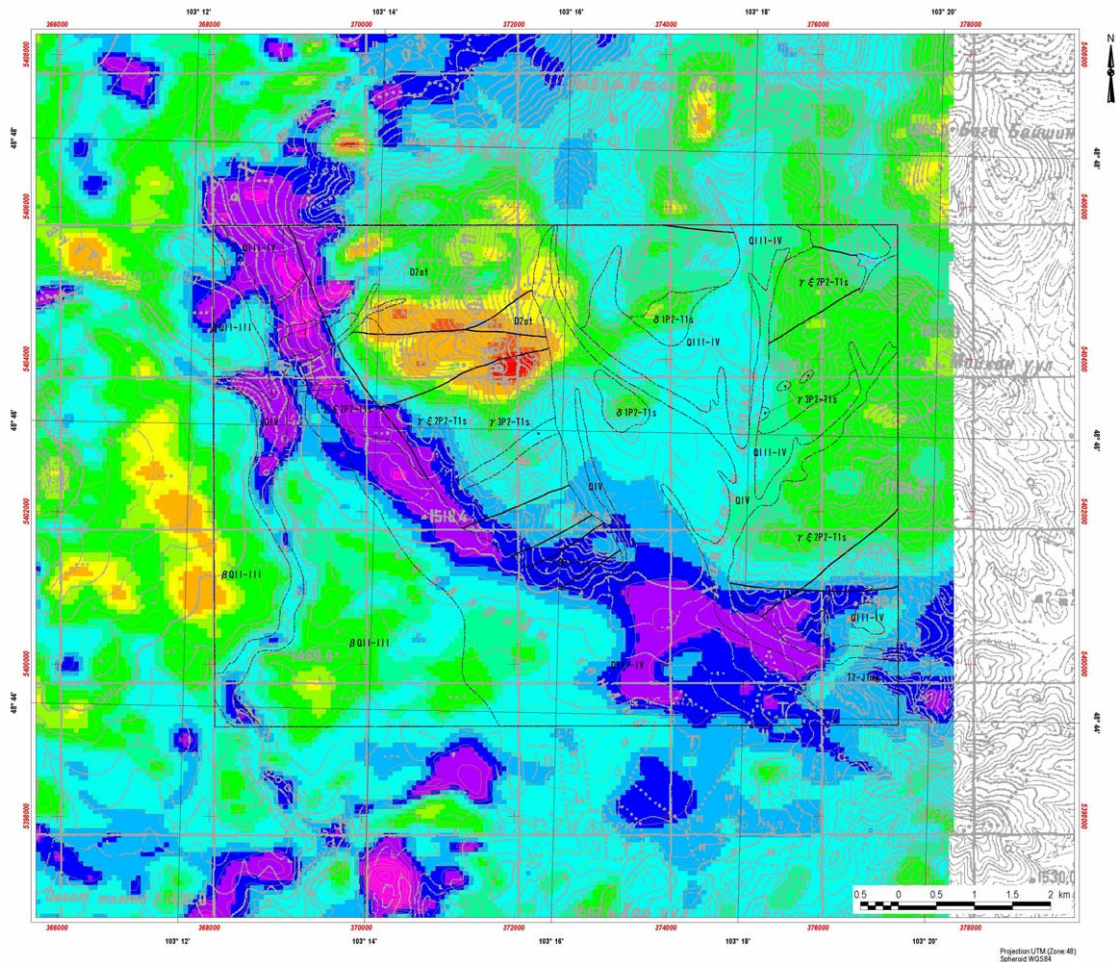


**LEGEND**

|                          |             |  |
|--------------------------|-------------|--|
| <b>Sedimentary Rocks</b> |             |  |
| Quaternary               | QIV         | Recent sediments: alluvial deposits: gravels, sand, silt and clay  |
|                          | QIII-IV     | Upper - Recent sediments: alluvial and colluvial deposits: gravels, sand, silt and clay                                |
|                          | QIII-III    | Middle - upper quaternary: basalt with olivine-pyroxene.   |
| Triassic to Jurassic     | T1-J1ms     | Mogod suite: volcanic rocks and dykes: microdiorite, andesite, porphyry, liparite, dacite and tuffaceous conglomerate. |
| Devonian                 | D1st        | Middle series: sandstone, siltstone, andesite, dacite, it's tuff.  |
| <b>Plutonic Rocks</b>    |             |  |
| Permian to Triassic      | γ SP2-T1s   | Selenge Complex: granite.  |
|                          | γ ε SP2-T1s | Selenge Complex: Lower Triassic: moderate to fine grained, granite to syenite.   |
|                          | δ SP2-T1s   | Selenge Complex: diorite.  |
| <b>Structure</b>         |             |  |
|                          |             | Fault  |
| <b>Mineralization</b>    |             |  |
|                          |             | Mineral showing.   |
|                          |             | Section line   |

Fig.51 Geological map, geological section and mineral showings in the Tsookher mert area.





**LEGEND**

**Sedimentary Rocks**

- Quaternary
  - Q1V Recent sediments: alluvial deposits: gravels, sand, silt and clay
  - Q11-IV Upper - Recent sediments; alluvial and colluvial deposits: gravels, sand, silt and clay
  - Q11-III Middle -upper quaternary: basalt with olivine-pyroxene.
- Triassic to Jurassic
  - T1-11ac Mogod suite: volcanic rocks and dykes: microdiorite, andesite, porphyry, liparite, dacite and tuffaceous conglomerate.
- Devonian
  - D1et Middle series; sandstone, siltstone, andesite, dacite, it's tuff.

**Plutonic Rocks**

- Permian to Triassic
  - γ 3P2-T1s Selenge Complex: granite.
  - γ 2P2-T1s Selenge Complex: Lower Triassic: moderate to fine grained, granite to syenite.
  - δ 1P2-T1s Selenge Complex: diorite.

**Structure**

- Fault

**Airborne survey**

**Reduced to Pole Magnetic Field (nT)**

- 60200 - 62200
- 60400 - 60500
- 60300 - 60400
- 60200 - 60300
- 60100 - 60200
- 60000 - 60100
- 59900 - 60000
- 59800 - 59900
- 59700 - 59800
- 59600 - 59700
- 59500 - 59600
- 59400 - 59500
- 59300 - 59400
- 59200 - 59300
- 59100 - 59200
- 59000 - 59100
- 58900 - 59000
- 58800 - 58900

Fig.52 Total magnetic intensity of air borne survey in the Tsokher mert area.